Fakultät für Medizin
Institut für Virologie

Application of *in vitro* transcribed mRNA to analyze hepatitis B virus infection and its targeting by CRISPR/Cas9

Andreas Oswald

Vollständiger Abdruck der von der Fakultät für Medizin der Technischen Universität München zur Erlangung des akademischen Grades eines

Doktors der Naturwissenschaften (Dr. rer. nat.)

genehmigten Dissertation.

Vorsitzender: Prof. Dr. Dr. Stefan Engelhardt

Prüfende der Dissertation:

1. Prof. Dr. Ulrike Protzer
2. Prof. Dr. Michael Pfaffl

Die Dissertation wurde am 30.06.2020 bei der Technischen Universität München eingereicht und durch die Fakultät für Medizin am 03.11.2020 angenommen.

Table of content

Abbreviations

A	Adenine
AAV	Adeno-associated virus
AdV	Adenovirus, adenoviral vector
ALT	Alanine aminotransferase
APS	Ammonium persulfate
As	*Acidaminococcous sp.*
C	Cytosine
Cas9	CRISPR-associated protein 9
Cav-1	Caveolin-1
cccDNA	Covalently closed circular DANN
CMV	Cytomegalovirus
CRISPR	Clustered regularly interspaced palindromic repeat
CTB	Cell Titer Blue
CTP	Cytosine triphosphate
DHBV	Duck hepatitis B virus
DMSO	Dimethyl sulfoxide
DNase	Deoxyribonuclease
Dpi	Days post-infection
DR1	Direct repeat 1
DR2	Direct repeat 2
DSB	Double strand break
DZIF	Deutsches Zentrum für Infektionsforschung
FCS	Fetal calf serum
FITC	Fluorescein isothiocyanate
FSC	Forward scatter
G	Guanine
GAPDH	Glyceraldehyde-3-phosphate dehydrogenase gene
GFP	Green fluorescent protein
H	Hours
HBc	HBV core protein
HBeAg	Hepatitis B e antigen
HBs	HBV surface protein
HBsAg	Hepatitis B surface antigen
HBV	Hepatitis B virus, Hepatitis-B-Virus
HBx	HBV X protein
HDR	Homologous direct repair
HDV	Hepatitis D virus
HIV-1	Human immunodeficiency virus type 1
IFNα	Interferon-alpha
IFNβ	Interferon-beta
InDel	Insertion, deletion
IU	Infectious units
IVT	*In vitro* transcribed
L protein, LHBs	Large HBV surface protein

Lb	*Lachnospiricae bacterium ND2006*
LV	Lentivirus
M protein, MHBs	Middle HBV surface protein
MFI	Mean fluorescent intensity
MOI	Multiplicity of infection
mRNA	Messenger RNA
Nd	Not detectable
NHEJ	Non-homologous end joining
ns	Not significant
NTCP	Sodium taurocholate cotransporting polypeptide
P protein	Polymerase protein of HBV (reverse transcriptase, RNaseH, primer)
PBS	Phosphate buffered saline
PCR	Polymerase chain reaction
PCSK9	Proprotein convertase subtilisin/kexin type 9
PEG	Polyethylene glycol
pgRNA	Pregenomic RNA
PHH	Primary human hepatocytes
PRNP	Prion protein gene
PVDF	Polyvinylidene fluoride
qPCR	Quantitative PCR
qRT-PCR	Quantitative reverse transcription PCR
rcDNA	Relaxed-circular DNA
RFP	Red fluorescent protein
RIG-I	Retinoic acid inducible gene I
RNase	Ribonuclease
s	sec
S protein, SHBs	Small HBV surface protein
Sa	Staphylococcus aureus
S-CAR	Chimeric antigen receptor recognizing HBsAg
SDS	Sodium dodecyl sulphate
SDS-PAGE	Sodium dodecyl sulphate-polyacrylamide gel electrophoresis
shRNA	Short hairpin RNA
siRNA	Small interfering RNA
Sp	Streptococcus pyogenes
SSC	Side scatter
T	Thymine
TBS-T	Tris-buffered saline with Tween 20
TCR	T-cell receptor
TDP	Tyrosyl-DNA-phosphodiesterase
TEMED	Tetramethylethylenediamine
TXR	Texas Red
U	Uridine, unit
UTP	Uracil triphosphate
WT	Wild type
ARCA	Anti-reverse cap analog
RNAi	RNA interference

HCC	Hepatocellular carcinoma
WHO	World Health Organization
cDNA	Complementary DNA
sgRNA	Single guide RNA
crRNA	CRISPR RNA
tracrRNA	Trans-activating crRNA
PAM	Protospacer adjacent motif
Kb	Kilobases
ORF	Open reading frame
CDS	Coding sequence
SVP	Subviral particles
Bp	Base pair
pDNA	Plasmid DNA
UTR	Untranslated region
NGS	Next generation sequencing

Abstract

Hepatitis B virus (HBV) infection remains a global health burden, with approximately 257 million people chronically infected and 880.000 annual deaths worldwide. Despite a prophylactic vaccination efficient treatment of chronic HBV is still demanded. Current treatment options are using IFNα or nucleos(t)ide analogues which either act as antiviral agents showing severe side effects or are exclusively targeting reverse transcription step. Since both treatments fail to completely eradicate the viral persistence form the covalently closed circular (ccc)DNA or reduce viral transcription alternative, highly potent drugs are still of great interest for research. In this work we were interested to establish *in vitro* transcribed (IVT) mRNA synthesis to allow different experimental application. Therefore, we first established the production and optimized the final IVT mRNA constructs by comparing different cap structures (standard cap vs. ARCA) and nucleotide modifications (UTP and CTP analogs) in terms of cytotoxicity, protein expression and functionality. Our results demonstrated that implementation of ARCA cap and Pseudo-UTP/5mCTP nucleotide modifications revealed most improved characteristics compared to other variations. We applied the optimized IVT mRNA for different experimental setups: (1) analysis of early steps in HBV life cycle and (2) targeting of HBV DNA forms to reduce viral load. For the first aim we used IVT mRNA constructs encoding for Caveolin-1 a relevant factor involved in HBV trafficking which was not expressed in our target cell line (HepG2-NTCP-K7). IVT mRNA transfection led to the expression of functional protein in high amounts but with no effects on HBV life cycle. Next, we were interested if transient expression of HBV entry receptor NTCP would support HBV infection in non-hepatic and hepatic cell lines. Application of NTCP by IVT mRNA showed that the protein was expressed in all tested cell lines, but exclusively supported uptake and infection of HBV in hepatoma cell line HepG2. Therefore, we further characterized the impact of NTCP on HBV susceptibility using titrated amounts of IVT mRNA to enable NTCP expression at more physiological level. Our results indicated that already very low amounts of NTCP protein led to productive HBV infection in HepG2.

This finding indicated that transient expression of desired factors using IVT mRNA is a suitable tool to analyze their impact on cellular level or in viral life cycle, allowing easy and fast screening for interesting candidates. For the second aim, we used IVT mRNA encoding for *Streptococcus pyogenes* Cas9 and a combination of sgRNAs against HBV to analyze CRISR/Cas9 targeting efficiency towards different HBV DNA forms. Application of mRNA-based CRISPR/Cas9 showed that targeting of integrated HBV DNA forms led to efficient reduction of viral parameters but revealed low efficiency towards multiple, episomal targets. Further analysis of binding behavior (using a silenced Cas9 variant) and genome editing events (by next-generation sequences) supported the previous findings indicating that CRISPR/Cas9 functionality is limited when targeting episomal structures like cccDNA. In contrast to the establishment of IVT mRNA we were also interested to find a treatment option for chronic HBV infection targeting cccDNA and HBV transcripts simultaneously. Therefore, we combined CRISPR/Cas9 method with RNAi using AAV vector system. Our *in vitro* data revealed that transduction of the AAV system led to significant reduction of viral parameters when targeting cccDNA or HBV integrates. Therefore, we are interested if this combinatorial system can efficiently reduce viral load and if this would allow reconstitution of anti-HBV immunity in the upcoming *in vivo* experiments.

In summary we demonstrated that IVT mRNA is a promising tool to apply for various experimental setups supporting fast and strong expression of functional proteins. We showed that titration of IVT mRNA encoding for NTCP led to dose-dependent functionality allowing analysis of effects on physiological level. Our experiments towards CRISPR/Cas9 efficiency indicated that targeting of episomal structures is strongly reduced. Therefore, additional optimizations have to be implemented to achieve efficient targeting of cccDNA. In contrast, our combinatorial AAV-based system revealed high efficiency in cell culture which needs to be validated in future *in vivo* experiments.

Zusammenfassung

Eine Infektion mit dem Hepatitis B Virus (HBV) führt nach wie vor zu globalen gesundheitlichen Problemen mit bis zu 257 Millionen chronisch Infizierten und weltweit rund 880.000 jährlichen Toten. Die Notwendigkeit einer effizienten Therapie gegen chronische HBV Infektionen, ist trotz einer prophylaktischen Impfung, hoch. In der vorliegenden Arbeit waren wir daran interessiert die Synthese von *in vitro* transkribierter (IVT) mRNA zu Etablieren und für verschiedene wissenschaftliche Fragestellungen zu verwenden. Hierzu wurde zunächst die Produktion etabliert und die fertigen IVT mRNAs durch den Vergleich von verschiedenen Cap-Strukturen, sowie Nukleotid-Modifikationen bezüglich Zellverträglichkeit, Protein Expression und Funktionalität, optimiert. Unsere Ergebnisse zeigten, dass die Verwendung von ARCA und Pseudo-UTP/5mCTP modifizierten mRNAs die besten Eigenschaften im Vergleich zu anderen Varianten zeigten. Folglich, wurden die optimierten mRNA Konstrukte für Experimente in unterschiedlichen Projekten verwendet: (1) Analyse der ersten Schritte im HBV Lebenszyklus und (2) die Inaktivierung verschiedener HBV DNA Formen zur Reduktion der Viruslast. Für das erste Teilprojekt haben wir mRNA verwendet, die für Caveolin-1 kodiert, einen wichtigen Faktor des intrazellulären HBV Transports, welcher in unseren Zielzellen (HepG2-NTCP-K7) fehlt. Die Transfektion von IVT mRNA führte zur Expression von großen Mengen an funktionellem Protein, jedoch ohne einen Effekt auf den HBV Lebenszyklus. Als nächstes waren wir daran interessiert, ob die kurzzeitige Expression des Eintrittsfaktors für HBV, NTCP, die Infektion mit HBV in nicht-hepatischen und hepatischen Zellen ermöglicht. Das Einbringen von NTCP mittels IVT mRNA zeigte Proteinexpression in allen getesteten Zelllinien, jedoch war die Aufnahme und Infektion von HBV spezifisch nur in HepG2 Zellen zu messen. Darauf basierend analysierten wir den Einfluss auf die HBV Permissivität in diesen Zellen durch die Titration unsere IVT mRNA zur Expression von physiologischen NTCP Konzentrationen. Unsere Ergebnisse zeigten, das bereits niedrige Konzentration an NTCP ausreichen, um eine HBV Infektion zu ermöglichen.

Wir konnten aufzeigen, dass eine kurzzeitige Expression von zu untersuchenden Faktoren mittels IVT mRNA ein praktisches Werkzeug darstellt, um deren Einfluss auf zellulärer Ebene oder auf den viralen Lebenslauf zu analysieren. Für die Durchführung des zweiten Projekts verwendeten wir IVT mRNA die für das Cas9 Protein von *Streptococcus pyogenes* kodiert und eine Kombination aus mehreren sgRNAs gegen HBV, um die CRISPR/Cas9 Effizienz gegen verschiedene HBV DNA-Formen zu untersuchen. Die Verwendung von mRNA basiertem CRISPR/Cas9 zeigte, dass die Anwendung gegen integrierte, jedoch nicht gegen mehrere, episomale HBV Sequenzen, zu einer effizienten Reduktion von viralen Parametern führte. Weitere Analysen zur Bindungsfähigkeiten und der Editierraten innerhalb des Genoms zeigte, dass CRISPR/Cas9 eine verringerte Effizienz gegen episomale Zielsequenzen, wie die virale cccDNA, aufweist. Zusätzlich zu den mRNA basierten Projekten, lag ein weiterer Aspekt dieser Arbeit auf der Entwicklung einer möglichen Behandlung für chronische HBV Infektionen, die sowohl die cccDNA, als auch die HBV Transkripte parallel angreift. Hierzu kombinierten wir die CRISPR/Cas9 und RNAi Technologie mittels eines AAV-basierten Vektorsystems miteinander. Unsere *in vitro* Daten zeigten, dass die Verwendung des Systems gegen cccDNA und integrierte HBV DNA zu einer signifikanten Reduktion von viralen Paramatern führte. Ob die Verwendung des Systems eine effiziente Reduktion der Viruslast, sowie eine Rekonstitution der anti-HBV Immunantwort ermöglichen kann, wird in zukünftigen *in vivo* Versuchen untersucht.

Zusammenfassend konnten wir zeigen, dass IVT mRNA eine vielversprechende Methode ist, die für verschiedene Ansätze verwendet werden kann, da sie eine schnelle und hohe Proteinexpression ermöglicht. Wir konnte aufzeigen, dass die Titration von IVT mRNA kodierend für NTCP zu einer Dosis-abhängigen Funktionalität führte, die eine Analyse unter physiologischen Bedingungen ermöglicht. Unsere Ergebnisse im Bezug auf die Effizienz von CRISPR/Cas9 impliziert, dass der limitierende Schritt dieser Methode auf episomale Zielstrukturen zurückzuführen ist. Demzufolge muss das System für einen effizienteren Einsatz gegen die cccDNA weiter optimiert werden. Im Gegensatz dazu konnten wir aufzeigen, dass die Verwendung unseres kombinatorischen AAV-basierten Systems bereits hoch effizient zu seien scheint, was jedoch in weiterführenden Experimenten validiert werden muss.

1. Introduction

1.1. Hepatitis B virus

The present thesis is focusing on different aspects related to basic virology and treatment options of chronic hepatitis B virus (HBV) infection. Therefore, the following chapters introduce the molecular biology of HBV, its infection cycle and treatment options.

1.1.1. Classification of HBV

Worldwide 257 million people are chronically infected with HBV, causing 887,000 annual deaths, which are related to liver cirrhosis and hepatocellular carcinoma (HCC) (Schweitzer et al. 2015, WHO 2017). HBV is classified as prototype of the *Hepadnaviridae* family consisting of hepatotropic DNA viruses which are species-specific and divided in two genera: *Orthohepadnavirus* and *Avihepadnavirus* (Schaefer 2007). The *Orthohepadnavirus* members mainly infect mammals (e.g. woodchucks via woodchuck hepatitis B virus (WHBV) and primates via HBV) and share 70% nucleotide homology between them (Summers et al. 1978, Schaefer 2007). The *Avihepadnavirus* members infect birds (e.g. ducks via duck hepatitis B virus, DHBV) and share about 80% homology among them (Mason et al. 1980). Homology between both genera is around 40% but they share a common genome organisation. As replication of these viruses occurs via an RNA intermediate, they are designated as *Pararetroviruses* (Hu et al. 2017).

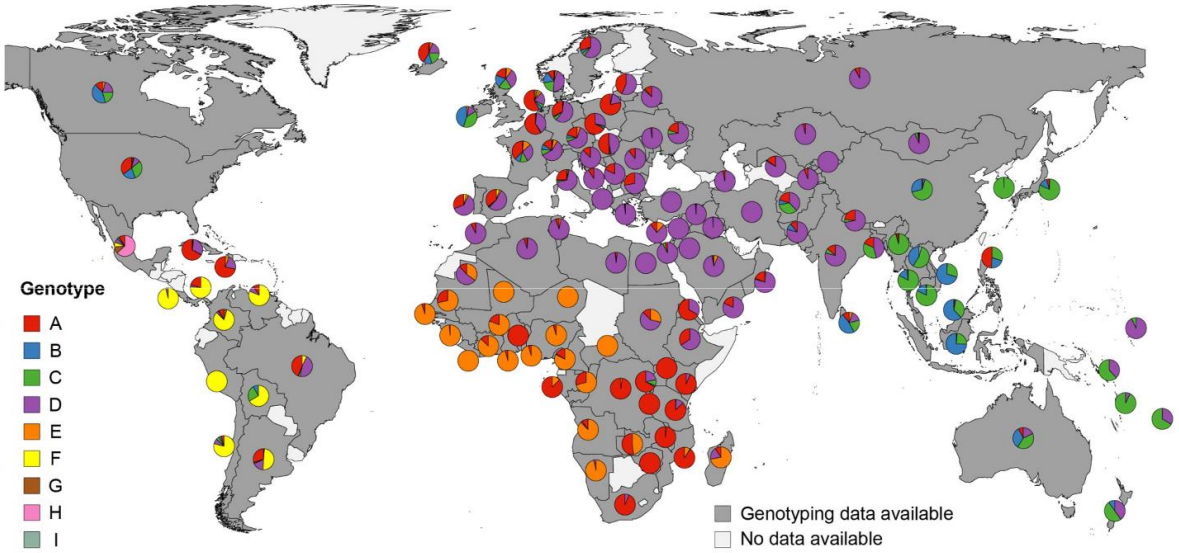

Figure 1: Graphical representation of worldwide HBV genotype distribution. Pie charts reflects statistical representation of each HBV genotype in each respective region (Velkov et al. 2018).

Based on nucleotide divergence of 7.5% of whole genome sequences, HBV can be divided phylogenetically into nine genotypes (A–I). Those genotypes can be further subdivided in sub-genotypes which differ > 4% in their nucleotide sequences (Kramvis 2014, Pourkarim et al. 2014, Velkov et al. 2018). The different genotypes are distributed geographically. Genotype A is predominantly found in European countries, South Africa and central America. Genotypes B and C occur most frequently in Asia, Oceania and Australia, genotypes F and H are prevalent in Southern and Central America. Genotype D can be found worldwide, whereas genotype E is predominant in Western and Central Africa, genotype G in parts of Europe and America and genotype I in Asia (Kramvis 2014). A proposed new genotype J was isolated from a Japanese patient in 2009 (Tatematsu et al. 2009). Additionally, based on the epitopes of the surface protein, HBV can be classified in nine different serological subtypes. In summary four major serotypes *ayw, ayr, adw* and *adr* were defined (Kramvis 2014).

1.1.2. Structure of HBV particles

Infectious virions of HBV also called “Dane particles” (Fig. 2) have a size of 42 nm in diameter and are enveloped by an outer layer consisting of small (S), middle (M) and large (L) surface proteins (hepatitis B surface antigen, HBsAg) embedded in a lipid layer. Within this lipid envelope 120 dimers of 180 (T=3) or 240 (T=4) core protein subunits are forming an icosahedral, inner nucleocapsid (core particle, hepatitis B core antigen, HBcAg) (Dane et al. 1970, Crowther et al. 1994, Nassal 2015). Inside this shell resides the viral genome as a partially double-stranded, partially closed, “relaxed circular” (rc)DNA. The viral polymerase protein (P protein) is covalently linked to the (-)-strand of the rcDNA and plays a role in the reverse transcription step (Gerlich et al. 1980). Besides infectious particles, HBV infected cells also form non-infectious subviral-particles (SVPs), which occur either as 22 nm in diameter filaments or as 25 nm in diameter spheres. SVPs exclusively consist of envelope proteins and lack nucleocapsid and rcDNA, respectively (Hu and Liu 2017).

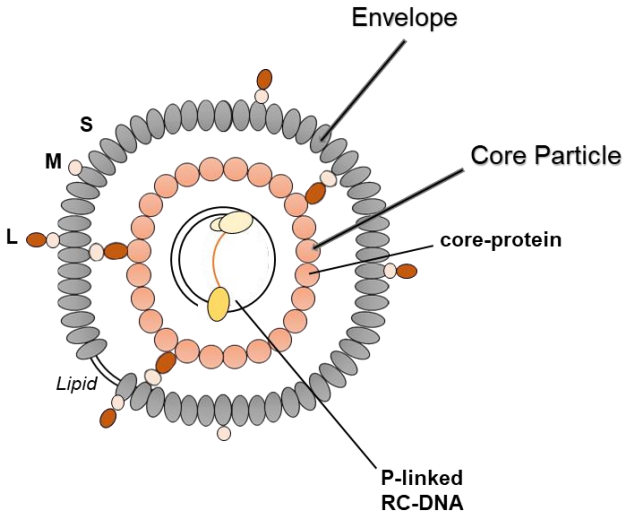

Figure 2: Schematic representation of Hepatitis B virus particle. Virus particle consisting of outer envelope, embedded in lipid layer. The envelope is formed out of surface proteins S (small), M (middle), L (large), which enclose the nucleocapsid (core particle). The core particle is composed of core proteins and the relaxed-circular DNA (rcDNA) which is linked to viral polymerase (P).

1.1.3. HBV genome organisation

The genome of HBV is the smallest amongst DNA viruses with a total length of 3.2 kilobases (kb), consisting of four open reading frames (ORFs) which are partially or fully overlapping (Fig. 3). These four ORFs encode for all seven viral proteins, the three HBV surface proteins which harbor the same C-terminal region but are extended N-terminally by preS2 and preS1 domains, respectively. Translation from different in-frame start codons lead to expression of the small (S), middle (M) and the large (L) HBsAg proteins (Ho et al. 2020). The subunits for the viral nucleocapsid are encoded by the ORF C and can harbor an additional N-terminal peptide (precore, preC) which is proteolytically processed and secreted as hepatitis B e antigen (HBeAg) (Seeger et al. 2015). HBeAg is involved in triggering anti-HBV immune responses and is used as a serological marker (Ho et al. 2020). ORF P encodes for the viral polymerase which serves as reverse transcriptase, RNAseH and primer during rcDNA synthesis (Seeger and Mason 2015). HBV X protein (HBx, X) is responsible for efficient infection and viral transcription of HBV (Lucifora et al. 2011). All additional regulatory elements such as the two enhancers (Enh1, Enh2), promotors (core, S1, S2 and X), polyadenylation, encapsidation (ε) and replication signals (DR1, DR2) are located in those ORFs (Karayiannis 2017).

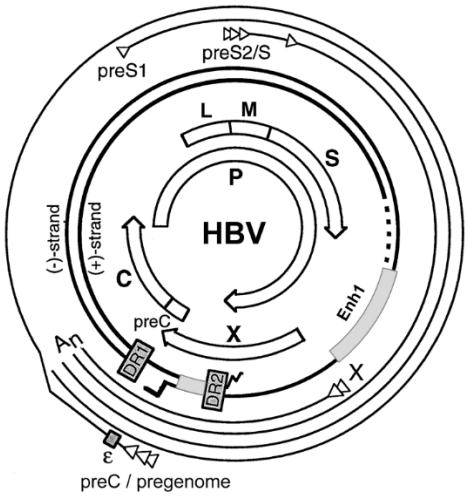

Figure 3: Genome organisation of HBV. Inner circle shows the four overlapping ORFs: LMS (surface proteins), P (viral polymerase P), C (core proteins) and X (X protein). Regulatory elements Enh1, DR1/2 and encapsidation signal ε are located within different ORF regions. Outer lines depict transcribed viral mRNAs with respective start codons shown by white arrowheads. Modified from (Protzer et al. 2000).

1.1.4. HBV life cycle

The HBV life cycle is depicted in Fig 4. For viral entry in susceptible cells, “Dane particles” attach to glycosaminoglycan side chains of cellular surface heparan sulphate proteoglycans (Schulze et al. 2007). Next, the myristoylated preS1 domain specifically binds to sodium-dependent taurocholate co-transporting polypeptide (NTCP), which was described as entry receptor of HBV and hepatitis D virus (HDV) (Yan et al. 2012, Ni et al. 2014). This integral membrane glycoprotein is involved in the uptake of glycine/taurine-conjugated bile acids and is exclusively expressed on hepatocytes (Hagenbuch et al. 1994, Appelman et al. 2017). Overexpression of NTCP was shown to support HBV infection (Lempp et al. 2016). Uptake of viral particles is driven by clathrin-dependent endocytosis in primary hepatocytes (Huang et al. 2012). Interestingly, in HepaRG cells uptake of HBV is dependent on Caveolin-1 (Cav-1) but not on clathrin expression to achieve productive infection (Macovei et al. 2010). After endocytosis, uncoating of viral particles induces the release of genome-containing nucleocapsids into the host cell cytoplasm where they are translocated to the nuclear membrane. There, the nucleocapsid shell disassembles at the nuclear basket and releases rcDNA into the nucleus (Schmitz et al. 2010). Cellular factors are involved in the repair of rcDNA to form fully double-stranded, covalently closed circular DNA (cccDNA) (Schreiner et al. 2017). This persistent form resides episomally in the nucleus of infected cells and serves as template for transcription by host RNA polymerase II for all viral transcripts, including subgenomic mRNAs, the pregenomic RNA (pgRNA) and precore RNA. As mentioned above, precore RNA is translated and processed to HBeAg which is secreted in the supernatant of infected cells. pgRNA serves as template for viral polymerase (P protein) and HBV core protein expression and is reverse transcribed by P protein into rcDNA within *de novo* formed nucleocapsids in the cytoplasm (Nassal 2015, Seeger and Mason 2015). Those rcDNA containing nucleocapsids can be either re-shuttled to the nucleus to increase the stable cccDNA pool or transported to the endoplasmatic reticulum where it is enveloped and finally secreted (Nassal 2015). Secretion of enveloped particles and filaments is driven by multivesicular bodies (Jiang et al. 2015). In contrast, subviral spheres exit the cells via endoplasmatic reticulum and Golgi complex (Patient et al. 2007).

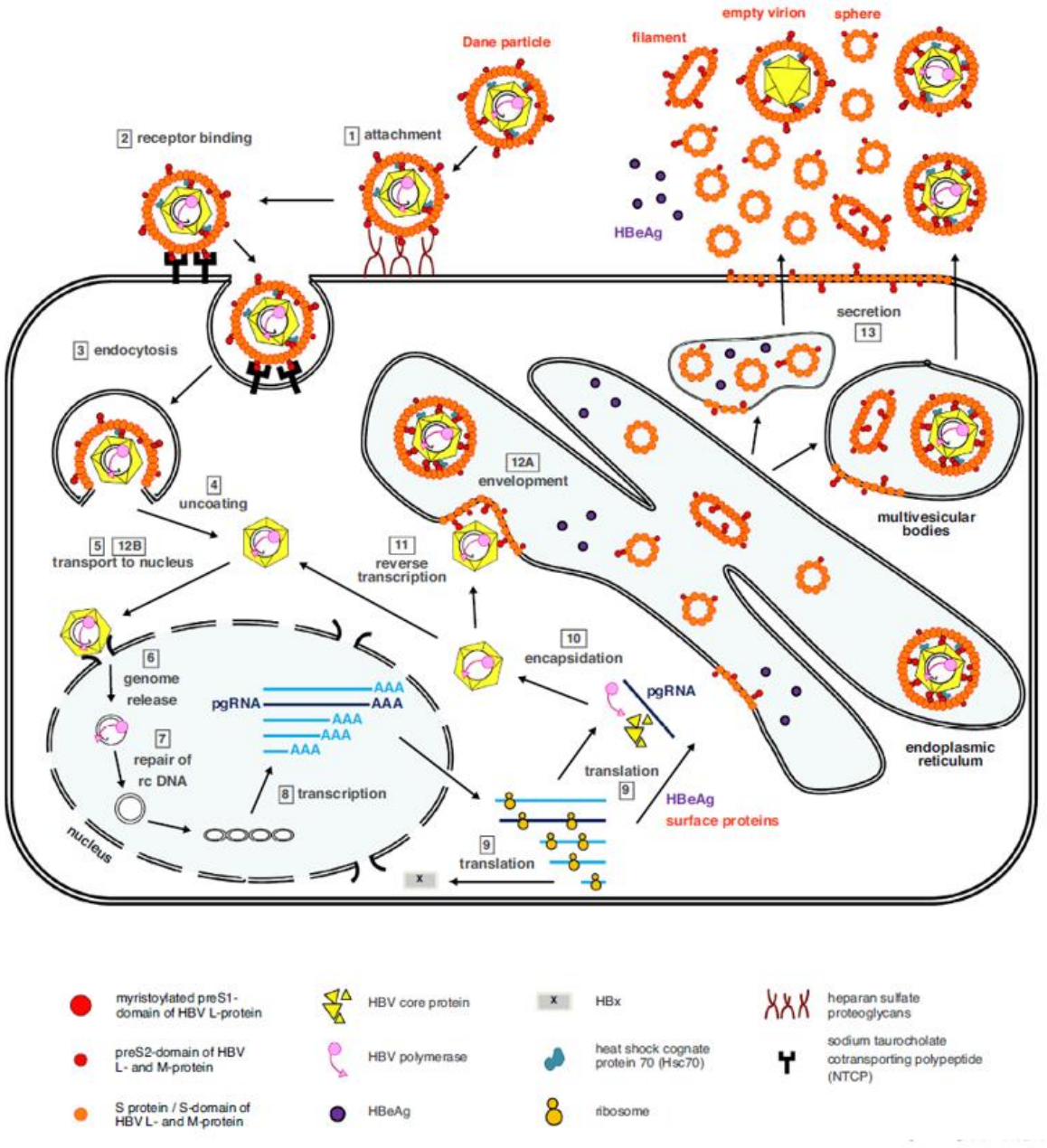

Figure 4: Schematic presentation of HBV life cycle. Attachment of viral particles to heparan sulfate proteoglycans and interaction with sodium taurocholate co-transporting polypeptide (NTCP) leads to endocytosis. In the cytoplasm of infected cells, particles are uncoated and nucleocapsid is transported to nucleus. There, conversion of rcDNA to cccDNA and transcription of viral transcripts occurs, leading to translation of viral proteins in the cytoplasm. pgRNA is encapsidated and reverse transcribed in the *de novo* formed nucleocapsids which are enveloped and secreted (Ko et al. 2017).

1.1.5. Persistence form of HBV: cccDNA

The viral persistent form cccDNA has a high stability and represents the major problem for treatment of chronic HBV infection, due to the lack of directly targeting anti-HBV drugs (Schreiner and Nassal 2017) During infection rcDNA, which was released in the nucleus, is deproteinized and RNA oligomer linkage is removed. It was postulated, that the removal of DNA-linked viral polymerase is driven by tyrosyl-DNA phosphodiesterase-2 (TDP2) which can cleave tyrosyl-5' DNA linkages (Koniger et al. 2014). Deproteinized rcDNA further serves as functional precursor of cccDNA (Guo 2017). The conversion of rc- to cccDNA in the nucleus of infected hepatocytes is a multistep process which still remains elusive. HBV cccDNA exists as episomal DNA in the nuclei of infected cells where it is packaged into a minichromosome interacting with cellular histones and nucleosomal proteins (Bock et al. 1994).

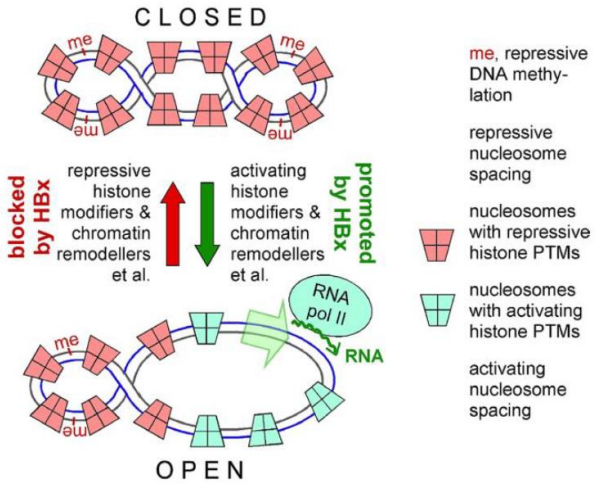

Figure 5: Epigenetic modulation of cccDNA by HBx. HBx is involved in blocking steps (e.g. repressive histone modifiers) and promoting steps (e.g. activating histone modifiers) regulating transcriptional activity of cccDNA (Nassal 2015).

Histone composition mainly consists of histones H3 and H2B and lower amounts of histones H4, H2A and H1 (Bock et al. 2001). Posttranslational modifications of these histones are focusing on active transcription indicated by enrichment of respective modifications. (Tropberger et al. 2015) For example it is know that, methylation patterns affect cccDNA transcription whereas acetylation of H3 and H4 histones influence HBV replication (Pollicino et al. 2006, Riviere et al. 2015). Viral HBx protein plays an important role in modulating the epigenetic status of cccDNA (Fig. 5) and the subsequent transcription by RNA polymerase II (Nassal 2015).

1.1.6. Epidemiology and current treatment of HBV

HBV can be transmitted by blood or blood products, sexual intercourse and most important vertically during birth from mother to child (Stevens et al. 2017, RKI 2018). In healthy adults, infection with HBV is often asymptomatic, one third develops an acute, icteric hepatitis and only 0.5–1% have the risk to develop a fulminant hepatitis with liver failure. Chronic hepatitis in adults is developed in 5–10% of all cases (RKI 2018). This number completely changes in children up to six months and patients under immune suppression who develop chronicity in 90% or 30–90% of the cases (Schweitzer et al. 2015, RKI 2018).

During acute and chronic HBV infection, viral control is mediated by the immune system which can lead to liver damage. Several weeks after infection with HBV, HBsAg can be detected in the serum of patients which mainly consists of SVPs. One to two weeks after appearance of HBsAg, alanine aminotransferase (ALT) concentrations in the patient blood increases which serves as an indicator for liver inflammation. Anti-HBc antibodies can be detected already at this time, whereas anti-HBs antibody levels can be measured several weeks after infection when HBsAg is cleared. Once HBsAg is detectable for more than six months, HBV infection is assumed to be chronic, indicating the failure of the immune system to clear the infection. Chronic hepatitis B is characterized by three phases: replicative phase (low HBV DNA levels, increased ALT levels), inactive phase (HBeAg seroconversion, HBV DNA and ALT concentrations decreased) and in 20–30% of cases reactivation phase (HBV DNA and/or ALT levels increase) leading to liver cirrhosis and hepatocellular carcinoma (Trepo et al. 2014).Currently, seven anti-viral treatment options against chronic hepatitis B are approved by the Food and Drug Administration (FDA): interferon-a2b, pegylated interferona2α and nucleos(t)ide analogues like entecavir (ETV), lamivudine (LAM), adefovir, telbivudine, tenofovir (TDF) and tenofoviralafenamid (TFA) (Rajbhandari et al. 2016). IFNα triggers immunomodulatory effects and act as antiviral agents, but has several side-effects like fatigue, bone marrow suppression, depression or unmasking of autoimmune diseases (Zoulim et al. 2016). In contrast, nucleos(t)ide analogues target viral reverse transcription of pgRNA to rcDNA which leads to the reduction of viral load in the patient serum.

The major disadvantage of nucleos(t)ide analogues treatment is based on missing targeting of viral transcripts and cccDNA which leaves eradication of the virus incomplete (Boni et al. 2019). Besides targeting reverse transcription step, another approach using core protein allosteric modulators (CpAM), like phenylpropenamide (PPA) or heteroaryldihydropyrimidine (HAP) modulating capsid assembly demonstrated promising results in early clinical trials (Lok et al. 2017). Currently, newly-synthesized versions of these compounds, like HAP-derivate Bay41-4109 or HAP_R01, are being tested *in vitro* showing promising inhibition capacity of HBV replication (Stray et al. 2006, Ko et al. 2019). Still, *in vivo* application and clinical trials have to confirm functionality of CpAMs to become a suitable treatment option for HBV. Since current treatment options fail to clear the virus from chronically infected hepatocytes further research is needed. The following chapters describe different therapies which might be promising candidates for treatment of chronic HBV.

1.1.7. Engineered T cell therapy

Acute HBV infection is resolved by strong polyclonal T cell responses leading to clearance of the virus. During chronic infections only scarce and oligoclonal T cell responses are present which are failing to control the virus and prevent disease progress (Thimme et al. 2003, Rehermann et al. 2005). It was shown that T cells can target HBV by killing infected hepatocytes but also by silencing cccDNA using secreted cytokines in a noncytolytic fashion. Additionally, killing of infected cells lead to cell division which further moderates cccDNA loss (Allweiss et al. 2018). A possible way to compensate the missing immune response is based on adoptive T cell therapy using T cells grafted with T cell receptors (TCR) or chimeric antigen receptors (CAR) against the envelope or the core protein of HBV (Boni et al. 2019). Transfer of these engineered T cells was demonstrated to significantly reduce HBV infection in mouse models (Kruse et al. 2018, Festag et al. 2019, Wisskirchen et al. 2019). Adoptive T cell therapy is a promising tool in chronic HBV patients, as data show only low off-targeting effects (Qasim et al. 2015). Nevertheless, adoptive T cell therapy has limitations concerning the amount of donor T cells and transduction efficiency of TCR/CAR constructs.

Additionally, treatment is time and cost intensive (apheresis of autologous T cells, genetic modification and expansion) and not suitable for every patient (Ranganathan et al. 2016).

1.1.8. Monoclonal antibody strategy

Immunotherapies using human derived monoclonal antibodies (mAb) have shown great clinical success treating different types of cancers, autoimmune or inflammatory diseases (Li et al. 2017). Further, treatment of chronic viral infections via mAb has already shown promising clinical outcomes when neutralizing HIV infection (Scheid et al. 2016, Schoofs et al. 2016). The anti-viral capacities of mAbs include neutralizing effects, blocking of viral entry, mediating cytotoxic killing or phagocytosis and triggering of sustained host immune responses *in vivo* (DiLillo et al. 2014, Pelegrin et al. 2015, Schoofs et al. 2016). For HBV, mAbs specific for viral surface protein (HBsAg) are of great interest for treatment of chronic infection. Several studies have demonstrated anti-viral effects of different neutralizing mABs in animal models and phase I human studies but failed to eradicate the virus (Neumann et al. 2010, Zhang et al. 2016). Another approach published by Li et al. 2017 demonstrated an anti-viral effect through fragment crystallizable (Fc)-dependent effector functions using mAbs against preS1 domains (Li et al. 2017). Still, application of mAbs might be ineffective as data suggests that circulating HBsAg can act as decoy reducing antibody titers and their ability to target and neutralize virions or infected cells (Seeger et al. 2007).

1.1.9. RNA interference

As mentioned above current treatment options do not target translation from viral transcripts. Since the HBV genome is relatively small and harbors four overlapping ORFs, its transcripts have a common 3’ end, allowing to simultaneously target all viral messenger (m)RNAs (Gish et al. 2015, Michler et al. 2016). This makes it an interesting target for RNA interference (RNAi), a method which uses small interfering RNAs (siRNA) complementary to target sequences. After complementary binding of siRNAs, mRNAs are degraded by RNA-induced silencing complex (RISC).

Introduction of RNAi system into target cells can be performed either by viral vectors encoding for short hairpin (sh)RNAs which are processed intracellularly by Dicer protein or using direct transfection of siRNA (Fischer 2015, Gish et al. 2015).

Michler *et al.* demonstrated that application of shRNA against HBV using adeno-associated vectors (AAV) for delivery significantly reduces expression of viral proteins and viral load *in vitro* and *in vivo* (Michler et al. 2016, Michler et al. 2020). Therefore, RNAi is another promising tool to target chronic HBV infection but still has to overcome some challenges, one being the delivery and the other being the overexpression of shRNA can lead to activation of innate immunity and inflammatory responses (Hornung et al. 2005, Judge et al. 2006). Further, RNAi targeting is limited to viral transcripts but has no effect on cccDNA.

1.1.10. Therapeutic vaccination

Therapeutic vaccination is aiming to overcome immune-tolerance of HBV in the liver by reactivation of HBV-specific B and T cell responses. Different vaccine therapies against chronic HBV have been evaluated in clinical trials, e.g. Theravax (DV-601) (S, core protein, iscomatrix adjuvant + ETV) or ABX203 (S, core protein + NUCs) (Spellman et al. 2011, Al Mahtab et al. 2018). A novel approach was established by Backes *et al.* using HBsAg/HBcAg-protein prime followed by Modified-Vaccinia-Virus-Ankara (MVA-HBcore and MVA-HBs) boost called TherVacB (Backes et al. 2016). Administration of this vaccination scheme into HBV transgenic mice resulted in activation of neutralizing antibodies, a polyclonal $CD8^+$ T cell response against HBV core and S antigens and induced potent $CD4^+$ T cell responses. Further studies in this direction were performed to improve the vaccination efficiency like additional CpG treatment or siRNA treatment against HBV to reduce viral load before starting therapeutic vaccination (Kosinska et al. 2019, Michler et al. 2020). Based on these promising results TherVacB is currently transferred to clinical phase I trials to further validate functionality in humans.

1.1.11. CRISPR/Cas9

Besides reactivation of anti-HBV immunity and reduction of viral load, targeting the viral persistence form cccDNA is another option to cure chronic infection. Therefore, different endonucleases can be applied like transcription activator-like effector nuclease (TALENs), zinc-finger nucleases (ZFNs) or CRISPR (clustered regularly interspaced short palindromic repeats)–Cas (CRISPR-associated genes) (Chandrasegaran et al. 2016). Especially, CRISPR/Cas9 has become a suitable tool for such applications as targeting is determined by single guide (sg)RNAs which can be easily designed using different online tools. In contrast targeting by TALENs and ZNF is dependent on the protein structure of the respective protein, which is accomplished by demanding protein engineering. This requires profound knowledge and technology, which impede broad and easy application (Eid et al. 2016). Nevertheless, different studies using TALENS, ZNF or and CRISPR/Cas9 showed that targeting of HBV sequences can lead to significant reduction of viral parameters *in vitro* and *in vivo* (Cradick et al. 2010, Bloom et al. 2013, Seeger et al. 2014, Li et al. 2018).

Since in this study CRISPR/Cas9 is used to target HBV sequences, the following chapters are focusing on CRISPR origin, classification and molecular biology.

1.2. CRISPR

1.2.1. Innate and adaptive prokaryotic immunity

Eukaryotic cells have established multiple defense strategies against foreign invaders like bacteria or viruses. Prokaryotes (bacteria and archaea) also have various defense mechanisms to deal with viruses which are subdivided by their principles of action in three groups: (a) resistance (b) immunity and (c) dormancy (Makarova et al. 2012). Resistance is based on change or physical masking of receptors responsible for virus binding, whereas dormancy consists of a diverse antitoxin (TA) system which tends to hinder virus reproduction (Labrie et al. 2010). The immune system can be naturally divided into the nonspecific innate immunity and the highly specific adaptive immunity. Both depend on the ability to distinguish between genomes of invaders (non-self) from the host (self) genome. Different forms of innate immunity are well described like restriction-modification (RM) modules which label self genomic DNA with methyl-groups and cleave unmodified non-self DNA. Another mechanism is DNA phosphorothioation (DND system) which labels DNA by adding phosphorothioation instead of methyl-groups (Kovall et al. 1999, Eckstein 2007). Two additional systems: bacteriophage exclusion (variation of RM theme) and prokaryotic Argonaute proteins (Arg) were newly discovered (Swarts et al. 2014, Barrangou et al. 2015).

In contrast to innate immunity where targeting of non-self invaders is not directed, the adaptive defense system CRISPR is highly specific (Jansen et al. 2002). This system was first described by Ishino *et al.* 1987 in *Escherichia coli* strain K12 and later in other bacterial species like *Streptococcus pyogenes* (Ishino et al. 1987, Hoe et al. 1999). It is characterized by a cluster of short sequence repeats (SSR) (specific for each bacterial species) interspaced by sequences of foreign origin e.g. bacteriophages or exogenous plasmids (van Belkum et al. 1998, Barrangou 2013).

The system can be found in all archaeal strains, but only in 30 – 40% of bacteria species. Probably this is based on the temperature dependency of CRISPR system reflected by ubiquitous distribution in hypothermophiles but only in one-third of mesophiles (Makarova et al. 2011). To this date many different CRISPR systems were described form various bacterial strains, which differ in functionality and targeting.

1.2.2. CRISPR/Cas9 classification

The CRISPR system can be divided in two main classes which differ in their composition and complexity of the effectors modules. Class 1 consists of a complex of various effector proteins, whereas Class 2 harbors a single, large protein like Cas9, Cas12 or Cas13, which is functionally analogous to the Class 1 effector complex (Fig. 6a). The effector proteins of each Class can be subdivided into four distinct, partially overlapping, functional modules (Fig. 6b) (Makarova et al. 2013, Makarova et al. 2015).

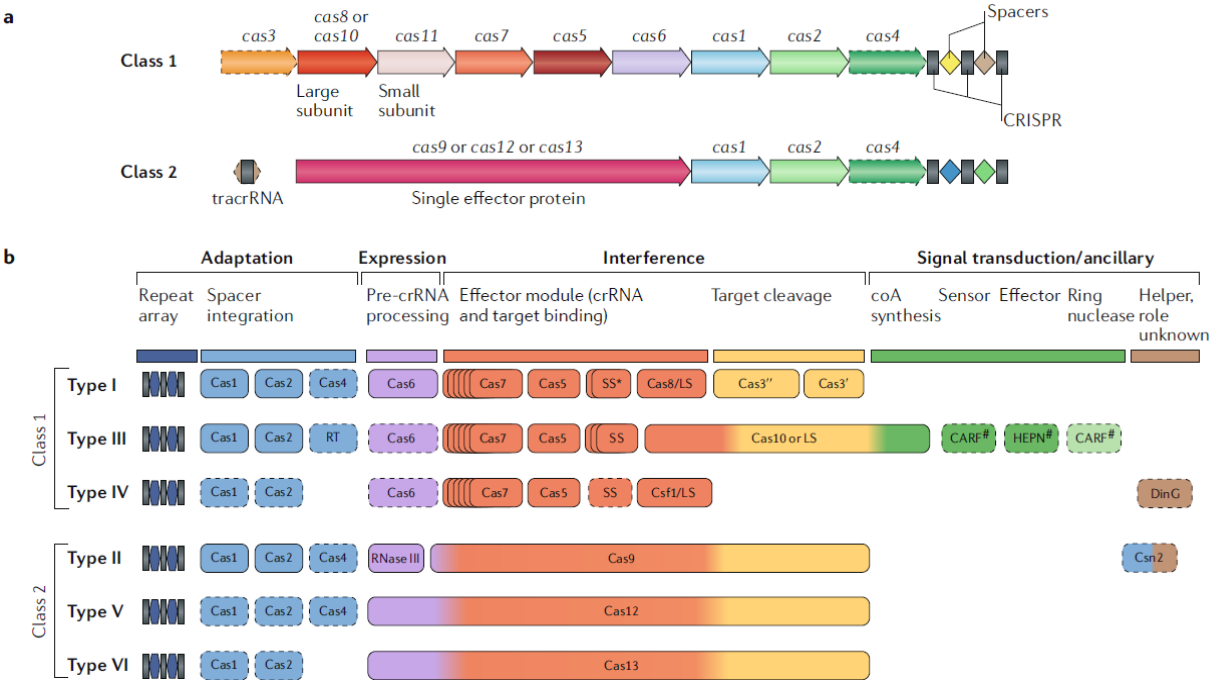

Figure 6: Schematic representation of CRISPR system. (a) Genome organisation of Class 1 and Class 2 system encoding for CRISRP associated proteins. (b) Subdivision of Class 1 and 2 CRISPR proteins in four modules: adaption, expression, interference and signal transduction/ancillary (Makarova et al. 2020).

The adaption module encodes for the Cas1 integrase, which is involved in spacer insertion, Cas2, the structural subunit of the adaption complex, Cas4 nuclease important for some subtypes, Csn2 (Subtype II-A) and reverse transcriptase (RT in type III system). The expression pre-CRISPR RNA (pre-crRNA) processing module is encoding for Cas6 enzyme for most Class 1 systems. In Class 2 the processing step is performed either by bacterial RNase III (type II) or by the large Cas protein (type V and VI) which harbors a distinct catalytic centre able to perform processing. The interference module is encoding for proteins involved in target recognition and cleavage.

As mentioned already in Class I system multiple effector proteins are involved in this step, namely Cas3 (sometimes fused to Cas2), Cas5-Cas8, Cas19 and Cas11 which are combined differently depending on subtype. In Class II the effector module is encoding for a single, large protein (Cas9, Cas12 or Cas13) which combines crRNA/target binding and target cleavage function (Makarova et al. 2020). The last module, signal transduction/ancillary, consists of genes linked to CRISPR system but with mostly unknown function. The only exception is type III where an essential signal transduction pathway was identified which involves activation of Csm6 (or Csx1) and higher eukaryotes and prokaryotes nucleotide-binding (HEPN) RNAse by cyclic oligoA binding to the CRISPR-associated Rossmann fold (CARF) domain of Csm6. The binding initiates non-specific RNA degradation by Csm6 which prevents phage infection and propagation (Kazlauskiene et al. 2017).

1.2.3. Biotechnology application of CRISPR class II system

Since the interference or effector module of CRISPR Class II consists of a single large protein incorporating all essential functions, it was possible to use the system for biotechnological applications. Currently, the most frequently used CRISPR systems originate from *Streptococcus pyogenes* (Sp), *Staphylococcus aureus* (Sa) (both type II), *Lachnospiraceae bacterium ND2006* (Lb), *Acidaminococcous sp.* (As) (both type V) and *Leptotrichia shahii* (Ls) (type VI). Whereas, Cas9 (Sp and Sa) and Cas12a (Lb/As) are targeting DNA structures, Cas13 (Ls) can be applied to target RNA sequences (Cong et al. 2013, Ran et al. 2015, Zetsche et al. 2015, Cox et al. 2017). As this study focuses on targeting HBV DNA the following chapters are explaining the characteristics of type II and V CRISPR systems, including the involved components.

1.2.3.1. The effector proteins: Cas9 and Cas12a

Different important factors are involved in the CRISPR system: effector protein (Cas9 or Cas12a, respectively), crRNA, transencoded crRNA (tracrRNA, only type II) and protospacer adjacent motif (PAM). Type II effector protein Cas9 of *Streptococcus pyogenes* harbors two distinct lobes responsible for recognition (REC) and nuclease activity (NUC). The REC lobe consists of a long alpha-helix (Bridge Helix),

REC1 and REC2 domain. It was shown that REC1 and Bridge Helix domains are important for different recognition steps during guide and target heteroduplexing: recognition of repeat:anti-repeat duplex of crRNA:tracrRNA interaction in a species-specific manner (REC1) and recognition of the backbone phosphate in the PAM-proximal 8-nt “seed” region (Bridge Helix). REC2 was described to be not involved in recognition (Nishimasu et al. 2014). The NUC lobe is encoding for the PAM-interacting (PI) domain recognizing the PAM structure on the non-complementary strand which is essential for DNA cleavage. The PAM motif is specific for each bacterial strain and consists of different nucleotide sequences, for type II: SpCas9 (5’-NGG-3’ or 5’-NGA-3’), SaCas9 (5’-NNGRRT-3’) (Nishimasu et al. 2015).

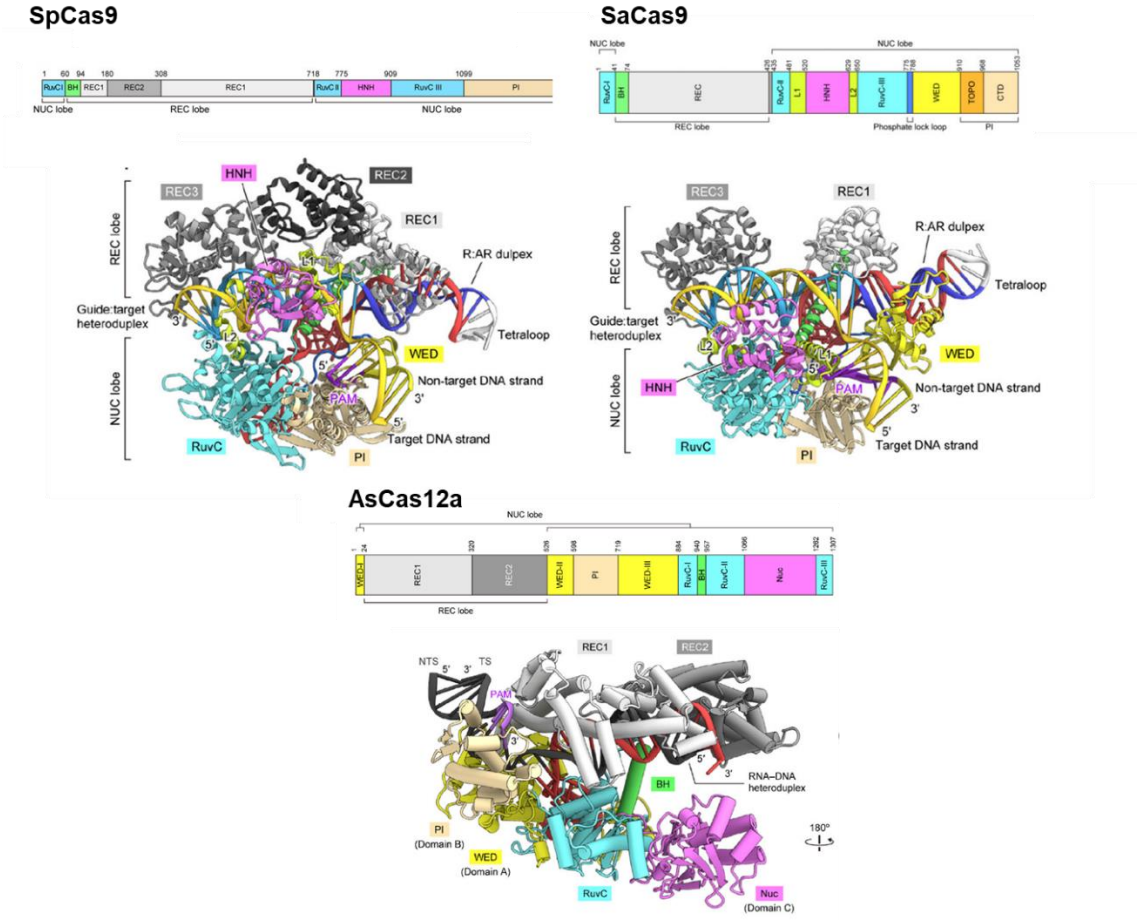

Figure 7: Genome organisation and crystal structure of Class 2 type II (SpCas9 and SaCas9) and V (AsCas12a) effector proteins. Modified from (Nishimasu et al. 2014, Nishimasu et al. 2015).

Within the NUC lobe both endonuclease domains RuvC and HNH are located. Sequence comparison revealed that type II Cas9 proteins share high similarity with IscB, a distinct family of TnpB homologs, which encode for nucleases associated with RuvC-like family of RNase H fold nucleases (Koonin et al. 2017). The RuvC domain was identified to cleave the non-complementary DNA strand by a two-metal mechanism whereas HNH domain cleaves the complementary strand using a single-metal mechanism (Gasiunas et al. 2012, Chen et al. 2013, Jinek et al. 2013). The structure described here is unique for SpCas9, as different type II effector proteins (e.g. SaCas9) have different organization (Fig. 7, top). Compared to type II SpCas9, type V Cas12a effector protein shows sequence and structural divergence (Fig.7, bottom). In contrast to Cas9, Cas12a harbors only one RuvC-like nuclease domain which cleaves both strands. Additionally, Cas12a recognizes a T-rich PAM motif (5'-TTTV-3') (Strecker et al. 2019, Swarts et al. 2019). For biotechnology applications the sequences of respective effector proteins were human codon optimized to enhance protein expression (Gustafsson et al. 2004). To allow transport of Cas9/Cas12a into the nucleus, two nuclear localization signals (NLS): 3' SV40 T-Antigen and 5' Nucleoplasmin were incorporated to enhance cleavage efficiency (Cong et al. 2013).

1.2.3.2. Guide RNAs for CRISPR

As mentioned above CRISPR targeting is depending on the interaction of effector proteins with guide (g)RNAs. For type II systems these gRNAs are consisting of two separate RNAs: crRNA and tracrRNA (Fig. 8, left).

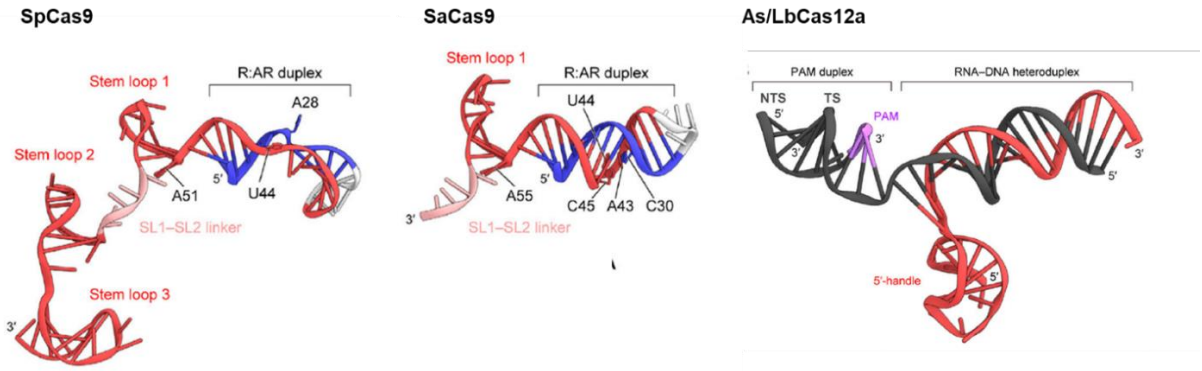

Figure 8: Crystal structure of CRISPR Class 2 type II (SpCas9 and SaCas9) and type V (AsLbCas12a and LbCas12a) guide RNAs. Modified from (Hirano et al. 2016, Yamano et al. 2016).

Pre-crRNA is processed by bacterial RNAse III to 42 nucleotide (nt) full-length mature crRNA which is subdivided in a 5' 20 nt spacer and 22 nt repeat unit. The spacer unit is important for DNA targeting and represents the sequence upstream of a PAM motif at the target site.

Studies of crRNA sequence demonstrated that 5' deletion of up to 3 nt reduces off-target events but 3' deletions within the "seed region" (nucleotides 9-20) diminished functionality (Semenova et al. 2011, Wiedenheft et al. 2011, Jinek et al. 2012, Fu et al. 2014). The repeat unit acts as linker between crRNA and tracrRNA, which is essential for efficient cleavage. The second part of gRNA, the 89 nt long tracrRNA consists of two subunits: anti-repeat (24 nt 5') which is binding to the repeat unit of crRNA and a 65 nt long sequence forming three stem-loop secondary structures. Deletion of 3' stem loops 2 and 3 was described to significantly reduce cleavage efficiency is indicative for their function in Cas9 protein interaction (Mekler et al. 2016). For biotechnological applications the two RNAs were fused to form a single guide RNA (sgRNA) which was shown to further enhance genome editing efficiency (Jinek et al. 2012).

In contrast to type II sgRNAs, processing of type V crRNA molecules is driven directly by the effector protein Cas12a. For targeting and interaction with Cas12a no additional tracrRNA is needed, as type V crRNA (Fig. 8, right) structurally differs from the type II variant. It consists of a 24 nt guide sequence essential for targeting and a 19 nt scaffold sequence which reveals a pseudoknot structure and interacts with Cas12a (Yamano et al. 2016).

1.2.4. Genome editing and cellular repair pathways

Several steps are involved in CRISPR to achieve genome editing. First, apo-Cas9 (inactive) protein interacts with sgRNA forming a "pre-target" state complex which is internalized into the nucleus. After recognition of the respective PAM sequence and initial binding of crRNA ("seed nucleation"), fully-active state is achieved through binding of whole crRNA sequence (Jiang et al. 2015). In this state both DNA strands of target sequence are cleaved 3 bp 5' of PAM by RuvC (non-complementary) and HNH (complementary) endonuclease domains forming a double-strand break (DSB) producing blunt ends. In contrast cleavage by Cas12a effector proteins lead to DSB 19/24 bp 3' of PAM in a staggering fashion leading to 5' overhangs (Jinek et al. 2012, Yamano et al. 2016).

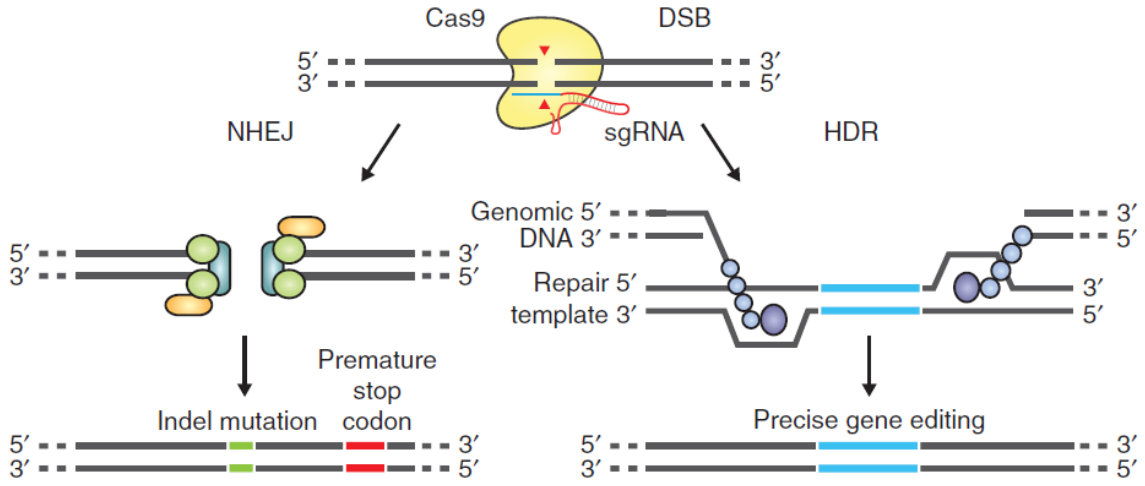

Figure 9: Cellular repair mechanism. CRISPR/Cas9 induced double strand breaks (DSB) can be repaired by non-homologues end-joining (NHEJ) or homology-direct repair (HDR). NHEJ repair can lead to insertion or deletion (InDel) mutations and premature stop codon formation. HDR lead to precise repair using sister allel sequence or introduced templates. (Ran et al. 2013)

DSB introduced by CRISPR can be repaired by two cellular repair mechanisms (Fig. 9): non-homologous end joining (NHEJ) or by homology-directed repair (HDR). NHEJ is an error-prone mechanism adding random DNA fragments to both DSB ends which are subsequently linked by endogenous repair machinery (Moore et al. 1996). Most Cas9-induced DSB are repaired by NHEJ and since no repair template is applied, small nucleotide insertions or deletions (InDels) can lead to frameshift mutations (Waters et al. 2014). Those characteristics are beneficial to acquire knockouts of certain genes, as InDels often result in premature stop codons. In contrast, HDR is more precise than NHEJ since it requires a DNA template for the repair e.g. from sister chromatid during S- or G_2-phase of cell cycle (Liu et al. 2018). HDR is frequently used to introduce certain sequences into Cas9-induced DSB by simultaneous delivery of DNA templates harboring homologous and desired sequences. These knock-in approaches were demonstrated to have low frequency of positive populations (Lino et al. 2018). Li *et al.* indicated that three kinds of entities coexist after application of Cas9: wild-type sequences, NHEJ-repaired sequences and a smaller quantity of HDR-repaired sequences (Li et al. 2014).

1.2.5. Delivery of CRISPR system

For delivery of CRISPR systems, different vehicles can be used which are subdivided into three general groups: physical delivery, viral vectors and non-viral vectors. For physical delivery microinjection and electroporation are most frequently used, whereas hydrodynamic delivery is currently under investigation (Yang et al. 2013, Yin et al. 2014, Paquet et al. 2016). Different viral vectors can be applied for CRISPR delivery, e.g. adenoviral (AdV), AAV or lentiviral (LV) based systems. Many groups are currently using AdV or LV vectors to deliver CRISPR/Cas9 as both systems offer enough packaging capacity for different Cas9 constructs and several sgRNAs (Heckl et al. 2014, Kabadi et al. 2014, Maddalo et al. 2014, Roehm et al. 2016, Voets et al. 2017). AAVs in contrast have limited space (~ 4.5 kb), therefore either Cas9 and one sgRNA or two separate AAV constructs are used for delivery. AAV delivery is more beneficial for *in vivo* applications, as it does neither trigger immune responses nor integrate. New applications are using smaller Cas9 variants, like SaCas9 (Bestor 2000, Follenzi et al. 2007, Ahi et al. 2011, Ran et al. 2015). Non-viral delivery vehicles can be based on lipid nanoparticles/liposomes or lipoplexes/polyplexes which are used to transport nucleic acids. Thereby, Cas9 and sgRNAs can be delivered as plasmid DNA (pDNA) or RNP complex (Zuris et al. 2015, Wang et al. 2016). It was demonstrated that application of CRISPR by lipid nanoparticles, like lipofectamine, can be highly efficient *in vitro* and *in vivo* (Schwank et al. 2013, Liang et al. 2015, Zuris et al. 2015). Also, delivery of CRISPR pDNA using FuGENE-6, a non-liposomal formulation, was shown to be highly efficient resulting in inactivation of target genes (Kennedy et al. 2014).

Another very promising way to introduce CRISPR/Cas9 or other proteins of interest into target cells is to use non-viral delivery of *in vitro* transcribed (IVT) mRNA. As the aim of this study was to apply IVT mRNAs for different applications, the following chapters are focusing on IVT mRNAs based on structural features, applications and their advantages over other methods.

1.3. *In vitro* transcribed mRNA

mRNA is encoding for different genes and serves as template for protein synthesis. It is built up of four ribonucleoside bases: adenosine (A), guanosine (G), cytidine (C) and uridine (U) which are linked via a phosphate group. In the 1970s first experiments were performed using IVT mRNAs encoding for poliovirus-specific RNA in HeLa cells and rabbit globin mRNA *in vivo* (Koch 1973, Dimitriadis 1978). These experiments proved that IVT mRNA can serve as promising tool for different applications. Unfortunately, high instability (half life ~ 7h) and activation of innate immunogenicity by mRNA constructs rendered this approach unsuitable at this point of time (Diebold et al. 2004, Heil et al. 2004, Loo et al. 2011).

1.3.1. Structural elements of IVT mRNA

The mRNA sequence can be subdivided in five distinct domains: 5' cap, 5' untranslated region (5' UTR), coding sequences or open reading frame (CDS, ORF), 3' UTR and 3' poly(A) tail (Fig. 10).

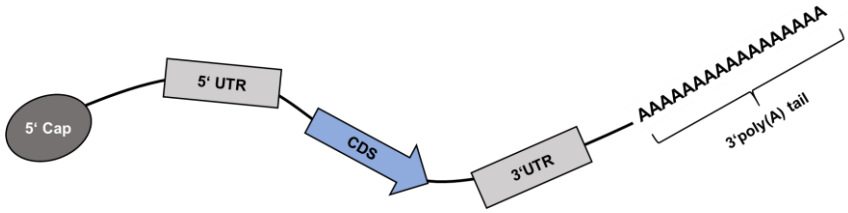

Figure 10: Schematic representation of mRNA structure. mRNA consists of 5' Cap structure, 5' untranslated region (UTR), coding sequence (CDS), 3' untranslated region (UTR) and 3' poly(A) tail.

The 5' cap protects the mRNA from degradation by exonucleases and is important for binding of initiation factor 4E, a key factor during translation (Ramanathan et al. 2016). The poly(A) tail, consisting of 50–250 adenosine residues, is involved in nuclear export, recruitment of translation initiation factors and improvement of stability and half life by protecting mRNA from nuclease degradation (Jalkanen et al. 2014, Patel et al. 2019).

The 5’ UTR plays an important role in mRNA translation through interaction with translation machinery, whereas 3’ UTR interacts with microRNA (miRNA) or decay-promoting proteins, which have an influence on mRNA stability (Barrett et al. 2012). The CDS or ORF is encoding for the gene of interest, harboring 5’ start and 3’ stop codons.

1.3.2. Improvements of IVT mRNA

To improve translational activity of introduced IVT mRNA, it was shown that codon optimization is essential to increase expression of encoded protein (Kariko et al. 2012). In the context of Cas9 mRNA it was also described that uridine depletion in ORF sequence further enhance protein expression and lead to improved genome editing (Vaidyanathan et al. 2018). Additionally, incorporation of certain UTR elements can either enhance protein expression (e.g. 5’ Kozak UTR) or improve mRNA stability (3’ ß-globin UTR) (Kozak 1987, Holtkamp et al. 2006). Further, during the last years significant improvements were made through addition of cap-analogs or chemical modifications to mRNA synthesis procedure.

1.3.2.1. Introduction of alternative cap analogs

In eukaryotic cells all mRNAs harbor a 7-methylguanosine (m7GpppG) standard cap (also referred as Cap 0) which are also used for *in vitro* transcription (Vaidyanathan et al. 2018). Since these standard caps may be incorporated in reverse orientation due to one additional transcription initiation site, currently synthesized mRNA is using anti-reverse cap analogs (ARCA, Fig. 11). IVT with such alternative caps lead to increased yield of correct-capped mRNAs enhancing translational efficiency (Pasquinelli et al. 1995, Jemielity et al. 2003, Grudzien-Nogalska et al. 2007). Further improvements of cap structures implementing Cap 1 ($^{m7}GpppN_{2'Om}N$) or Cap 2 ($^{m7}GpppN_{2'Om}N_{2'Om}$) which are described as less immunogenic are currently ongoing (Furuichi et al. 2000, Zust et al. 2011, Devarkar et al. 2016). Vaidyanathan *et al.* established a co-transcriptional capping strategy called CleanCap which allows production of Cap 1 IVT mRNAs with enhanced IVT capping efficiency and protein expression (Vaidyanathan et al. 2018).

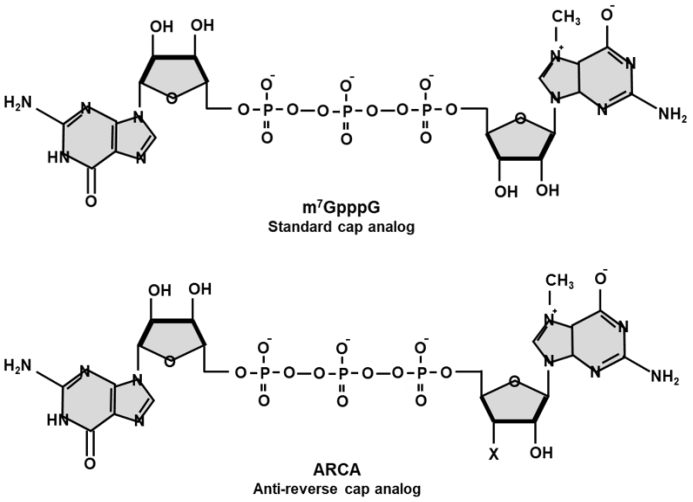

Figure 11: Graphic representation of Cap structures. Standard cap analog (m7GpppG, top) and anti-reverse cap analog (ARCA, bottom). Substitution of the 3'-OH of the m7 guanine moiety by 3'-O-methyl group (X) in ARCA lead to incorporation of correct orientated cap and higher yield of functional mRNA.

1.3.2.2. Introduction of modified nucleotides

Incorporation of modified nucleotides like Pseudo-UTP (Ψ-UTP), 5-Methoxy-UTP (5moUTP), N^1-Methylpseudo-UTP (me^1Ψ-UTP) or 5-Methyl-CTP (m^5CTP) was described to reduce innate immune responses and improve mRNA activity (Fig. 12). Incorporation of m^5CTP and Ψ-UTP in first generation mRNAs showed limited TLR signaling, reduction of 2'-5'-oligoadenylate synthetase and PKR (Kariko et al. 2005, Anderson et al. 2010, Anderson et al. 2011). Further, it was demonstrated that Ψ-UTP, me^1Ψ-UTP and m^5CTP modified mRNAs have high binding affinity to RIG-I but fail to activate downstream signalling (Durbin et al. 2016). So far different combinations were used *in vitro* and *in vivo* revealing improved characteristics compared to unmodified mRNAs (Warren et al. 2010, Zangi et al. 2013, Pardi et al. 2015). Thereby, it is important to mention that optimized combinations have to be adjusted according to each experimental setup (e.g. cell line, encoded gene).

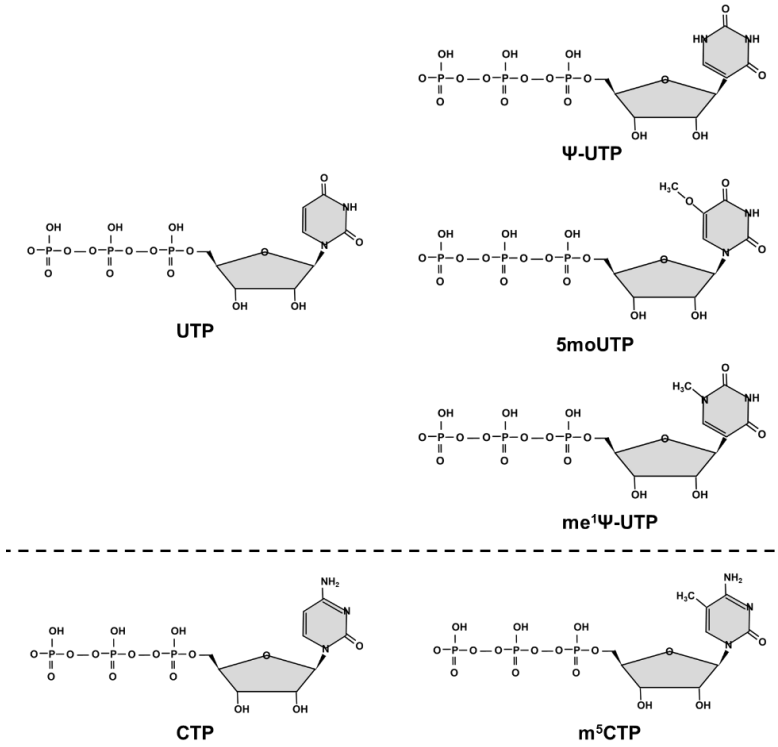

Figure 12: Structure of nucleotide analogs. UTP analogs: Pseudo-UTP (Ψ-UTP), 5-Methoxy-UTP (5moUTP), N^1-Methylpseudo-UTP ($me^1Ψ$-UTP). CTP analog: 5-Methyl-CTP (m^5CTP).

1.3.3. Advantages of IVT mRNA for gene therapy approaches

As mentioned already, most gene therapy applications are using viral vectors or pDNA systems to introduce their genes of interest into target cells. Production of pDNA in high yields is cost-effective but transfection efficiency *in vitro* and *in vivo* is very low (Rettig et al. 2010). In contrast to pDNA viral vectors like AAVs, AdVs or LVs show high transduction efficiency and high protein expression, but production is work and cost intensive. Further, induction of immune responses (AdVs and LVs), risk of integrational mutagenesis (LVs) and long-term expression of genome-modifying proteins (e.g. CRISPR/Cas9) lead to significant safety concerns towards viral vectors and impede broad clinical translation (Mallon et al. 2014, Steichen et al. 2014). Therefore, application of IVT mRNA offers many advantages: transient expression, reduction of off-targeting, low immunogenicity and no risk of insertion. Nevertheless, production of IVT in high yields remains cost intensive, in the future further improvements concerning enhanced production might be beneficial (Steinle et al. 2017). Though, IVT mRNA offers multiple advantages over current viral and non-viral vectors and is a promising tool for basic and translational science.

2. Aim of the study

Since the full viral life cycle of HBV is still elusive and until now no treatment, targeting its persistence form cccDNA is available, the following study addressed these issues.

The first aim was to establish the IVT mRNA method to investigate different aspects related to HBV infection: the introduction of factors involved in viral life cycle and CRISPR/Cas9 genome editing against HBV DNA.

Therefore, we first aimed to improve IVT mRNA functionality concerning cell viability, transfection efficiency and protein expression by implementation of different modifications (Cap structures and nucleoside analogous) and to compare those modified mRNAs in our non-dividing cell culture systems.

After optimization, we wanted to apply the optimized IVT mRNA investigating the viral life cycle or anti-HBV treatment. To decipher details of viral uptake, we used IVT mRNAs encoding for Caveolin-I and NTCP proteins which are both described as important factors but are missing in certain cell lines prohibiting to investigate their specific role in certain steps of HBV infection.

In a next step, IVT mRNA should be used for the establishment of an mRNA based CRISPR/Cas9 system to investigate targeting efficiency against different types of HBV DNAs (cccDNA, integrated and episomal). We aimed to use SpCas9 IVT mRNA and modified sgRNAs targeting HBV sequences in different HBV related cell lines to analyze distinct parameters indicating for HBV replication, as well as genome editing efficiency after treatment. To compare this transient expressed system, we planned to implement an AAV based CRISPR/Cas9 application to investigate long-term effects.

The second aim of the study was to establish a combinatorial AAV based system using CRISPR/Cas9 and RNAi method to target chronic HBV infection. In cooperation with Carolin Schmelas (University Heidelberg) we wanted to improve the system and to analyze its functionality *in vitro* in different cell lines. For further optimization we were aiming to implement the findings of our IVT mRNA CRISPR/Cas9 analysis into the combinatorial system to enhance efficiency in future *in vivo* applications.

3. Results

3.1. Optimization of IVT mRNA for CRISPR/Cas9 application

3.1.1. ARCA cap increased protein expression and transfection efficiency

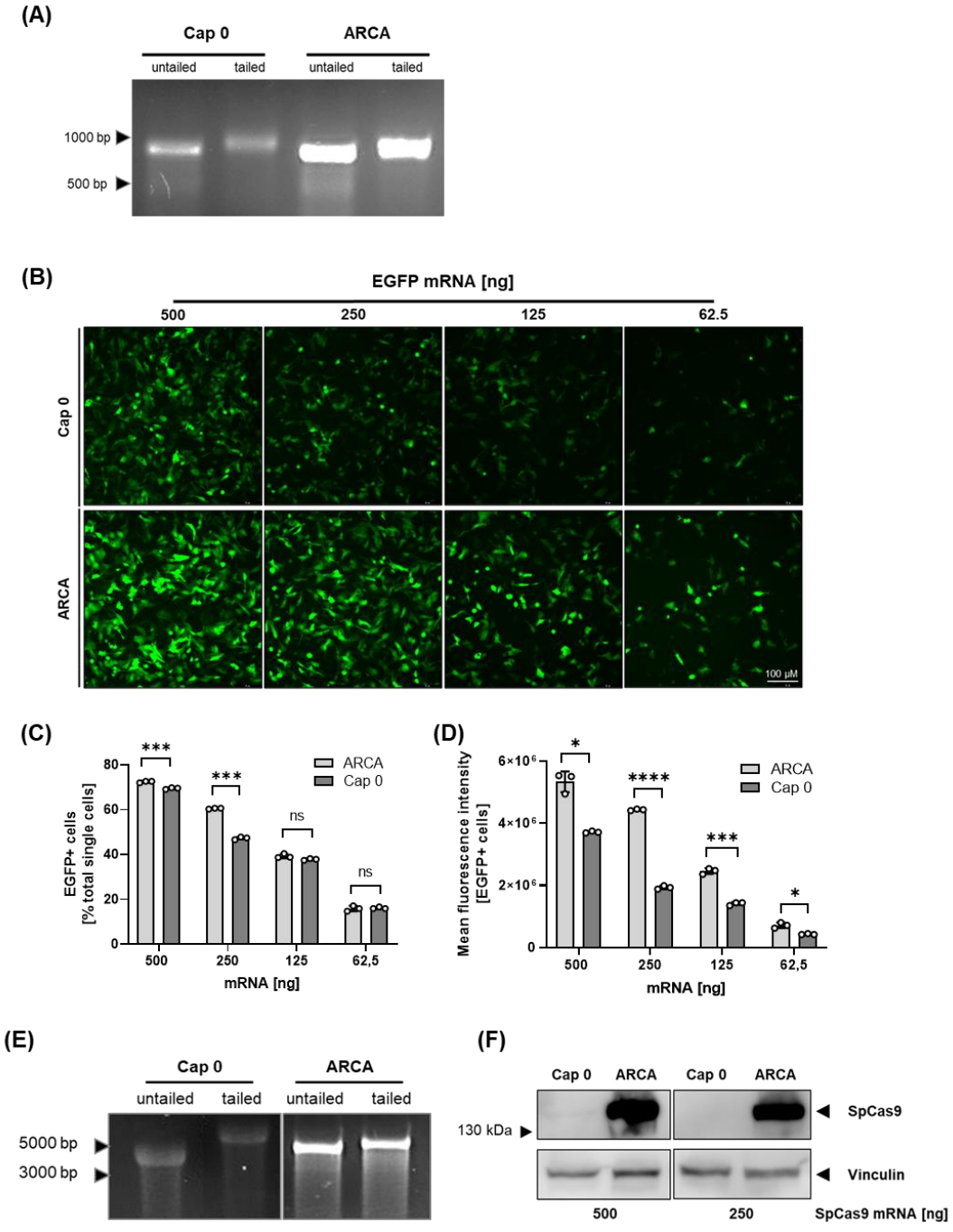

Figure 13: Comparison of protein expression between Cap 0 and ARCA. (A) Analysis of production of tailed and untailed Cap 0 and ARCA capped EGFP IVT mRNA on 2% agarose gel. (B) Fluorescence images of differentiated HepG2 cells 24 h post transfection with 2-fold titration of Cap 0 or ARCA capped EGFP IVT mRNA (500–62.5 ng). ►

◄ (C) Flow cytometry analysis of EGFP$^+$ HepG2 cells 24 h post transfection with 2-fold titrated EGFP IVT mRNA and calculation of mean fluorescence intensity (MFI, D) of EGFP$^+$ cells. (E) Analysis of Cap 0 or ARCA capped SpCas9 IVT mRNA. (F) Western Blot analysis of SpCas9 protein expression in differentiated HepG2 cells 24 h post transfection with 500 ng and 250 ng of SpCas9 IVT mRNA. Statistical significance was determined using unpaired Students *t*-test with Welsh's correction. (*: $p < 0.05$; **: $p < 0.01$; ***: $p < 0.001$; ****: $p < 0.0001$).

For the establishment of highly functional IVT mRNA different optimization steps, like using alternative cap structures, nucleotide modifications or UTR elements, can be applied to improve cell viability by reducing activation of innate immunity, protein expression and stability. To improve our IVT mRNA we first analyzed two different cap analogs: m7GpppG (standard cap analog, Cap 0) and ARCA (anti-reverse cap analog, Cap 0). The difference between these two variants is based on a substitution of the 3-OH of the m7guanine moiety by 3'-O-methyl group in ARCA cap leading to incorporation of cap exclusively in correct orientation. To compare these cap variants, we produced Cap 0 and ARCA capped IVT mRNA encoding enhanced green fluorescent protein (EGFP). Analysis on 2% agarose gel (Fig.13 A) showed produced untailed and tailed mRNAs of both approaches. To validate EGFP expression we transfected a 2-fold titration of IVT mRNA starting from 500 ng per well in differentiated HepG2 cells. 24 h post transfection we monitored EGFP expression using fluorescence microscopy (Fig. 13 B) which revealed titration dependent expression of EGFP with higher signal intensity using ARCA capped mRNA. To determine transfection efficiency and quantify protein expression we performed flow cytometry analysis for IVT mRNA EGFP transfected cells. Results (Fig. 13 C) showed dose-dependent transfection efficiency which was significantly increased using high IVT mRNA amounts of 500 ng and 250 ng with ARCA capped variants. Calculation of mean fluorescent intensity (MFI, Fig. 13 D) revealed significantly increased EGFP expression in cells transfected with ARCA capped mRNA in all tested amounts. To validate these results with another protein, we produced IVT mRNA encoding for *Streptococcus pyogenes* Cas9 (SpCas9) capped with both analogs. Again, analysis of produced mRNA on 2% agarose gel (Fig. 13 E) demonstrated production of both constructs as well as successful tailing. To determine SpCas9 expression we transfected differentiated HepG2 cells with 500 ng and 250 ng of both cap variants. 24 h post transfection we isolated protein and performed Western Blot analysis.

Result (Fig. 13 F) showed a strong SpCas9 signal in samples transfected with ARCA capped mRNA for both tested amounts, but only a faint signal when treated with 500 ng Cap 0 capped mRNA. The signal of housekeeping protein Vinculin was comparable between all tested samples.

3.1.2. Low immunogenicity but high genome editing using modified sgRNAs

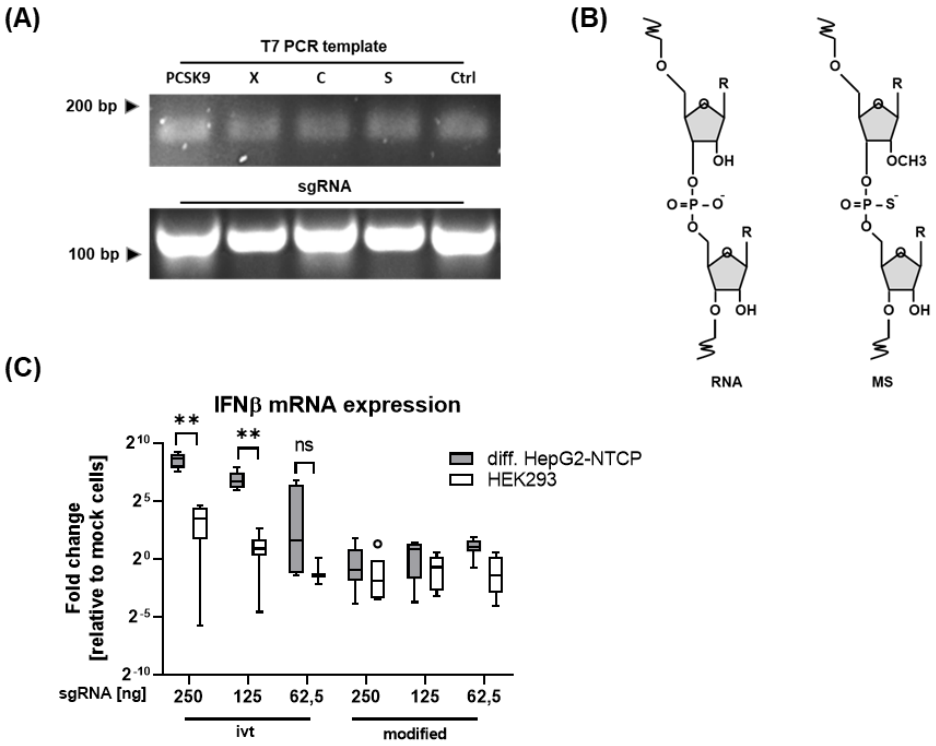

Figure 14: Comparison of IVT sgRNA with modified sgRNAs. (A) Analysis of IVT sgRNA production using 1% agarose gel for PCR template (top) and 2% agarose gel for IVT sgRNA (bottom). (B) Structure of unmodified (left) and 2'-O-methyl 3'phosphorothioate (MS) modified sgRNAs (right). (C) qPCR analysis of IFNβ expression 24 h post transfection of 2-fold titrated IVT sgRNA or modified sgRNA in differentiated HepG2 and HEK293 cells. Statistical significance was determined using unpaired Students *t*-test with Welsh's correction. (*: $p < 0.05$; **: $p < 0.01$; ***: $p < 0.001$; ****: $p < 0.0001$).

Since CRISPR is a two-component system, we also had to identify the most efficient sgRNA variant. Therefore, we first established a protocol to produce T7 IVT derived sgRNAs, which is described in detail in the methods (5.2.4.). We used this protocol to produce templates for different targets like host genes (PCSK9), HBV genes (ORF X, ORF C, ORF S) or nonsense/Ctrl sequences.

Analysis of PCR reaction for all targets on 1% agarose gel (Fig. 14 A, top) showed bands of around 150 bp indicating successful template production. Using these templates for T7 IVT reaction led to production of all sgRNA constructs which were analyzed on 2% agarose gel displayed strong bands at around 100 bp (Fig. 14 B, bottom). To compare functionality with T7 IVT derived sgRNAs we ordered synthesized and stabilized sgRNAs (Merck). In contrast to T7 derived RNA, these sgRNAs lack additional phosphates at 5', which can trigger innate immunity and are harboring a 2'-O-methyl 3'phosphorothioate (MS) modification (Fig. 14 B), demonstrating higher functionality as described previously (Pichlmair et al. 2006, Hendel et al. 2015). To analyze activation of innate immunity by sgRNAs, to exclude negatively affects in the experimental setup, we transfected differentiated HepG2 and HEK293 cells with 2-fold titration of PCSK9 sgRNA. 24 h post transfection we isolated total RNA and performed cDNA synthesis. As described previously transfection of IVT sgRNA can trigger innate immune responses by activation of retinoic acid inducible gene I (RIG-I) signaling (Wienert et al. 2018). To determine activation, we measured expression of Interferon-β (IFNβ), which is regulated via nuclear factor 'kappa-light-chain-enhancer' of activate B-cells (NF-kB) pathway, in our transfected cells using qPCR. As results indicated (Fig. 14 C) activation of innate immunity was triggered by IVT sgRNAs in a dose dependent manner, showing significant activation in HepG2 post transfection of 250 ng or 125 ng sgRNA, respectively. Activation of innate immunity in HEK293 was only observable when transfecting 250 ng sgRNA. In contrast modified sgRNA did not induce IFNβ expression independent of cell line and dosage used.

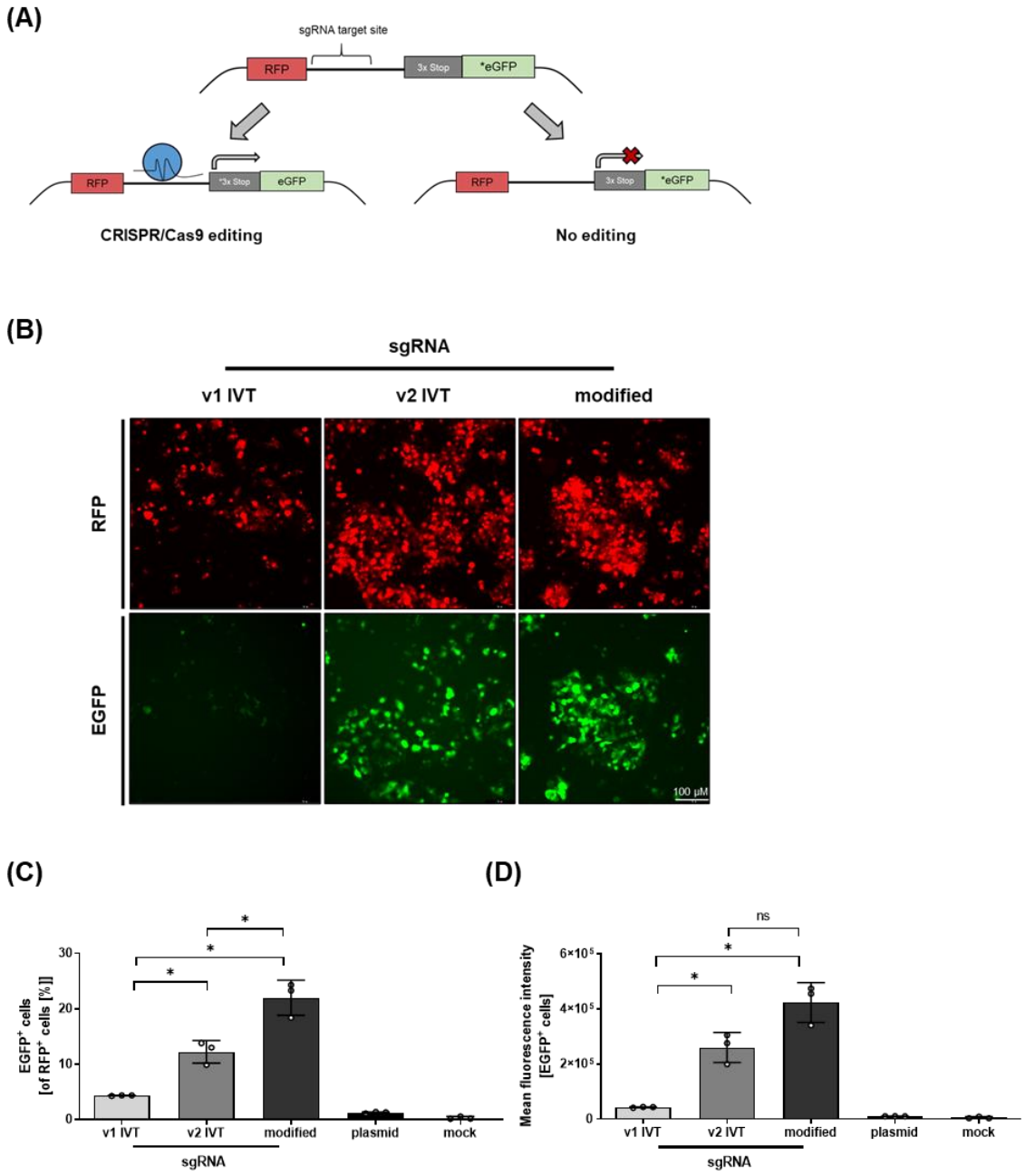

Figure 15: Functional comparison of IVT and modified sgRNAs. (A) Schematic representation of single strand annealing (SSA) assay consisting of RFP (constitutively expressed), sgRNA target site, 3x stop codons and EGFP (out of frame). (B) Fluorescence image of SSA assay comparing v1/v2 IVT with modified sgRNA 5 days post transfection into HEK293. $EGFP^+$ cells indicate CRISPR/Cas9 genome editing. Flow cytometry analysis of (C) $EGFP^+$ cells and (D) calculated MFI of SSA assay 5 days post transfection into HEK293. Statistical significance was determined using unpaired Students *t*-test with Welsh's correction (*: $p < 0.05$; **: $p < 0.01$; ***: $p < 0.001$; ****: $p < 0.0001$).

To further validate and optimize our CRISPR/Cas9 approach we established an easy and fast screening assay, single strand annealing assay (SSA), which was used to detect genome editing after transfection of our constructs. Therefore, we generated a plasmid (pDNA-SSA) harboring a cassette of red fluorescent protein (RFP; in frame), sgRNA target site, 3X stop codons (in frame) and EGFP (out of frame) under control of a human cytomegalovirus (CMV) promotor (Fig. 15 A). Targeting by functional Cas9 protein and correct sgRNA leads to introduction of DSB which can introduce frameshift mutations allowing expression of EGFP, if either or both factors are missing or sgRNA is unspecific no editing occurs. Expression of RFP protein is independent of genome editing and serves as transfection control. As mentioned before, modified sgRNA were described to increase genome editing (Hendel et al. 2015). Therefore, we used our SSA to compare two different IVT sgRNA constructs (v1: with additional 5' GGG; v2: no additional 5' GGG) with our modified sgRNA. For screening, we transfected 250 ng pDNA-SSA in HEK293, which demonstrated better transfection efficiencies with plasmid than HepG2 and no activation of innate immunity after sgRNA transfection. 24 h post introduction of pDNA-SSA we transfected 250 ng of ARCA capped SpCas9 mRNA with 125 ng of each respective sgRNA. Five days post transfection, we analyzed genome editing using fluorescence microscopy to detect $EGFP^+$ cells (Fig. 15 B). Results revealed lowest numbers of positive cells for v1 IVT when compared to v2 IVT or modified sgRNA, respectively. To quantify positive cells and determine signal intensity, we performed flow cytometry analysis of treated samples. As results (Fig. 15 C) indicated transfection of SpCas9 mRNA with modified sgRNAs led to significantly increased numbers of $EGFP^+$ cells in comparison to v1 IVT but not to v2 IVT. Quantification of EGFP expression by calculation of MFI (Fig. 15 D) revealed that transfection with modified sgRNA showed significantly increased levels when compared to IVT variants.

The results indicated that modified sgRNAs demonstrated preferable characteristics, like no activation of innate immunity, efficient genome editing and were therefore used for all further experiments.

3.1.3. Increased genome editing using ARCA capped SpCas9 IVT mRNA

As already shown, ARCA capped mRNA led to higher transfection efficiency and protein expression than Cap 0 capped mRNA in differentiated HepG2. Since we were interested to optimize our CRISPR/Cas9 system, we wanted to achieve optimal experimental conditions in terms of expression as well as high genome editing rates.

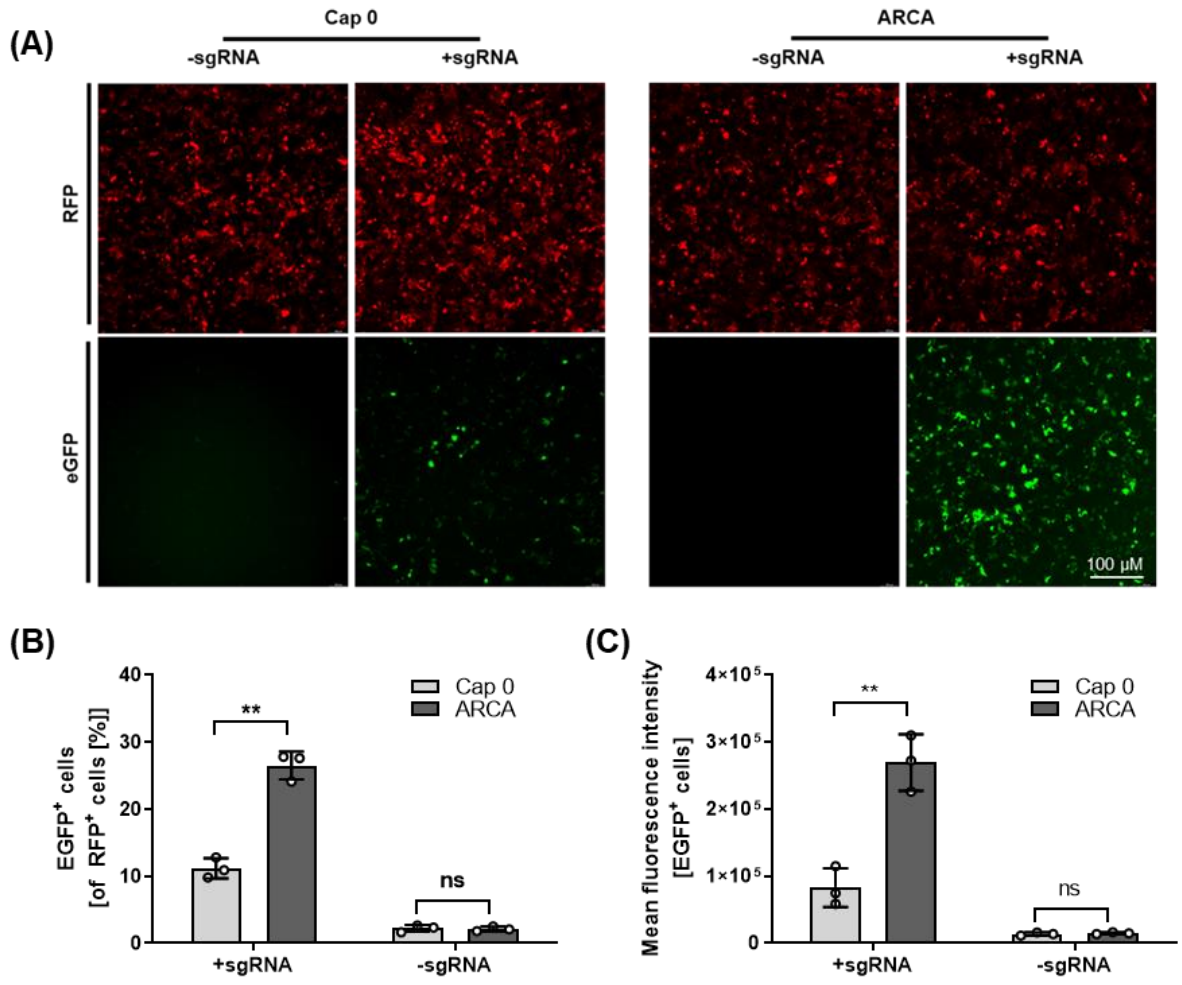

Figure 16: Functional analysis of cap structures. (A) Fluorescence images of SSA assay comparing Cap 0 and ARCA capped SpCas9 IVT mRNA 5 days post transfection in HEK293. EGFP$^+$ cells indicate for CRISPR/Cas9 genome editing. Flow cytometry analysis of (B) EGFP$^+$ cells and (C) calculated MFI for SSA assay 5 days post transfection into HEK293 cells. Statistical significance was determined using unpaired Students *t*-test with Welsh's correction (*: $p < 0.05$; **: $p < 0.01$; ***: $p < 0.001$; ****: $p < 0.0001$).

Therefore, we transfected 250 ng ARCA or 250 ng Cap 0 capped SpCas9 mRNA with 125 ng modified sgRNA and repeated our SSA assay to analyze genome editing efficiency five days post transfection. Fluorescence microscopy of transfected cells (Fig. 16 A) showed increased amounts of $EGFP^+$ cells when using ARCA capped IVT mRNA compared to the standard cap. Determination of $EGFP^+$ cells (Fig. 16 B) using flow cytometry displayed significantly increased numbers using ARCA compared to standard cap. Additionally, calculation of MFI (Fig. 16 C) of $EGFP^+$ cells demonstrated significant higher protein expression when transfecting ARCA capped SpCas9 mRNA.

In summary results indicated that ARCA capped mRNA supports higher protein expression (EGFP and SpCas9) leading to increased genome editing efficiencies in SSA assays than Cap 0. Therefore, in all further experiments ARCA capped mRNA was used.

3.1.4. Improved characteristics with ψ-UTP/m^{5}CTP modified IVT mRNA

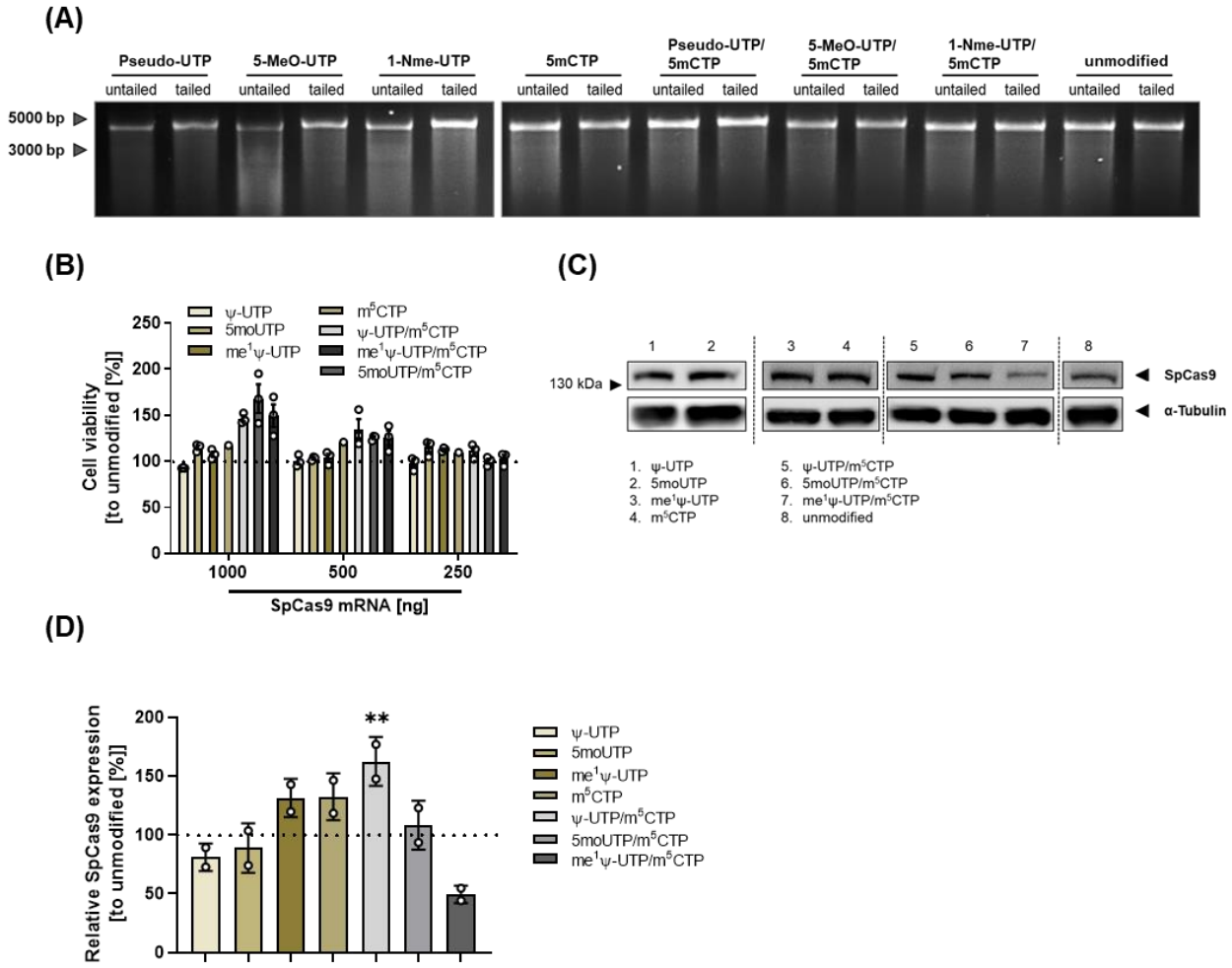

Figure 17: Comparison of nucleotide modifications. (A) Analysis of produced modified untailed and tailed SpCas9 IVT mRNAs using 2% agarose gel. (B) Determination of cell viability 24 h post transfection via CTB assay of 2-fold titrated SpCas9 IVT mRNA modifications in differentiated HepG2 cells. (C) Western Blot analysis of SpCas9 protein expression 24 h post transfection of modified IVT mRNAs into differentiated HepG2 cells. α-tubulin was used as loading control. (D) Relative quantification of SpCas9 protein expression of modified IVT mRNAs to α-tubulin loading control, normalized to unmodified SpCas9 mRNA in differentiated HepG2 cells. Statistical significance was determined with one-way ANOVA (*: $p < 0.05$; **: $p < 0.01$; ***: $p < 0.001$; ****: $p < 0.0001$).

As already mentioned, besides the optimization of 5'cap structures, introduction of nucleotide modifications can further improve IVT mRNAs by improving stability as well as protein expression and by reducing immunogenicity. Several nucleotide modifications are commercially available to exchange all four natural nucleotides.

Here, we used substitutions for UTP (Pseudo-UTP (ψ-UTP), 5-Methoxy-UTP (5moUTP), N^1-Methylpseudo-UTP (me^1ψ-UTP)) and CTP (5-Methyl-CTP (m^5CTP)) which are supplemented to T7 IVT reaction in 1:1 ratios, leading to mRNAs containing 50% natural and 50% analog for each respective nucleotide. To analyze the impact of nucleotide modifications on cell viability, protein expression and functionality in our SSA assay, we first produced single (UTP or CTP analog) and double (UTP and CTP analog) modified IVT mRNAs encoding for SpCas9. Produced mRNAs were analyzed on 2% agarose gel (Fig. 17 A) showing expected bands for untailed and tailed IVT mRNAs of each construct. To determine effects on cell viability we transfected differentiated HepG2 with 1000 ng, 500 ng or 250 ng of each construct. 24 h post transfection we performed CellTiter Blue (CTB) assay and normalized the measurement to cells transfected with unmodified IVT mRNAs. Results (Fig. 17 B) indicated that introduction of two nucleotide modifications highly increase cell viability, especially when using higher amounts (1000 ng and 500 ng) of mRNA for transfection. Implementation of double modifications ψ-UTP/m^5CTP, 5moUTP/m^5CTP and me^1ψ-UTP/m^5CTP demonstrated best cell viability compared to unmodified and single modifications in high dosages, which showed no significant improvement. Transfection of 250 ng IVT mRNA revealed slight differences to unmodified control. To compare SpCas9 protein expression, we transfected differentiated HepG2 with 500 ng of each construct. 24 h post transfection we isolated protein and performed Western Blot analysis which showed specific SpCas9 expression with all tested modifications (Fig. 17 C). Relative quantification of SpCas9 expression to housekeeper α-tubulin (Fig. 17 D) indicated the highest protein levels using ψ-UTP/m^5CTP modifications. In comparison to unmodified control, also me^1ψ-UTP, m^5CTP single modifications and 5moUTP/m^5CTP led to increased protein expression. In contrast decreased expression was observable when using ψ-UTP, 5moUTP single and me^1ψ-UTP/m^5CTP double modification.

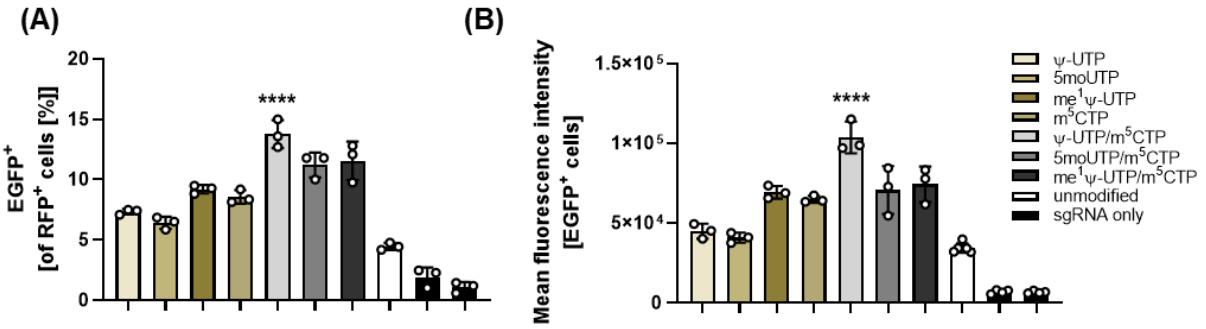

Figure 18: Functionality comparison of nucleotide modification. Flow cytometry analysis of SSA assay 24 h post transfection of 250 ng IVT SpCas9 with respective modification and modified sgRNA into HEK293 cells. (A) Determination of EGFP$^+$ cells relative to SSA plasmid transfected (RFP$^+$) cells. (B) Calculation of MFI of EGFP$^+$ cells. Statistical significance was determined using one-way ANOVA (*: $p < 0.05$; **: $p < 0.01$; ***: $p < 0.001$; ****: $p < 0.0001$).

To analyze the impact of modification on genome editing efficiency, we performed an SSA assay using 250 ng of each modified SpCas9 IVT mRNA and 125 ng of modified sgRNA per well. In contrast to previously performed SSA assays, flow cytometry was carried out 24 h post transfection of CRISPR/Cas9 system, to allow easier comparison. Results indicated improved genome editing efficiency for all modifications, showing increased numbers of EGFP$^+$ cells and higher MFI values compared to unmodified control (Fig. Fig 18 A&B). In line with previous results, ψ-UTP/m^{5}CTP double modification revealed significant highest amounts of EGFP$^+$ cells and MFI value.

In conclusion, our results indicated that ψ-UTP/m^{5}CTP modified mRNA induced highest cell viability, protein expression and genome editing efficiency in both cell culture systems (HEK293 and differentiated HepG2) and was therefore used for all further experiments.

3.1.5. *In vitro* functionality of IVT mRNA based CRISPR variants

As already mentioned in the introduction, besides SpCas9, SaCas9 and LbCas12a systems have recently become more important, as they exhibit several advantages. Therefore, we were interested to establish both systems for future IVT mRNA applications.

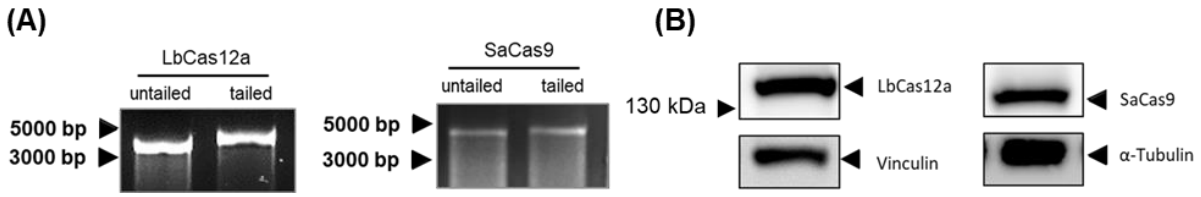

Figure 19: Alternative CRISPR/Cas9 systems. (A) Analysis of produced untailed and tailed LbCas12a and SaCas9 IVT mRNAs on 2% agarose gel. (B) Western Blot analysis of LbCas12a (140 kDa) and SaCas9 (130 kDa) 24 h post transfection into differentiated HepG2 cells. Vinculin and α-tubulin were used as loading control.

To test both variants we produced ARCA-ψ-UTP/m^5CTP IVT mRNAs encoding for each protein and analyzed the production on 2% agarose gel, displaying desired bands for untailed and tailed mRNA (Fig. 19 A). To verify expression of both proteins we transfected differentiated HepG2 cells with 500 ng of each mRNA. 24 h post transfection we isolated protein and performed Western Blot analysis. Results demonstrated (Fig. 19 B) strong expression of correctly sized proteins at 145 kDa (LbCas12a) and 130 kDa (SaCas9).

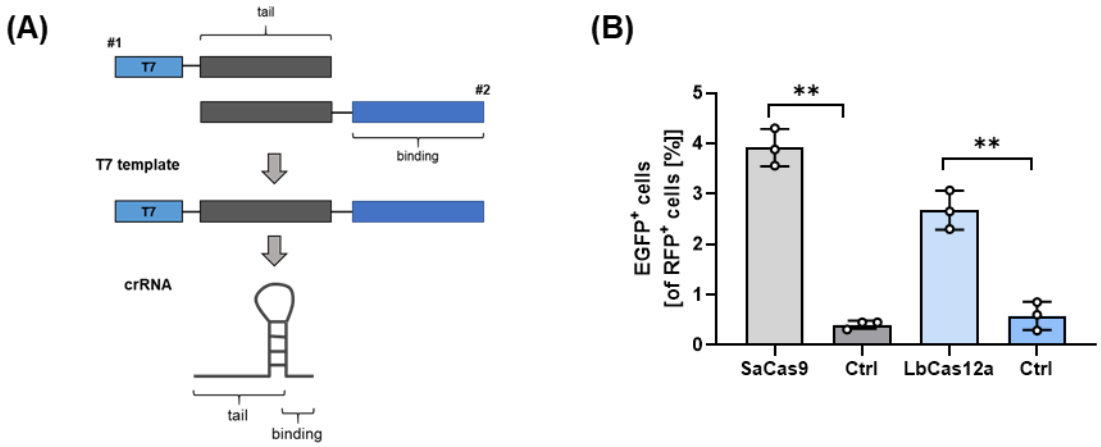

Figure 20: Functionality of alternative CRISPR/Cas9 systems. (A) Schematic representation of crRNA production. Primer #1 and #2 are used for PCR to generate template for T7 IVT synthesis. (B) Flow cytometry analysis of SSA-assay measuring EGFP$^+$ cells, 5 days post transfection of LbCas12a and crRNA or SaCas9 and sgRNA into HEK293, respectively. Statistical significance was determined using unpaired Students *t*-test with Welsh's correction (*: $p < 0.05$; **: $p < 0.01$; ***: $p < 0.001$; ****: $p < 0.0001$).

To analyze functionality, we produced IVT sgRNA for SaCas9 as described for SpCas9 by exchanging SpCas9 tracrRNA sequences with those of SaCas9. For LbCas12a we produced crRNA as described previously (Fig. 20 A) (Henning 2019). To analyze genome editing efficiency we cloned SSA-plasmids for both variants (pDNA-SSA-SaCas9 and pDNA-SSA-LbCas12a) and transfected them into HEK293 together with 250 ng of respective CRISPR IVT mRNA and 125 ng of crRNA or sgRNA, respectively. Five days post transfection we performed flow cytometry. Analysis of EGFP$^+$ cells (Fig. 20 B) showed low, but significant numbers in comparison to the controls for both CRISPR variants.

In summary the results indicated that both IVT mRNA based CRISPR/Cas9 variants were functional, but further optimizations especially concerning gRNAs have to be implemented.

3.2. Analysis of IVT mRNA transfection in non-dividing cell lines

3.2.1. IVT mRNA outperformed pDNA in non-dividing cells

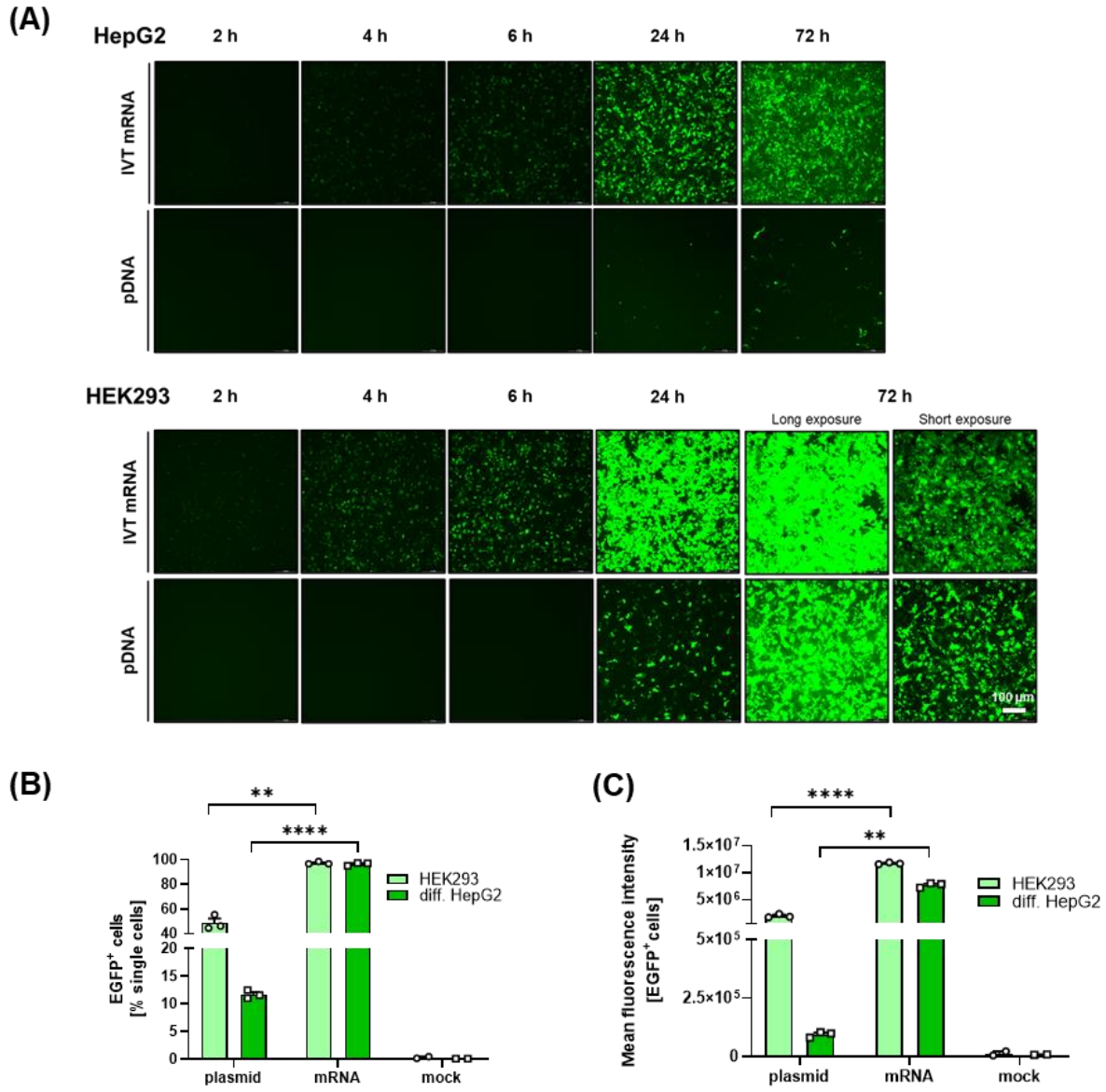

Figure 21: Comparison of pDNA with IVT mRNA. (A) Fluorescence images of depicted time points after transfection of 500 ng pDNA-EGFP or 500 ng IVT mRNA EGFP in differentiated HepG2 and HEK293 cells. Flow cytometry analysis of (B) EGFP$^+$ cells and (C) MFI of EGFP$^+$ cells, 24 h post transfection of pDNA-EGFP or IVT mRNA EGFP in differentiated HepG2 or HEK293 cell line. Statistical significance was determined using unpaired Students *t*-test with Welsh's correction (*: $p < 0.05$; **: $p < 0.01$; ***: $p < 0.001$; ****: $p < 0.0001$).

Introduction of missing genes in target cells is an important tool in basic research to investigate the impact of those factors on cellular pathways or the viral life cycle. To introduce such factors viral or non-viral vectors can be applied.

Here, we compared pDNA and IVT mRNA in terms of transfection efficiency and protein expression in non-dividing, differentiated HepG2 and easy to transfect HEK293. Therefore, we transfected both cell lines with 500 ng IVT mRNA or 500 ng pDNA encoding for EGFP protein, respectively. We monitored EGFP expression 2, 4, 6, 24 and 48 h post transfection using fluorescence microscopy. As results (Fig. 21 A) indicated, EGFP expression was detectable in both cell lines already 4 h after transfection of IVT mRNA with increasing signal intensity over time. For plasmid transfected cells expression could be detected 24 h post transfection in both cell lines, showing higher transfection efficiency and protein expression in HEK293 cells. To quantify these results, we performed flow cytometry analysis using 500 ng of IVT mRNA and 500 ng of pDNA transfected in HEK293 and differentiated HepG2, respectively. 24 h post transfection we measured $EGFP^+$ cells (Fig. 21 B) showing significant increased numbers of positive cells for both cell lines when transfecting IVT mRNA in comparison to pDNA. Calculation of MFI showed comparable results (Fig. 21 C) as signal intensities of IVT mRNA transfected cells were significantly increased in comparison to pDNA transfection.

In summary, the results indicated that IVT mRNA outperformed pDNA transfection in non-dividing cells, leading to high transfection efficiency and strong protein expression.

3.2.2. High transfection efficiency of IVT mRNA independent of cell type or encoded protein

Since these results indicated for high transfection efficiency and strong protein expression in non-dividing cells, we were interested if this was transferable to other hard to transfect cell lines like differentiated HepaRG or primary hepatocytes and if it was dependent of mRNA size or encoded protein.

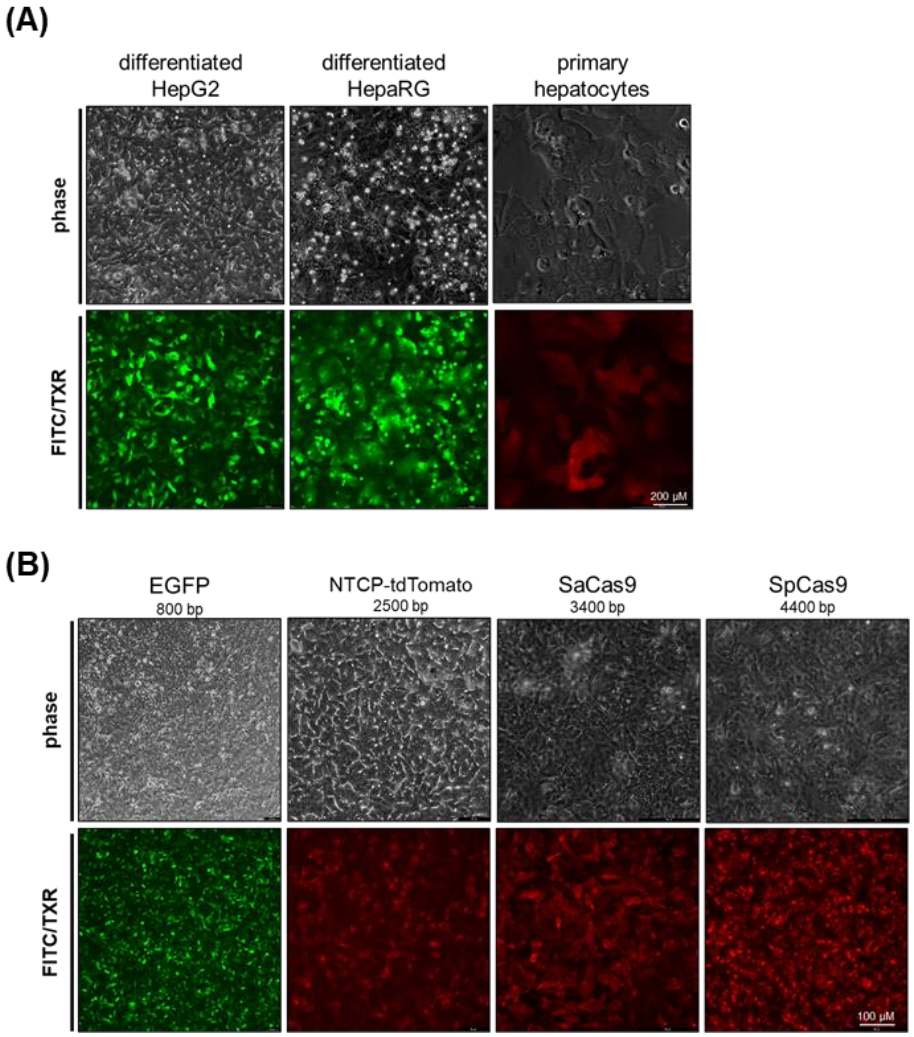

Figure 22: Protein expression in hard to transfect cells. (A) Fluorescence images 24 h post transfection of 500 ng IVT mRNA EGFP (FITC) or RFP (TXR) in differentiated HepG2 cells, differentiated HepaRG cells and primary hepatocytes. (B) Fluorescence images 24 h after transfection of 500 ng IVT mRNA encoding for EGFP (FITC), NTCP-tdTomato (TXR), SaCas9 or SpCas9 (TXR) in differentiated HepG2 cells.

To answer the first question, we transfected differentiated HepG2, HepaRG and primary hepatocytes with 500 ng of IVT mRNA encoding for EGFP or RFP and analyzed protein expression 24 h post transfection. Results (Fig. 22 A) of fluorescence microscopy showed high transfection efficiency and strong expression of EGFP (in HepG2 and HepaRG) and RFP (in primary hepatocytes). To analyze impact on transfection efficiency and protein expression by mRNA size or encoded protein, we utilized different sized IVT mRNAs encoding for EGFP (800 bp), NTCP-tdTomato (2.5 kb), SaCas9 (3.4 kb) or SpCas9 (4.4 kb). We transfected 500 ng of each IVT mRNA into differentiated HepG2 and analyzed cells 24 h post transfection by fluorescence microscopy. All tested mRNAs (Fig. 22 B) showed high transfection efficiency and protein expression independent of size or encoded protein.

Overall, results indicated that IVT mRNA demonstrated optimal characteristics for application in hard to transfect cells and for various proteins.

3.3. Supplementation of missing factors using IVT mRNA

3.3.1. Introduction of Cav-1 using IVT mRNA demonstrated protein expression but had no impact on HBV uptake

Introduction of missing genes into target cells is an important tool to investigate their function or an impact on viral life cycles. In this context we were interested in different factors described to be involved in the HBV life cycle. One of these factors is Cav-1 which is involved in endocytosis and was shown to be responsible for internalization of HBV in HepaRG cells (Macovei et al. 2010). Therefore, we were interested if Cav-1 also affects HBV uptake in our HepG2-NTCP-K7 cell line. Interestingly, Western blot analysis revealed that Cav-1 is not expressed in HepG2 or HepG2-NTCP-K7 cell line (data not shown). To investigate the impact of Cav-1 in HepG2-NTCP-K7 cell line we produced IVT mRNA encoding for Cav-1 and Cav-1-RFP.

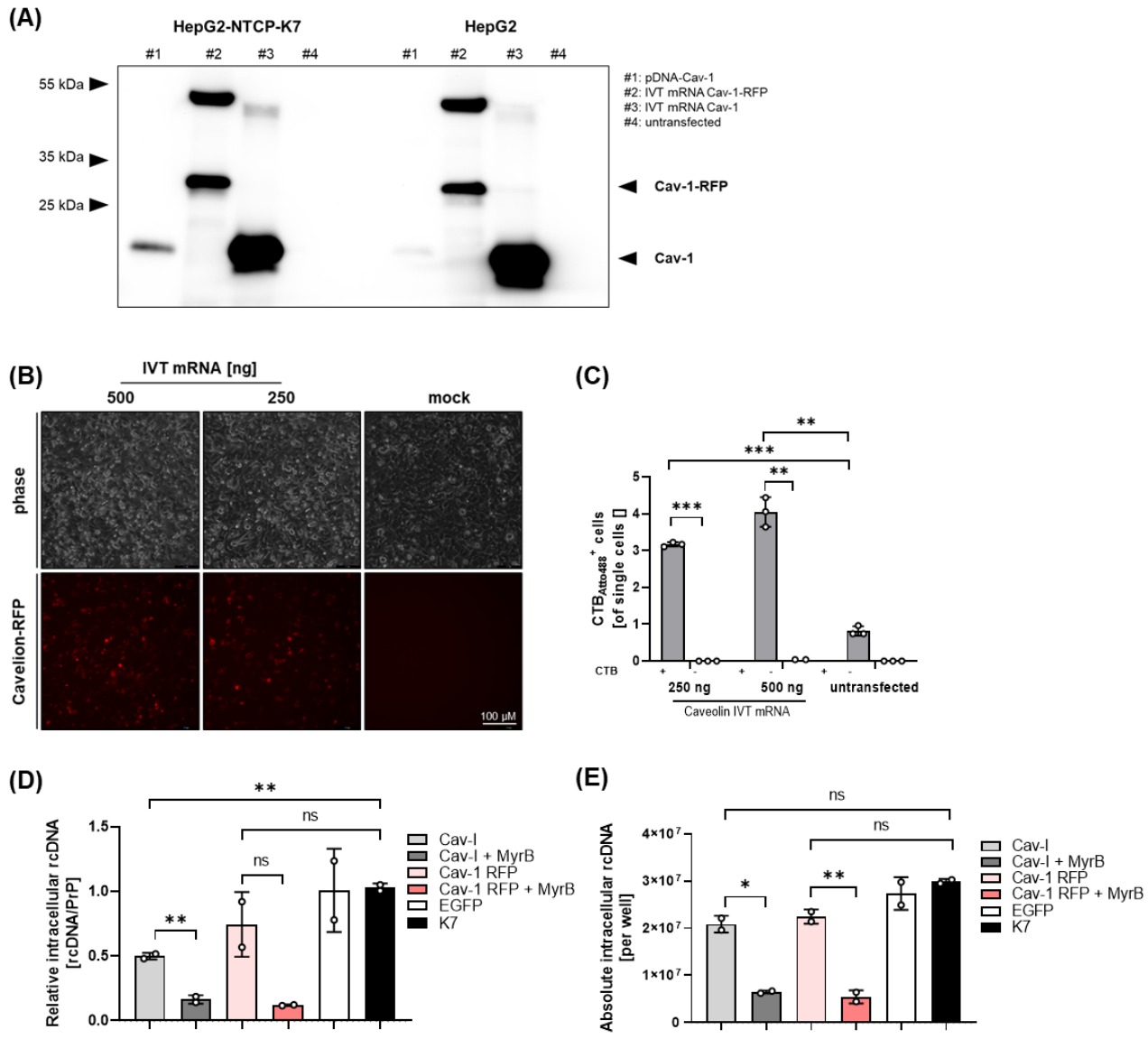

Figure 23: Characterisation of Cav-1 introduced by IVT mRNA. (A) Western blot analysis of Cav-1 and Cav-1-RFP 24 h post transfection in HepG2-NTCP-K7 and HepG2 cell line. (B) Fluorescence image 8 h post transfection of IVT mRNA Cav-I-RFP (500 ng and 250 ng) in HepG2-NTCP-K7 cell line. (C) Analysis of uptake functionality using Cav-1 substrate $CTB_{Atto488}$. Flow cytometry analysis was performed to determine internalized substrate in HepG2-NTCP-K7 transfected with 500 ng and 250 ng of IVT mRNA Cav-1 was performed with flow cytometry. Quantification of relative (D) and absolute (E) internalized HBV rcDNA, 6 h after HBV uptake assay measured with qPCR. Statistical significance was determined using Students *t*-test with Welsh's correction (*: $p < 0.05$; **: $p < 0.01$; ***: $p < 0.001$; ****: $p < 0.0001$).

To confirm protein expression, we transfected 500 ng of Cav-1 and Cav-1-RFP mRNA in differentiated HepG2 and HepG2-NTCP-K7 cells and performed Western Blot analysis 24 h post transfection. As our results showed (Fig. 23 A) application of both constructs led to strong protein expression of Cav-1 and the fusion construct (#2 and #3), in contrast to mock cells which had no detectable Cav-1 expression. To analyze transfection efficiency, we transfected 500 ng and 250 ng of Cav-1-RFP into differentiated HepG2-NTCP-K7 cells (Fig. 23 B) and monitored RFP^+ cells over time. Results showed high transfection efficiency for both tested concentrations with highest expression 8 h after transfection (data not shown). To confirm functionality of the introduced Cav-1 protein we performed an uptake assay using $Atto_{488}$ labelled Cholera Toxin B ($CTB_{Atto488}$) as described previously (Macovei et al. 2010). Therefore, we transfected HepG2-NTCP-K7 cells with 500 ng and 250 ng Cav-1 IVT mRNA and performed CTB assay 8 h post transfection. Determination of internalized $CTB_{Atto488}$ was performed with flow cytometry (Fig. 23 C) showing significant uptake of $CTB_{Atto488}$ in transfected cells (500 and 250 ng) when compared to non-treated or untransfected control cells. Finally, we were interested if introduction of Cav-1 protein had an impact on HBV uptake. Therefore, we transfected HepG2-NTCP-K7 with 250 ng Cav-1 and 250 ng Cav-1-RFP IVT mRNA and performed HBV uptake assay 8 h post administration. Internalized HBV DNA was analyzed 6 h after inoculation using qPCR analysis. Results (Fig. 23 D, E) showed intracellular HBV DNA in Cav-1 and Cav-1 RFP treated cells which was blocked by Myrcludex B. In comparison to untransfected control uptake was lower in Cav-1 harboring cells.

In summary, our results revealed that introduced Cav-1 mRNA had a high transfection efficiency and led to the expression of functional protein in high amounts. Still, introduction of Cav-1 did not improve uptake of HBV when comparing to naïve cells.

3.3.2. Transient introduction of NTCP in HepG2

Since this project was performed in cooperation with Anindita Chakraborty, the here mentioned data was already described in her PhD thesis (Chakraborty 2020).

3.3.2.1. IVT mRNA outperformed pDNA and AdV vector in differentiated HepG2

Another initial factor involved in the HBV life cycle is NTCP. Since NTCP is an essential factor involved in entry of HBV, we established a HepG2 derived cell line stably expressing NTCP (HepG2-NTCP-K7) which is used for different *in vitro* applications (Ko et al. 2018). One disadvantage of cell lines concerns differences in their cellular homeostasis (protein expression, pathway activation) when compared to cell population as they were selected for certain characteristics. To exclude such effects, transient expression of important factors is an alternative, which can be achieved by introduction of non-viral (pDNA or IVT mRNA) or viral (AdV) vectors. As IVT mRNA showed very promising results in above mentioned experiments, we were interested if the technique can be utilized to introduce NTCP into HepG2 cells, to support HBV infection. To verify, that IVT mRNA encoding for NTCP is the best method for transient expression in our cell lines we first compared transfection/transduction efficiency and protein expression with pDNA and AdV vectors encoding for fusion-protein NTCP-tdTomato.

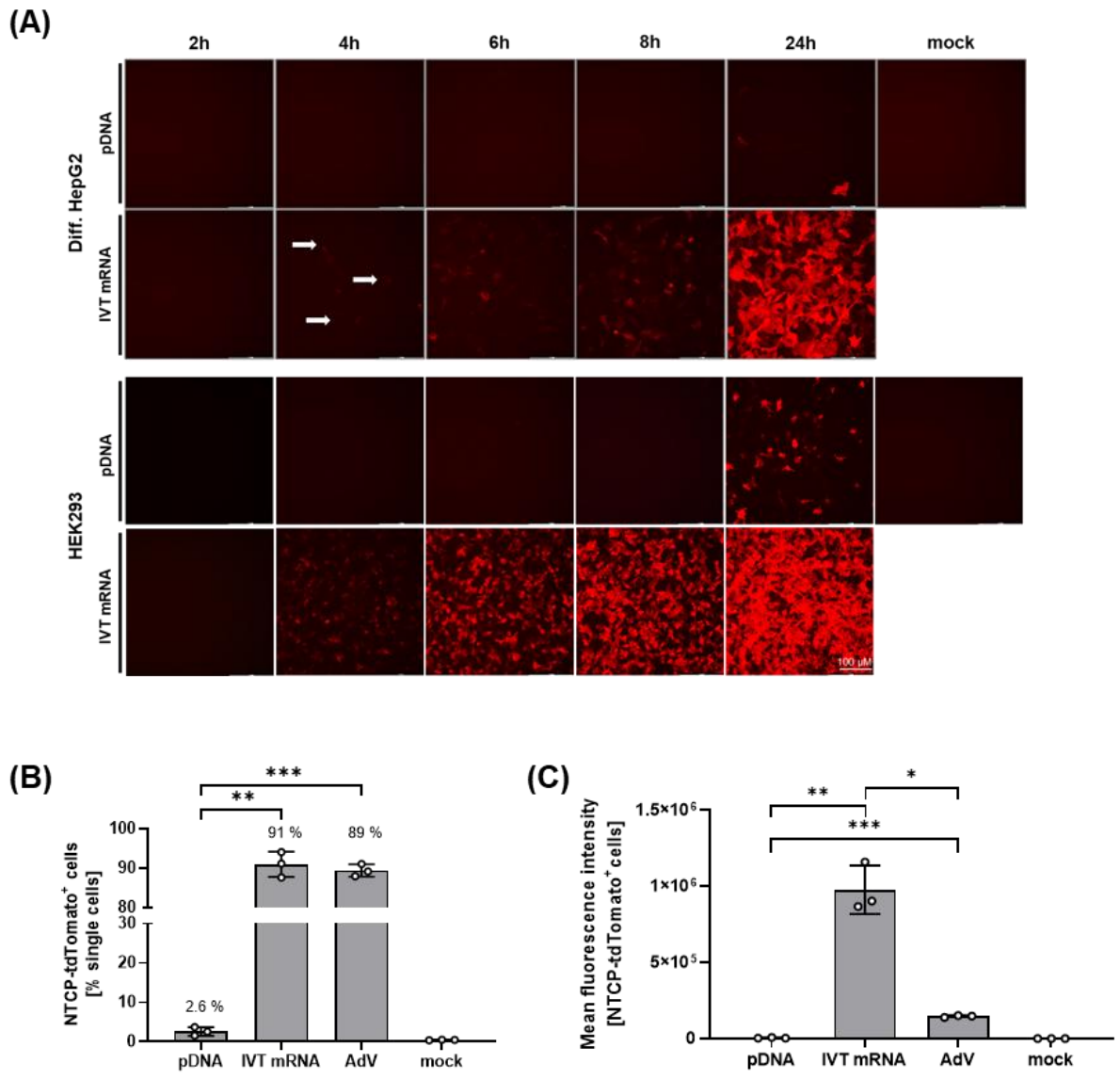

Figure 24: Analysis of different viral and non-viral vectors. (A) Fluorescence images of depicted time points after transfection of 500 ng pDNA-NTCP-tdTomato or 500 ng IVT mRNA NTCP-tdTomato in differentiated HepG2 cells. Flow cytometry analysis of NTCP-tdTomato$^+$ (B) and MFI (C) 24 h post transfection of 500 ng pDNA-NTCP-tdTomato or 500 ng IVT mRNA NTCP-tdTomato and transduction of MOI 1 AdV-NTCP-tdTomato in differentiated HepG2 cells. Statistical significance was determined using Students *t*-test with Welsh's correction (*: $p < 0.05$; **: $p < 0.01$; ***: $p < 0.001$; ****: $p < 0.0001$).

Previous results indicated that IVT mRNA encoding for EGFP revealed better performance than pDNA in HepG2 and HEK293. To verify those results, we transfected differentiated HepG2 and HEK293 with 500 ng of IVT mRNA or 500 ng pDNA and monitored expression over time.

Analysis of tdTomato$^+$ cells (Fig. 24 A) by fluorescence microscopy demonstrated expression of tdTomato in IVT mRNA transfected cells 4 h after transfection with higher signal intensity in HEK293 cells. Transfection with pDNA showed expression 24 h post transfection with low numbers of positive cells in HepG2 and HEK293. In comparison to these non-viral vectors, we were interested how adenoviral vectors would perform, as they support transduction of non-dividing cells (Steinle et al. 2017). To address this question, we transfected differentiated HepG2 with 500 ng of IVT mRNA, 500 ng pDNA or transduced MOI 1 AdV encoding for NTCP-tdTomato. 24 h post administration we analyzed treated cells using flow cytometry. Results (Fig. 24 B) revealed that both IVT mRNA and AdV had comparable but significant higher numbers of tdTomato$^+$ cells (91% and 89%) in contrast to pDNA (2.6%). Interestingly, calculation of MFI (Fig. 24 C) indicated significant higher protein expression using IVT mRNA compared to AdV or pDNA, respectively.

In summary, IVT mRNA showed the best characteristics for our experimental setup and was therefore used for the following NTCP experiments.

3.3.2.2. Introduced NTCP led to dose-dependent protein expression

To analyze if introduction of NTCP by IVT mRNA supports HBV infection, we first evaluated the optimal time point, based on NTCP expression levels, to perform our experiments. Therefore, we transfected differentiated HepG2 cells with 250 ng IVT mRNA and analyzed NTCP expression 6, 12, 24, 48 and 72 h post transfection. To detect NTCP we used Atto$_{488}$ labelled Myrcludex B (MyrB$_{Atto488}$) which specifically interacts with expressed NTCP protein.

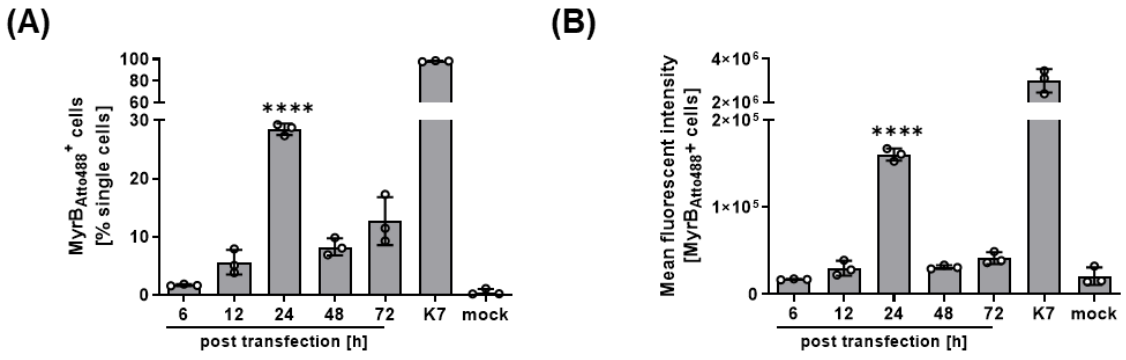

Figure 25: Time depending expression of NTCP protein. Flow cytometry analysis of MyrB$_{Atto488}$ at depicted time points post transfection of 250 ng IVT mRNA NTCP in differentiated HepG2 cells. Statistical significance was determined using one-way ANOVA (*: $p < 0.05$; **: $p < 0.01$; ***: $p < 0.001$; ****: $p < 0.0001$).

Detection of $MyrB_{Atto488}$ staining was performed with flow cytometry analysis (Fig. 25 A) showing the highest number of positive cells 24 h post transfection. Additionally, calculation of MFI (Fig. 25 B) revealed significant increased signal intensity 24 h post transfection in comparison to other time points. In contrast, HepG2-NTCP-K7 showed 100% NTCP positive cells and highest protein expression.

An important advantage of IVT mRNA is the possibility to easily titrate its concentration, allowing analysis of dose-dependent effects. As we were interested in how cellular and HBV related functions were influenced by different amounts of expressed NTCP, we performed a 2-fold titration starting from 1000 ng to 3.9 ng of IVT mRNA per well.

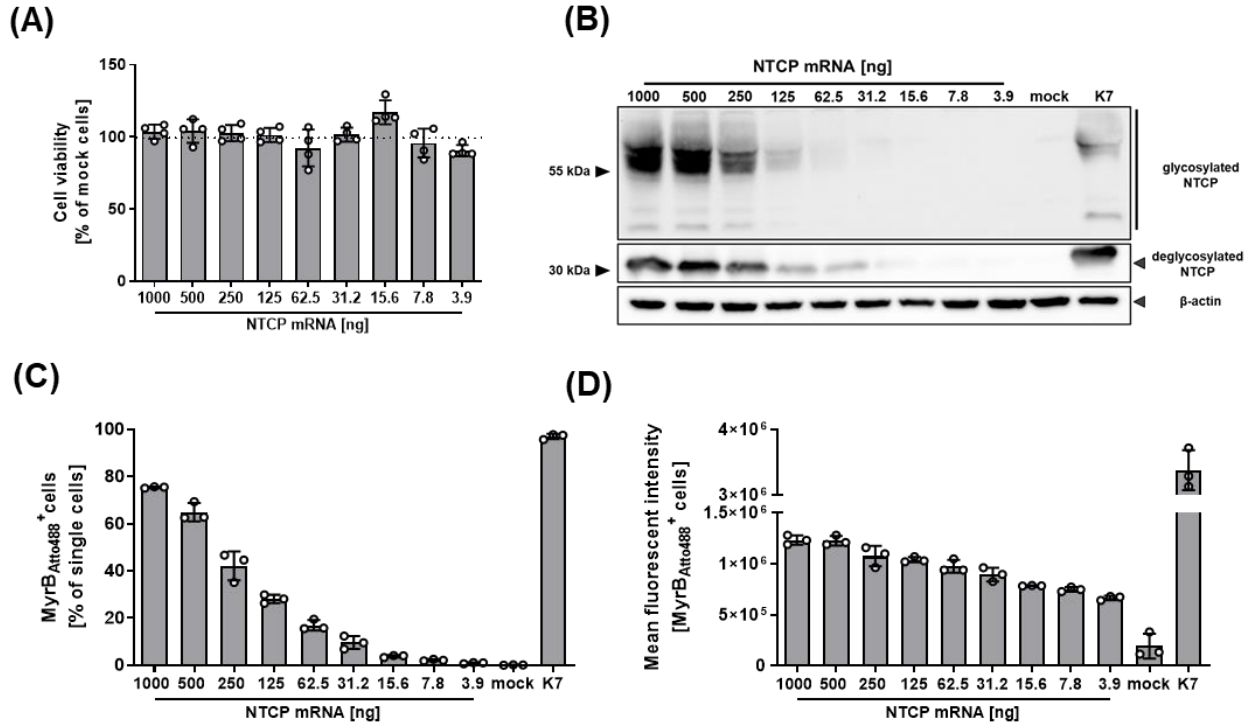

Figure 26: Characterization of IVT mRNA derived NTCP. (A) Determination of cell viability 24 h post transfection via CTB assay of 2-fold titrated IVT mRNA NTCP in differentiated HepG2 cells. (B) Western Blot analysis 24 h post transfection of 2-fold titrated IVT mRNA NTCP in differentiated HepG2. Detection of glycosylated (top) and deglycosylated NTCP (bottom). β-actin was used as loading control. Analysis of surface NTCP expression 24 h post transfection of 2-fold titrated NTCP IVT mRNA in differentiated HepG2 cells. Determination of $MyrB_{Arro488}^{+}$ cells (C) and calculation of MFI (E) was performed with flow cytometry.

Since transfection of extracellular RNAs can trigger immune responses and lead to cytotoxicity we first determined cell viability. Therefore, we transfected a 2-fold titration of NTCP IVT mRNA in differentiated HepG2 cells and performed CTB assay 24 h post administration. Results of the CTB (Fig. 26 A) showed no adverse effect for any of the tested concentrations when comparing to untreated control. To verify a dose-dependent expression of NTCP protein, we performed Western Blot analysis 24 h post transfection of IVT mRNAs. As NTCP is usually glycosylated, we additionally performed a deglycosylation step using PNGaseF treatment to allow detection of both, glycosylated (~50 kDa) and deglycosylated (~37 kDa), forms (Hagenbuch and Meier 1994, Ho et al. 2004, Doring et al. 2012). Western Blot analysis (Fig. 26 B) showed dose dependent expression of NTCP protein regarding both forms detectable for 1000 ng–15.6 ng of transfected IVT mRNA. To verify the expected localization of NTCP on cell surface we repeated $MyrB_{Atto488}$ staining 24 h post transfection of 2-fold titrated mRNA. Analysis of stained cells by flow cytometry (Fig. 26 C) revealed dose dependent expression of NTCP which was reflected by the calculated MFI (Fig. 26 D). In contrast to HepG2-NTCP-K7 control, total expression of NTCP, even for the highest amount of 1000 ng IVT mRNA, was lower in transfected cells.

In summary, our data suggested that titration of IVT mRNA allowed dose-dependent expression of encoded protein.

3.3.2.3. NTCP revealed dose-dependent cellular and HBV related function

NTCP is naturally involved in bile acid transport of hepatocytes. Therefore, we were interested if the introduced NTCP protein supports cellular function. To address this question, we repeated dose-dependent transfection of IVT mRNA in differentiated HepG2 cells and performed an NTCP specific uptake assay 24 h after, using radioactive labeled bile acids (taurocholate [^{3}H]). To verify specific uptake, we included MyrB to block NTCP dependent internalization of bile acids as a control.

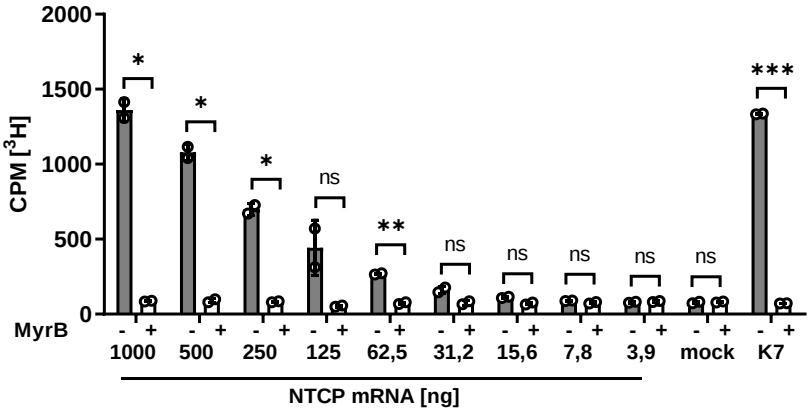

Figure 27: Radioactive bile acid uptake of transfected HepG2 cells. Uptake of ^{3}H taurocholate was determined 24 h post transfection of 2-fold titrated IVT mRNA NTCP into differentiated HepG2 cells. Measurement was performed using scintillation analyzer. Statistical significance was determined using unpaired Students *t*-test with Welsh's correction (*: $p < 0.05$; **: $p < 0.01$; ***: $p < 0.001$; ****: $p < 0.0001$).

Measurement of internalized radioactive bile acids (Fig. 27) demonstrated significant and dose-dependent uptake in cells transfected with 1000–62.5 ng of IVT mRNA which was blocked by MyrB treatment. No difference in uptake capability was detected compared to 1000 ng IVT mRNA with K7 cell line. Since we confirmed protein expression and functionality of the introduced NTCP protein, we were interested if HBV uptake and infection showed a dose-dependency. Therefore, we transfected differentiated HepG2 with 2-fold titrated IVT mRNA and performed either HBV uptake assay or HBV infection 24 h post administration of mRNA. HBV uptake was determined by qPCR measuring internalized HBV DNA 6 h after inoculation.

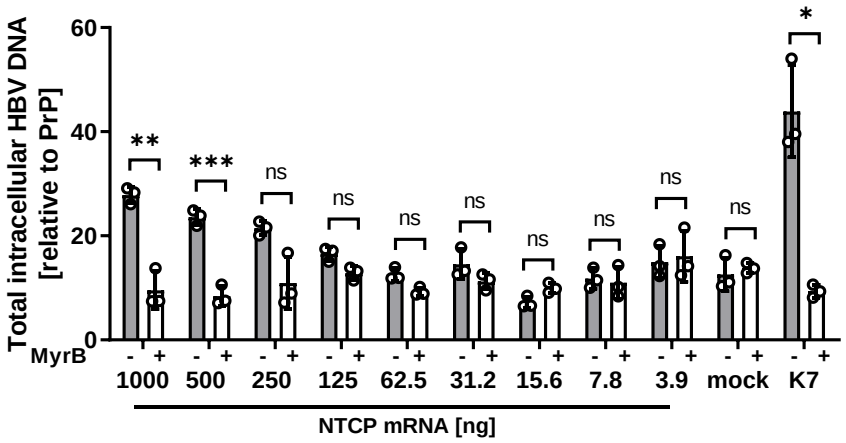

Figure 28: HBV uptake assay for transfected HepG2 cells. Measurement of internalized HBV DNA via qPCR was performed 24 h post transfection with 2-fold titrated IVT mRNA NTCP in differentiated HepG2 cells. 10 µM Myrcludex B was added as specific inhibitor for NTCP HBV interaction. Statistical significance was determined using unpaired Students *t*-test with Welsh's correction (*: $p < 0.05$; **: $p < 0.01$; ***: $p < 0.001$; ****: $p < 0.0001$).

Results (Fig. 28) demonstrated significant uptake in cells transfected with 1000 ng and 500 ng compared to MyrB control, whereas the effect at lower concentrations was not as pronounced or even absent. In contrast to transfection with 1000 ng, K7 cell line showed higher amounts of internalized HBV DNA.

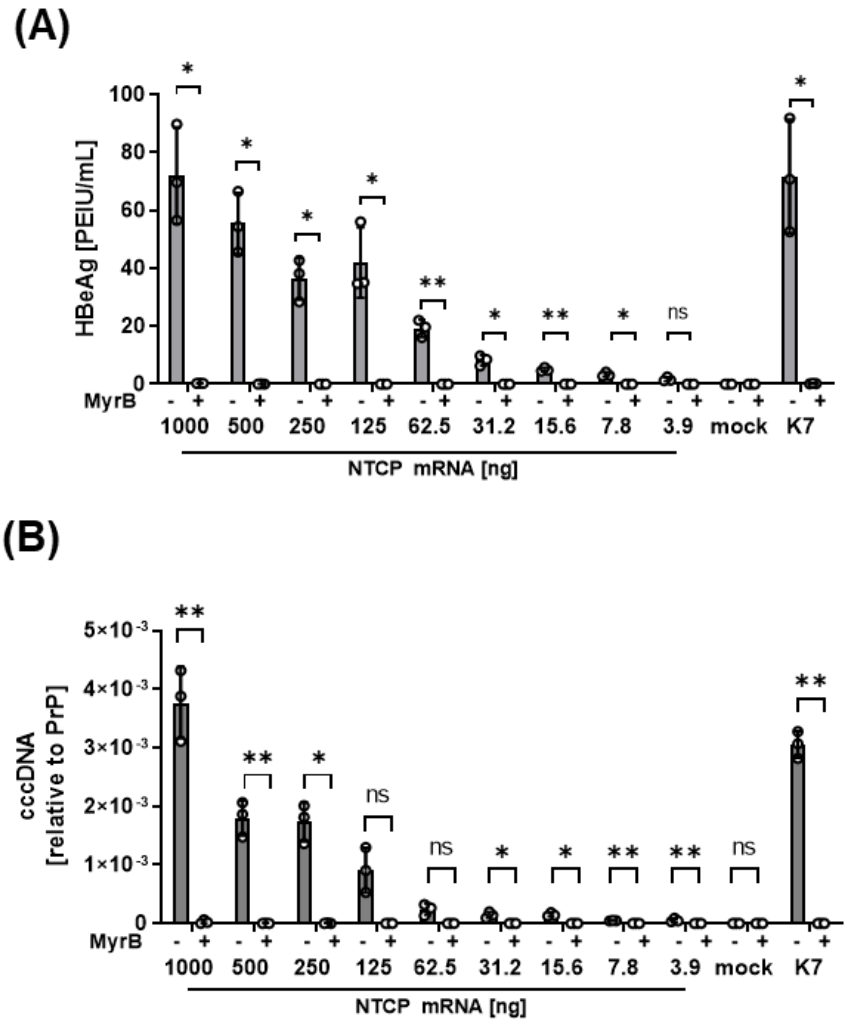

Figure 29: Analysis of NTCP dose-dependent infection with HBV. Differentiated HepG2 cells were transfected with 2-fold titrated IVT mRNA NTCP and infected with MOI 200 WT HBV 24 h post transfection. Measurement of HBeAg (A) and quantification of cccDNA molecules (B) were performed 7 days post infection. 10 µM Myrcludex B was added to infection to inhibit NTCP HBV interaction. Statistical significance was determined using unpaired Students *t*-test with Welsh's correction (*: $p < 0.05$; **: $p < 0.01$; ***: $p < 0.001$; ****: $p < 0.0001$).

To analyze infection capability of transfected cells, we measured HBeAg (Fig. 29 A) and cccDNA (Fig. 29 B) 7 days post infection. HBeAg results showed a significant and dose-dependent secretion in cells transfected with 1000 ng–7.8 ng, which was blocked by MyrB treatment. Compared to cells transfected with 1000 ng, HepG2-NTCP-K7 cells showed equal concentrations. Relative quantification of cccDNA revealed corresponding results, showing significant formation of cccDNA molecules in cells transfected with 1000 – 250 ng and 31.2–3.9 ng IVT mRNA.

Formation was blocked specifically when MyrB was added during HBV infection. Interestingly, formation of cccDNA in K7 cells was lower when compared to HepG2 transfected with 1000 ng IVT mRNA.

3.3.2.4. High transfection efficiency and protein expression in non-hepatic cells

As mentioned already, expression of NTCP on target cells is essential for HBV entry but still other factors are necessary for a full life cycle. Identification of those factors is a major goal in basic research to identify possible drug targets. Therefore, two different strategies were used in previous studies: Introduction of human NTCP in hepatocytes from different organism or into different human tissues to analyze their capability to support HBV infection. A major problem of comparing different cells is the expression level of introduced genes, which can vary drastically (data not shown). Therefore, we were interested if introduction of NTCP by IVT mRNA in different non-hepatic cell lines would lead to comparable expression levels supporting viral replication on a populational level. To address those questions, we selected HEK293 (human embryonic kidney), A549 (human lung carcinoma), HeLa (human cervix carcinoma) and U2OS (human osteosarcoma) cell lines which were already used in previous studies for establishment of NTCP harboring cell lines (Ni et al. 2014, Meredith et al. 2016). To analyze cytotoxicity and protein expression, we transfected all cells with 500 ng IVT mRNA and performed CTB assay as well as Western Blot analysis 24 h post transfection.

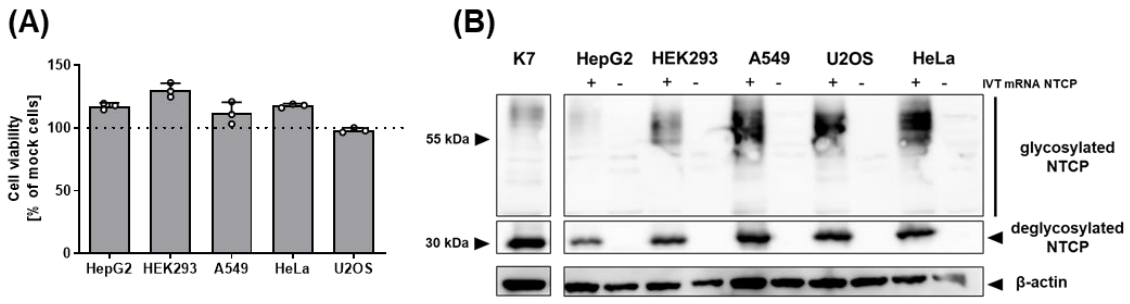

Figure 30: Characterization of NTCP protein introduced to non-hepatic cells. (A) Analysis of cell viability via CTB assay 24 h post transfection of 500 ng IVT mRNA NTCP into HepG2, HEK293, A549, HeLa and U2OS cell lines. (B) Western blot analysis 24 h post transfection of respective cell lines with 500 ng of IVT mRNA NTCP. Determination of glycosylated (top) and deglycosylated (bottom) was performed. β-actin was used as loading control.

CTB results (Fig. 30 A) showed no toxic effect in all tested cells. Western Blot analysis revealed specific expression of NTCP protein (Fig. 30 B) exclusively in IVT mRNA transfected cells. To verify transfection efficiency and correct protein expression, we repeated the experiment using 500 ng of NTCP-tdTomato IVT mRNA and analyzed expression 24 h after administration by fluorescence microscopy and flow cytometry.

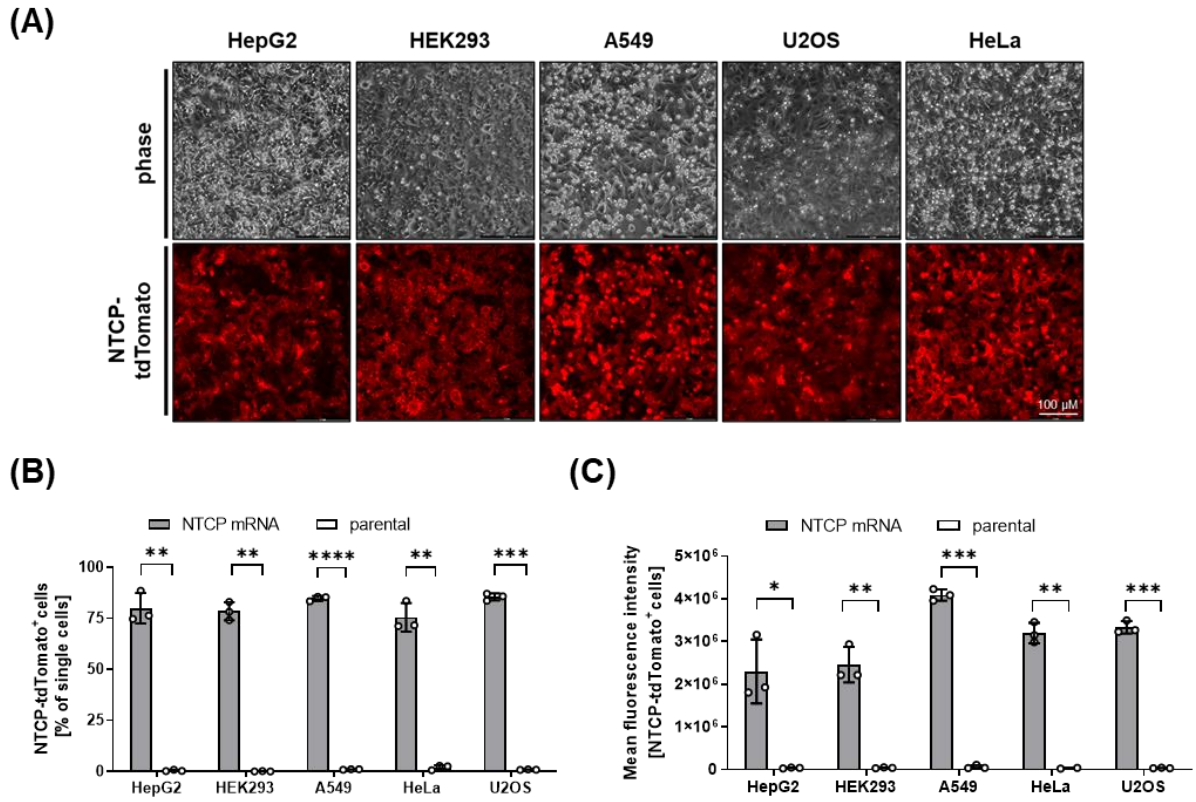

Figure 31: Analysis of NTCP localization. (A) Fluorescence images 24 h post transfection of respective cell lines with 500 ng IVT mRNA NTCP-tdTomato. Analysis of NTCP-tdTomato$^+$ (B) and MFI (C) of respective cells transfected with IVT mRNA NTCP-tdTomato was performed with flow cytometry. Statistical significance was determined using unpaired Students *t*-test with Welsh's correction (*: $p < 0.05$; **: $p < 0.01$; ***: $p < 0.001$; ****: $p < 0.0001$).

Results of fluorescence microscopy (Fig. 31 A) showed the correct localization of NTCP-tdTomato with integration into the cellular membrane in all tested cells with comparable signal intensity. Further, flow cytometry analysis revealed high numbers of tdTomato$^+$ cells (Fig. 31 B) in all tested cell lines which was reflected by comparable signal intensities determined calculation of MFI (Fig. 31 C).

To validate functionality of the introduced NTCP we repeated the radioactive bile acid uptake assay for all cell types.

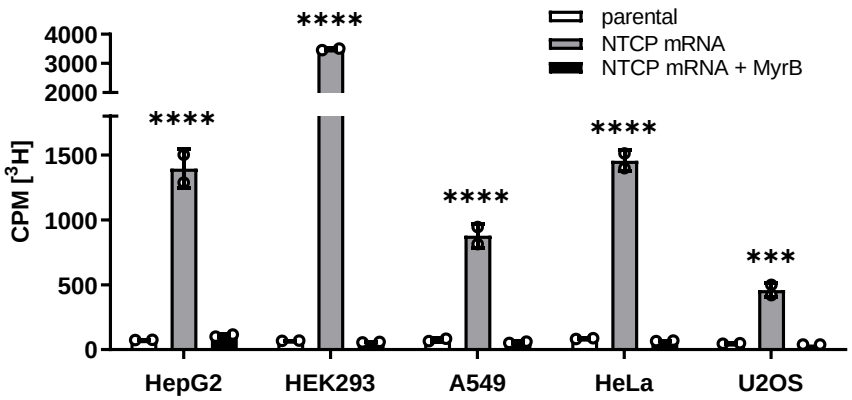

Figure 32: ^{3}H taurocholate uptake assay in non-hepatic cell lines. Internalized uptake of ^{3}H taurocholate in respective cell lines transfected with 500 ng IVT mRNA was performed 24 h post transfection using scintillation analyzer. Myrcludex B was added to assay to inhibit NTCP HBV interaction. Statistical significance was determined using 2-way ANOVA (*: $p < 0.05$; **: $p < 0.01$; ***: $p < 0.001$; ****: $p < 0.0001$).

Measurement of internalized radioactive bile acids was performed one day post transfection of 500 ng NTCP IVT mRNA. Results (Fig. 32) showed significant uptake in cells transfected with mRNA compared to parental cells which could be specifically blocked by MyrB treatment.

In summary, our results indicated that introduction of NTCP in non-hepatic cells using IVT mRNA led to high numbers of positive cells, which demonstrated strong expression of functional protein.

3.3.2.5. Non-hepatic cell lines supported transcription from HBV template

As mentioned previously several cellular factors and processes are involved in the HBV life cycle (e.g. nuclear import or transcriptional factors). To ensure the capability of our non-hepatic cell lines to use HBV sequences as transcriptional templates, we transduced all cell lines with MOI 1 of an AdV vector harboring a 1.3-fold overlength HBV sequence and EGFP to control transduction efficiency.

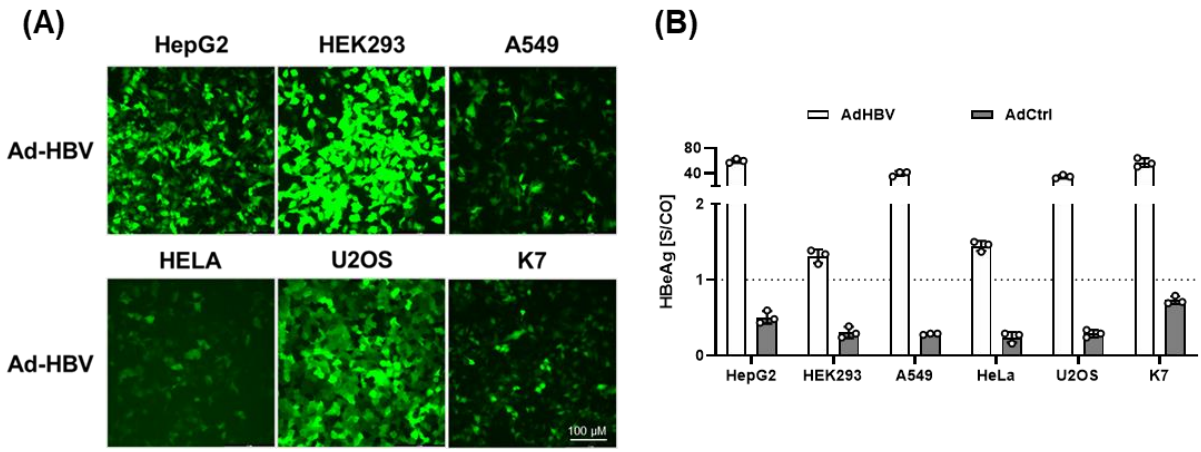

Figure 33: Analysis of HBV specific transcription in non-hepatic cell lines. (A) Fluorescence images of respective cell lines transduced with MOI 1 AdV-H1.3. harboring 1.3-fold HBV and EGFP sequence. (B) Measurement of HBeAg 7 days post transduction with AdV-H1.3. with BEP III.

Two days after transduction we monitored EGFP expression using fluorescence microscopy (Fig. 33 A), revealing different transduction efficiencies and signal intensities between all tested cell lines. To detect transcriptional activity of HBV, we measured HBeAg expression 7 days post transduction. Our results (Fig. 33 B) indicated HBeAg secretion in all transduced cells, with lowest secretion in HEK293 and HeLa cell lines.

3.3.2.6. Introduction of NTCP in non-hepatic cells did not support HBV life cycle

As a final experiment we were interested if transient expression with high transfection efficiency and strong protein expression would allow uptake or infection with HBV virus on a populational level. Therefore, we transfected all cells with 500 ng NTCP IVT mRNA and performed either HBV uptake or HBV infection 24 h post transfection. In contrast to previous experiments using only HepG2 and K7 cell lines, cells were cultivated in absence of 2.5% DMSO, due to cytotoxicity (data not shown).

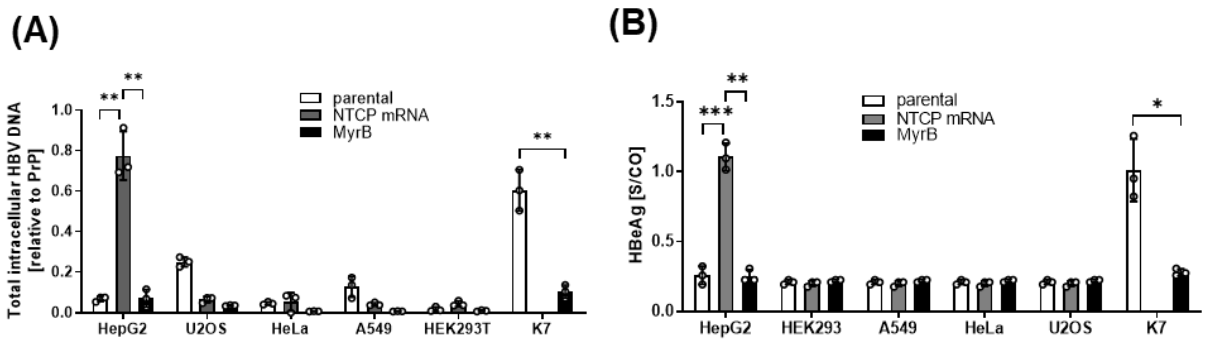

Figure 34: HBV uptake and infection of transfected non-hepatic cells. Analysis of HBV uptake and infection was performed 24 post transfection of 500 ng IVT mRNA NTCP in respective cell lines. (A) Determination of internalized HBV DNA 6 h post inoculation was performed with qPCR measurement. (B) Detection of secreted HBeAg was determined 7 days post infection. Statistical significance was determined using unpaired Students *t*-test with Welsh's correction (*: $p < 0.05$; **: $p < 0.01$; ***: $p < 0.001$; ****: $p < 0.0001$).

Measurement of internalized HBV DNA 6 h after inoculation (Fig. 34 A) demonstrated significant uptake of virus in transfected HepG2 and K7 control cells, which was blocked by MyrB treatment. In contrast, transfected non-hepatic cells did not support HBV uptake. Interestingly, parental U2OS and A549 showed low uptake of HBV independent of NTCP expression. Analysis of HBV infection by measurement of secreted HBeAg (Fig. 34 B) indicated HBV infection exclusively in transfected HepG2 and K7 cell lines showing significant higher amounts than the corresponding MyrB controls. All non-hepatic cells were negative for HBeAg expression independent of NTCP expression.

In summary introduction of NTCP by IVT mRNA displayed higher transfection efficiency than pDNA and stronger protein expression than AdV. Additionally, it supported dose-dependent protein expression and functionality. Transferring IVT mRNA into non-hepatic cell lines led to protein expression and specific uptake of bile acids but did not support HBV uptake or infection.

3.4. Analysis of CRISPR/Cas9 targeting against HBV DNA

3.4.1. CRISPR/Cas9 efficiency was target number dependent

CRISPR/Cas9 is used in multiple ways to target various sequences either for knock-out or knock-in applications. Additionally, it was also used as tool to target viruses like integrated HIV with the final goal to cure infection (Zhu et al. 2015). Since infected hepatocytes harbor the persistence form of HBV cccDNA, CRISPR/Cas9 became an interesting application to target chronic infection. Several groups demonstrated efficient targeting of HBV sequences in cell lines harboring an integrated form or against plasmids transfected into cells. Interestingly, targeting of cccDNA is less efficient while still showing significant reduction *in vitro*. In contrast, *in vivo* targeting of HBV sequences in transgenic mice but also targeting of injected pDNA-HBV1.3. molecules in mouse model showed drastically reduced efficiency (Ramanan et al. 2015, Liu et al. 2018). These previous findings were supported by our experiments using adenoviral based CRISPR/Cas9 against HBV showing significant reduction *in vitro* but no effect in *in vivo* situation (Schiwon et al. 2018).

Since eradication of cccDNA from infected hepatocytes is a crucial step to cure chronic infection, we were interested to identify limitations of CRISPR/Cas9 helping to improve its functionality.

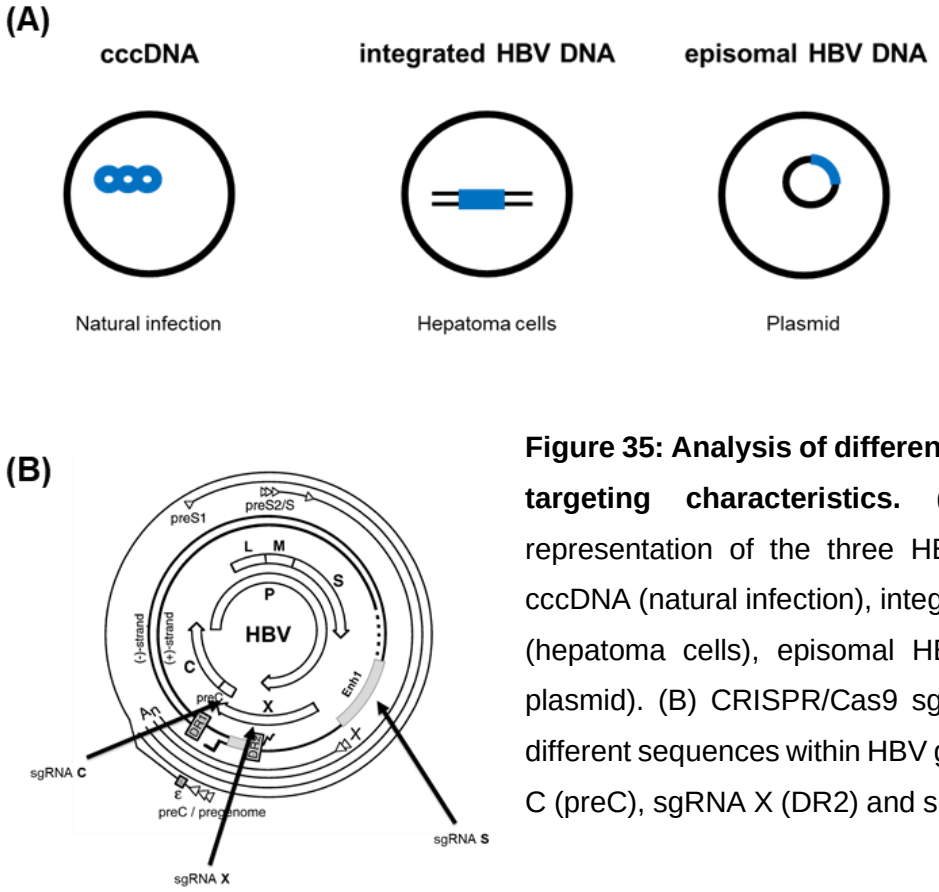

Figure 35: Analysis of different CRISPR/Cas9 targeting characteristics. (A) Schematic representation of the three HBV DNA forms: cccDNA (natural infection), integrated HBV DNA (hepatoma cells), episomal HBV DNA (pEpi-plasmid). (B) CRISPR/Cas9 sgRNAs targeting different sequences within HBV genome: sgRNA C (preC), sgRNA X (DR2) and sgRNA S (Enh1).

To narrow down the problem, we analyzed CRISPR/Cas9 targeting efficiencies against different target localizations and structures: cccDNA, integrated and episomal (Fig. 35 A). We applied our established IVT mRNA CRISPR/Cas9 method for transient expression of SpCas9 allowing fast screening in different cell lines. To ensure efficient targeting of HBV sequences, we used sgRNAs against pre core (sgRNA C), DR2 (sgRNA X) and Enh1 (sgRNA S) (Fig. 35 B) which are essential regions for HBV transcription and replication (Ramanan et al. 2015, Wang et al. 2015). Additionally, we applied a combination of two sgRNAs as previous studies showed significant increased genome editing efficiency (Wang et al. 2015). As control for CRISPR/Cas9 experiments we included a nonsense sgRNA which harbors randomized nucleotides and does not interact with HBV (Wang et al. 2017). As described already, targeting of integrated sequences is efficient against multiple targets including HBV. In a first step, we were interested how CRISPR/Cas9 efficiency differs when targeting cells harboring different copy numbers of target sequences. We chose three HBV cell lines HepG2-H1.3., HepG2.2.15 and HepG2-911.

HepG2-H1.3. harbors one copy of 1.3-fold overlength HBV genome, HepG2.2.15 four tandem copies of two head-to-tail orientated HBV sequences and HepG2-911 multiple integrates (average 13-16) as this cell was produced using piggyBac system (Sells et al. 1987, Kettlun et al. 2011, Hu et al. 2019).

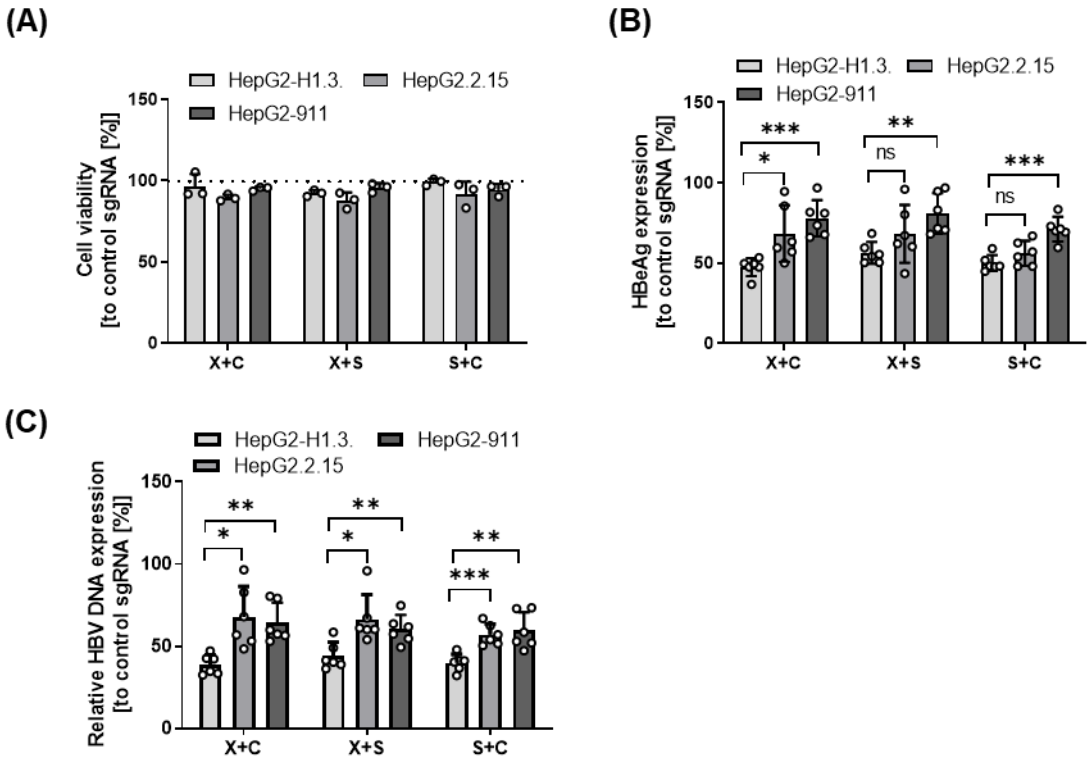

Figure 36: Comparison targeting efficiency against multiple, integrated targets. (A) Determination of cell viability via CTB assay 24 post transfection of 250 ng IVT mRNA SpCas9 and 125 ng of respective sgRNA combination in HepG2-H1.3., HepG2.2.15 and HepG2-911 cells. Analysis of anti-HBV effect, in the already mentioned cells, on secreted HBeAg (B) and relative HBV DNA levels with qPCR (C) 5 days post transfection of 250 ng IVT mRNA SpCas9 and 125 ng of respective sgRNA combination compared to control. Statistical significance was determined using unpaired Students *t*-test with Welsh's correction (*: $p < 0.05$; **: $p < 0.01$; ***: $p < 0.001$; ****: $p < 0.0001$).

To exclude cytotoxicity, we transfected all cell lines with 250 ng IVT mRNA SpCas9 and in total 125 ng of two modified sgRNAs per well and performed CTB assay one day post treatment. Results (Fig. 36 A) show comparable cell viability of all HBV specific sgRNA combinations when compared to cells transfected with nonsense sgRNA.

To investigate efficiency of CRISPR/Cas9 against integrated HBV, we repeated transfection of our CRISPR/Cas9 system and analyzed viral parameters 5 days after application. Measurements of HBeAg (Fig. 36 B) showed reduction in all cell lines for each combination when compared to nonsense control. When comparing to HepG2-911 reduction of HBeAg secretion was significant in HepG2-H1.3. cell line for all tested combinations. In contrast reduction of HBeAg to HepG2.2.15 was only significant using sgRNA X and sgRNA C but not for the other two combinations. Quantification of total HBV DNA (Fig. 36 C) revealed reduction in all tested cell lines and with all sgRNA combinations. In contrast to HBeAg, HepG2-H1.3. showed a significant reduction with all sgRNA combinations compared to both HepG2.2.15 and HepG2-911 cell lines, respectively.

3.4.2. Reduced CRISPR/Cas9 functionality against episomal HBV DNA

The next step was to analyze the efficiency of CRISPR/Cas9 against episomal structures like cccDNA or pDNA. Therefore, we used natural infection with HBV leading to formation of cccDNA molecules in the nucleus of infected cells. Additionally, we utilized a plasmid harboring a scaffold/matrix-associated region (S/MAR) sequence, which allows cell cycle dependent replication and a 1.3-fold overlength HBV sequence to establish HepG2-pEpi-H1.3. cell line (Piechaczek et al. 1999). For quantification of HBV templates, we determined cccDNA amounts 7 days after infection of HepG2-NTCP-K7 cells with MOI 500 and number of pEpi-H1.3. plasmid by qPCR.

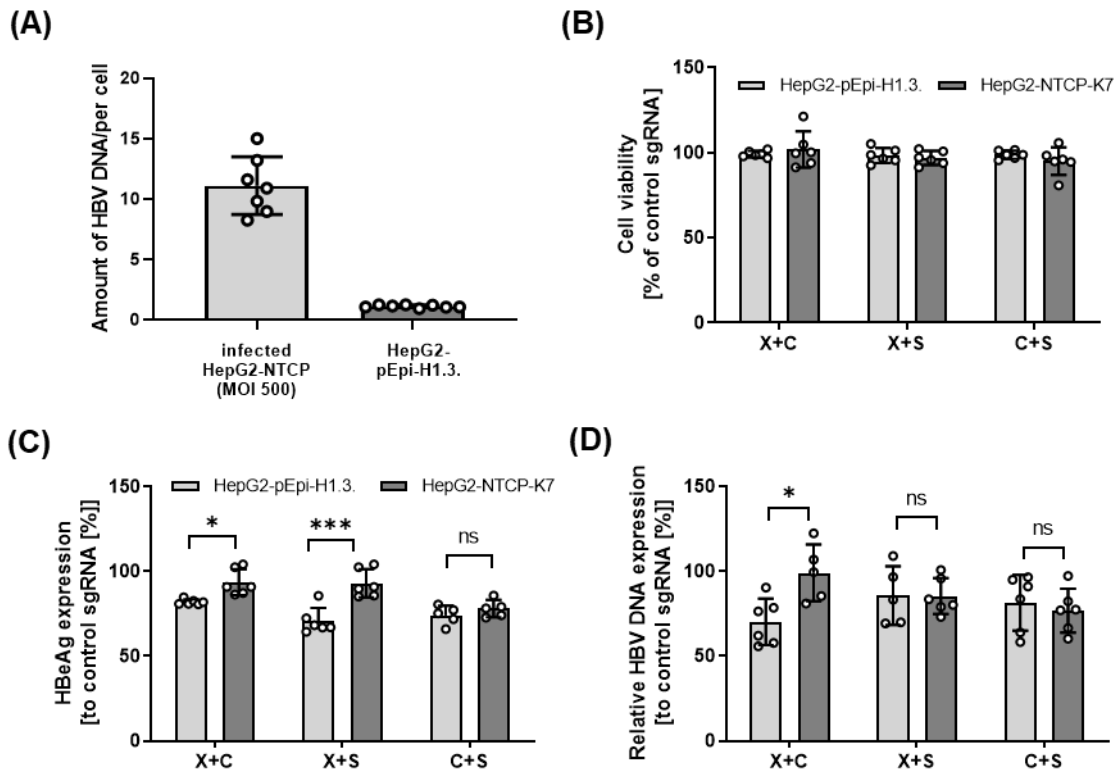

Figure 37: Comparison targeting efficiency against episomal structures. (A) Absolute quantification of cccDNA (MOI 500 WT HBV) 7 days post infection and pDNA-pEpi-H1.3. copy numbers determined with qPCR analysis and normalized to cell number. (B) Determination of cell viability 24 h post transfection of 250 ng IVT mRNA SpCas9 and 125 ng of respective sgRNA combination in infected HepG2-NTCP-K7 (MOI 500 WT HBV) and HepG2-pEpi-H1.3. cell line. Analysis of anti-HBV effect in HepG2-pEpi-H1.3. and infected HepG2-NTCP-K7 on secreted HBeAg (C) and relative HBV DNA levels with qPCR (D) 5 days post transfection of 250 ng IVT mRNA SpCas9 and 125 ng of respective sgRNA combination compared to control. Statistical significance was determined using unpaired Students *t*-test with Welsh's correction (*: $p < 0.05$; **: $p < 0.01$; ***: $p < 0.001$; ****: $p < 0.0001$).

Absolute quantification was performed using a dilution series of HBV/pEpi-H1.3. plasmid standard and was normalized to cell number (Stavrou et al. 2017, Xia et al. 2017). Results (Fig. 37 A) showed that MOI 500 infection led to formation of ~ 11 copies of cccDNA, whereas HepG2-pEpi-H1.3. cell line harbored 1 copy per cell. To investigate CRISPR/Cas9 effect in both cell lines we repeated transfection with 250 ng IVT mRNA SpCas9 and 125 ng of sgRNA combination in both cell lines.

24 h post transfection we performed a CTB assay (Fig. 37 B) indicating no adverse effect on cell viability in both cell lines. Viral parameters were measured 5 days post transfection. Analysis of HBeAg (Fig. 37 C) showed slight reduction for both cell lines compared to nonsense control. Still, the reductive effect in HepG2-pEpi-H1.3. was significantly increased when using sgRNA X/C or X/S compared to infected K7 cell line. The combination of sgRNA C and S showed comparable reduction in both cell lines. In contrast total HBV DNA expression (Fig. 37 D) was significantly reduced in HepG2-H1.3. compared to infected K7 exclusively with sgRNA X/C combination.

3.4.3. CRISPR limitations evoked reduced efficiency against episomal structures

As demonstrated in our previous experiments targeting of integrated HBV sequences showed higher efficiency than observed against episomal structures. To simplify investigation of this limitation, we chose HepG2-H1.3. and HepG2-pEpi-H1.3. cell line as both are harboring only a single copy of HBV template per cell allowing easier comparison of effects. One reason for reduced CRISPR/Cas9 efficiency might be related to different binding affinities against episomal compared to integrated sequences. To investigate if binding has an impact on CRISPR/Cas9 effect we used a silenced, dead SpCas9 (dSpCas9) protein which harbors two mutations within both catalytic domains of HNH (H841A) and RuvC (D10A) nuclease (Yao et al. 2018). Both mutations disrupt enzymatic activity of SpCas9 protein to introduce DSB into target sequence but have no impact on sgRNA-mediated binding. To compare effects on episomal or integrated HBV sequences, we transfected HepG2-H1.3. and HepG2-pEpi-H1.3. with either 250 ng dSpCas9 or SpCas9 IVT mRNA and 125 ng of modified sgRNA combinations.

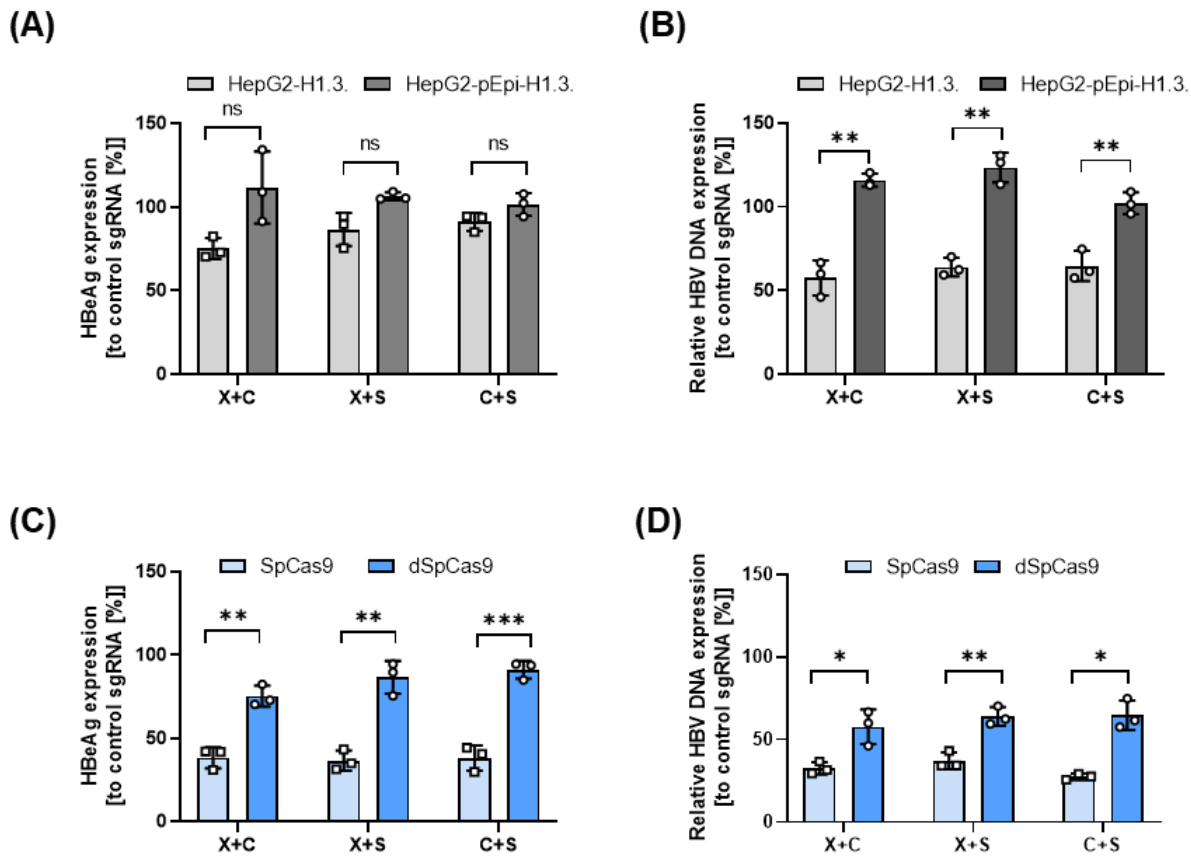

Figure 38: Analysis of CRISPR/Cas9 binding characteristics. Comparison of anti-viral effect on HBeAg secretion (A) and total HBV DNA (B) 5 days post transfection of 250 ng dSpCas9 with 125 ng of respective sgRNA combination in HepG2-H1.3. and HepG2-pEpi-H1.3 cells Determination of anti-HBV effect on HBeAg (C) and total HBV DNA with qPCR (D) in HepG2-H1.3. cells 24 h post transfection of 250 ng SpCas9 or dSpCas9 with respective sgRNA combination compared to control. Statistical significance was determined using unpaired Students *t*-test with Welsh's correction (*: $p < 0.05$; **: $p < 0.01$; ***: $p < 0.001$; ****: $p < 0.0001$).

24 h post transfection we performed CTB analysis showing no reduction of cell viability in HepG2-H1.3. and HepG2-pEpi-H1.3. (data not shown). To analyze effects on viral parameters we measured HBeAg expression 5 days post transfection. Results (Fig. 38 A) revealed no reduction of HBeAg in HepG2-pEpi-H1.3. Interestingly, transfection of dSpCas9 led to reduced secretion of HBeAg in HepG2-H1.3. for sgRNA X+C and X+S compared to nonsense control.

In contrast to HBeAg, relative quantification of total HBV DNA (Fig. 38 B) showed significant reduction in HepG2-H1.3. for all sgRNA combinations compared to HepG2-pEpi-H1.3., where no reduction was detectable. In comparison to dSpCas9 expression, HBeAg (Fig. 38 C) and total HBV DNA (Fig. 38 D) was further and significantly reduced in cells transfected with enzymatic active SpCas9.

In summary these results indicated that binding of SpCas9 protein might be affected when targeting episomal structures which could lead to a reducing CRISPR/Cas9 effect. To confirm this finding, further experiments like binding assays have to be performed.

3.4.4. CRISPR/Cas9 targeting induced lower numbers of genome editing against episomal HBV DNA

Besides differences in CRISPR/Cas9 binding, also genome editing between integral and episomal HBV DNA forms differ. Therefore, we amplified the targeting region of sgRNA S and analyzed genome editing events using NGS sequencing with Illumina PE250 machine (Novogene). For comparison analysis, we used HepG2-H1.3. and HepG2-pEpi-H1.3. treated with SpCas9 and sgRNA X and sgRNA S combination for 5 days.

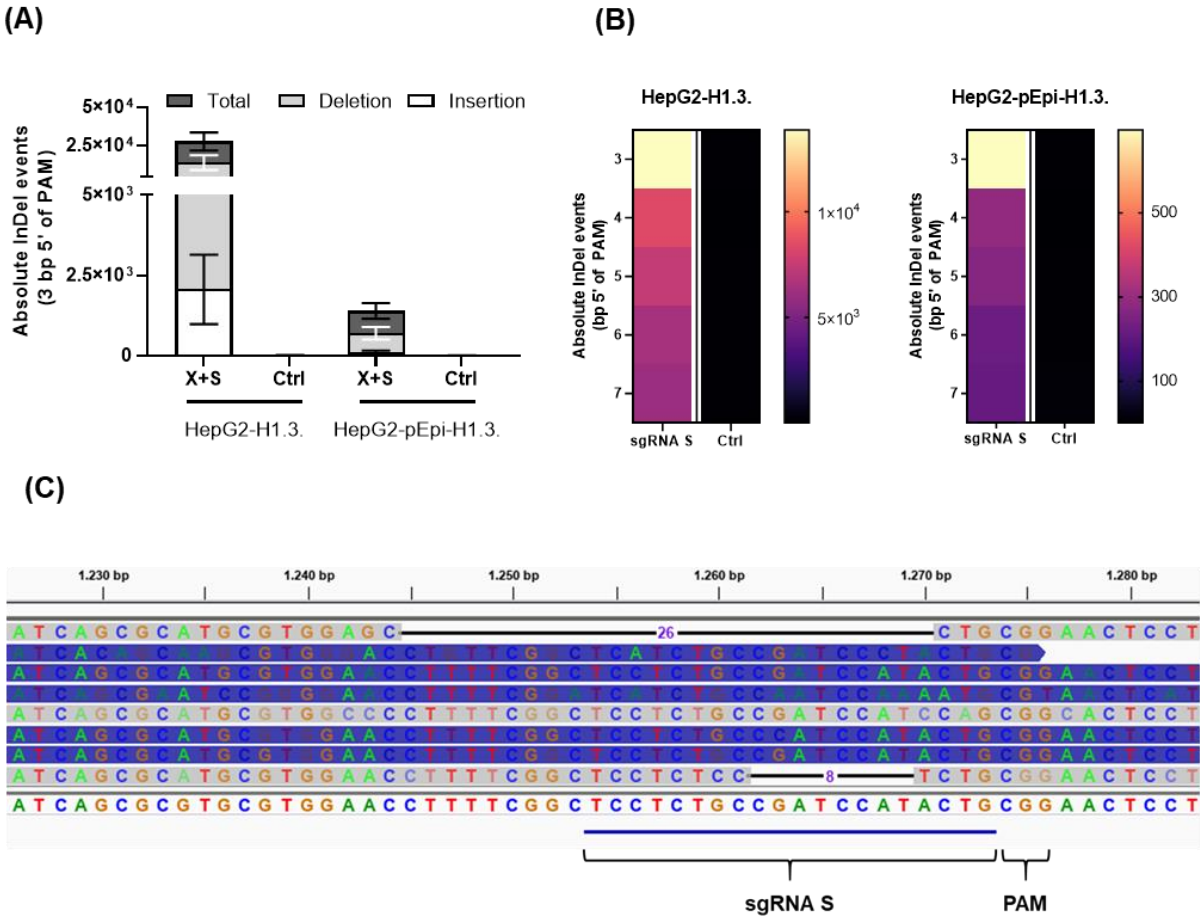

Figure 39: Next-generation sequencing of CRISPR/Cas9 editing. Genome editing was analyzed at certain regions upstream of PAM motif (NGG) within target site of sgRNA S. (A) Analysis of InDel mutations 3 bp 5' of PAM motif at target site in HepG2-H1.3. and HepG2-pEpi-H1.3. 5 days post treatment with 250 ng SpCas9 mRNA and 125 ng sgRNA X/S. (B) Absolute number of InDel events 3-7 bp 5' of PAM motif in both cell lines. (C) Sequence comparison of HepG2-H1.3. treated samples with WT HBV genome including sgRNA S target site and PAM motif.

To compare genome editing, we analyzed InDel events exclusively 3 bp upstream of PAM motif in comparison to WT HBV sequence. Genome editing events (Fig. 39 A) were detectable in both cell lines when compared to nonsense sgRNA treated samples. Interestingly, deletion events were more prominent than insertion events for both cell lines. When comparing absolute numbers of genome editing events, HepG2-H1.3. showed higher numbers of InDels at the depicted target site in comparison to HepG2-pEpi-H1.3. Sequence comparison of 3-7 bp 5' of PAM (Fig. 39 B) revealed genome editing at every location analyzed in both cell lines. Overall number of InDel events decreased with increasing distance to SpCas9 cleavage site 3 bp 5' of PAM motif. Additional to InDels, also larger deletions (Fig. 39 C) were observed for HepG2-H1.3. treated samples in contrast to HepG2-pEpi-H1.3 in which no such events were detectable.

In summary our NGS data indicated that CRISPR/Cas9 targeting of integrated HBV DNA (HepG2-H1.3.) led to more but not to qualitatively different genome editing events when compared to episomal target (HepG2-pEpi-H1.3.).

3.4.5. Long-term expression of CRISPR/Cas9 compensated for structure dependent effect

Previous experiments used IVT mRNA allowing transient expression of SpCas9 protein to investigate early events of CRISPR/Cas9 efficiency, by limiting protein amount and exposure time.

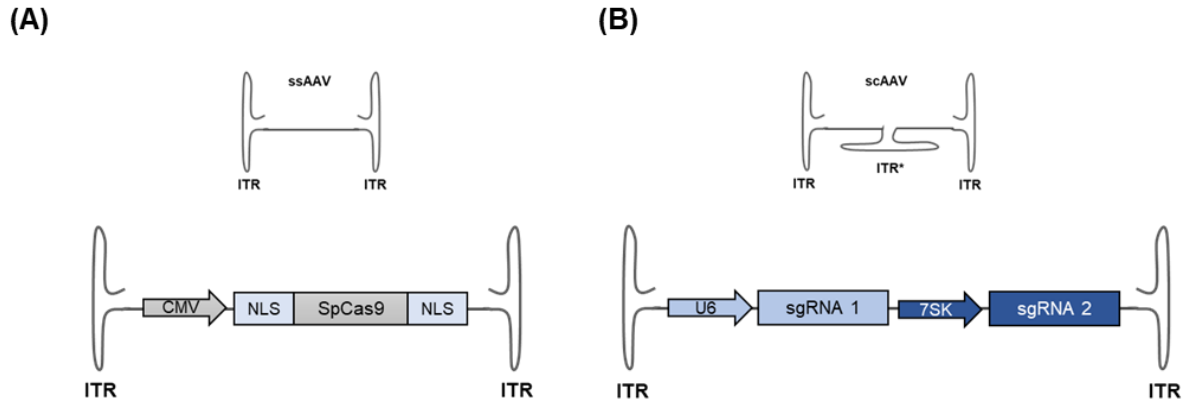

Figure 40: Schematic representation of AAV-SpCas9 constructs. (A) Single-stranded (ss) AAV encoding for SpCas9 under control of CMV promotor. SpCas9 harbors 5' SV40 and 3' Nucleoplasmin nuclear localization signal (NLS). (B) Self-complementary (sc) AAV encoding for two sgRNAs (sgRNA 1 and sgRNA 2) under the control of U6 or 7SK promotor.

To analyze if the described structural dependent effects could be overcome by prolonged overexpression of SpCas9, we repeated the experiments using two separated AAV vectors (Fig. 40) harboring either SpCas9 or a combination of two sgRNAs. To ensure strong expression of sgRNAs, we used self-complementary (sc)AAVs (A) which allow faster transgene expression than observed with conventional single-stranded (ss)AAVs (B) (McCarty 2008, Schmelas et al. 2018). For those experiments, we transduced HepG2-H1.3. and HepG2-pEpi-H1.3. with MOI $5x10^4$ for AAV-SpCas9 and MOI $1x10^5$ for AAV-sgRNAs.

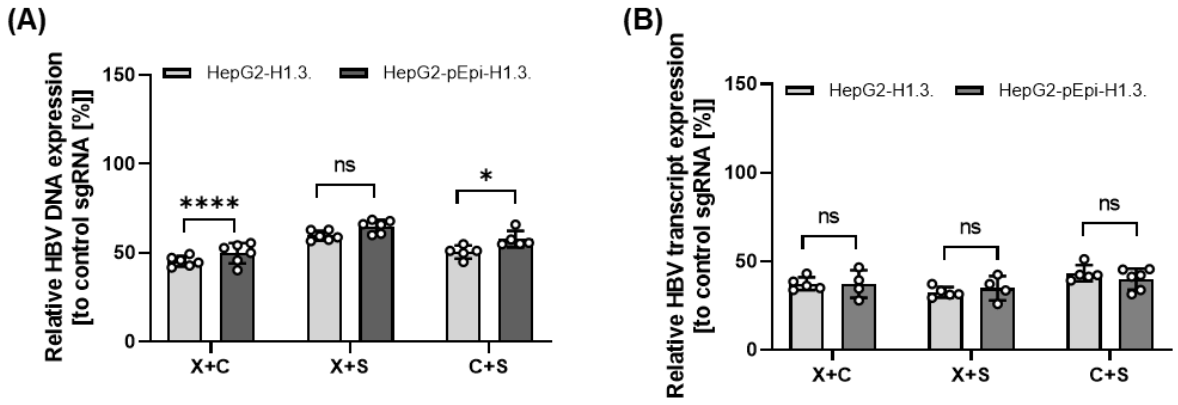

Figure 41: Analysis of long-term anti-viral effects using AAV-SpCas9. Determination of anti-HBV effects on total HBV DNA (A) and total HBV transcripts (B) was performed 14 days after transduction of AAV-SpCas9 and AAV-sgRNA (both titer 10^5) into HepG2-H1.3. and HepG2-pEpi-H1.3 cells. Statistical significance was determined using unpaired Students *t*-test with Welsh's correction (*: $p < 0.05$; **: $p < 0.01$; ***: $p < 0.001$; ****: $p < 0.0001$).

Two weeks post transduction we analyzed total HBV DNA and total HBV transcripts using qPCR method. Relative quantification of total HBV DNA (Fig. 41 A) showed reduction in both cell lines independent of sgRNA combination when compared to nonsense sgRNA control. For sgRNA combinations X/C and C/S reduction of HBV DNA was significantly increased in HepG2-H1.3. when compared to HepG2-pEpi-H1.3. Treatment with X/S sgRNA did not show a significant difference, but still HepG2-H1.3. had slightly lower expression of HBV DNA than HepG2-pEpi-H1.3. Analysis of total HBV transcripts expression (Fig. 41 B) indicated strong reduction in HepG2-H1.3. and HepG2-pEpi-H1.3. compared to nonsense control, but no significant difference between both cell lines was detectable.

In summary, these data suggested that long-term expression of CRISPR/Cas9 components could compensate for structure dependent effects, e.g. a reduced binding to episomal DNA.

3.5. Combinatorial treatment of HBV using CRISPR/Cas9 and RNAi containing AAV vectors

3.5.1. Improvement of AAV based system to allow efficient HBV targeting

As mentioned previously, current treatment options against HBV are mostly using nucleos(t)ide analogous targeting the reverse transcription step of the viral life cycle. The persistence form cccDNA and viral transcripts are not affected by those treatments, preventing complete cure of chronic infection. Therefore, we were interested to establish a combinatorial system targeting those elements by combining CRISPR/Cas9 with RNAi technology. Establishment, optimization and production were performed in cooperation with Carolin Schmelas and are described in her PhD thesis (Schmelas 2020). Our results indicated that targeting of HBV by CRISPR/Cas9 was already a suitable tool showing significant reduction of viral parameters after long-term expression. RNAi against HBV transcripts was demonstrated to be highly efficient when targeting the 3' overlapping region common for all transcripts using shHBV7 construct, reducing viral load *in vitro* and *in vivo*, supporting clearance of chronic HBV in addition to further treatments (e.g. TherVac).

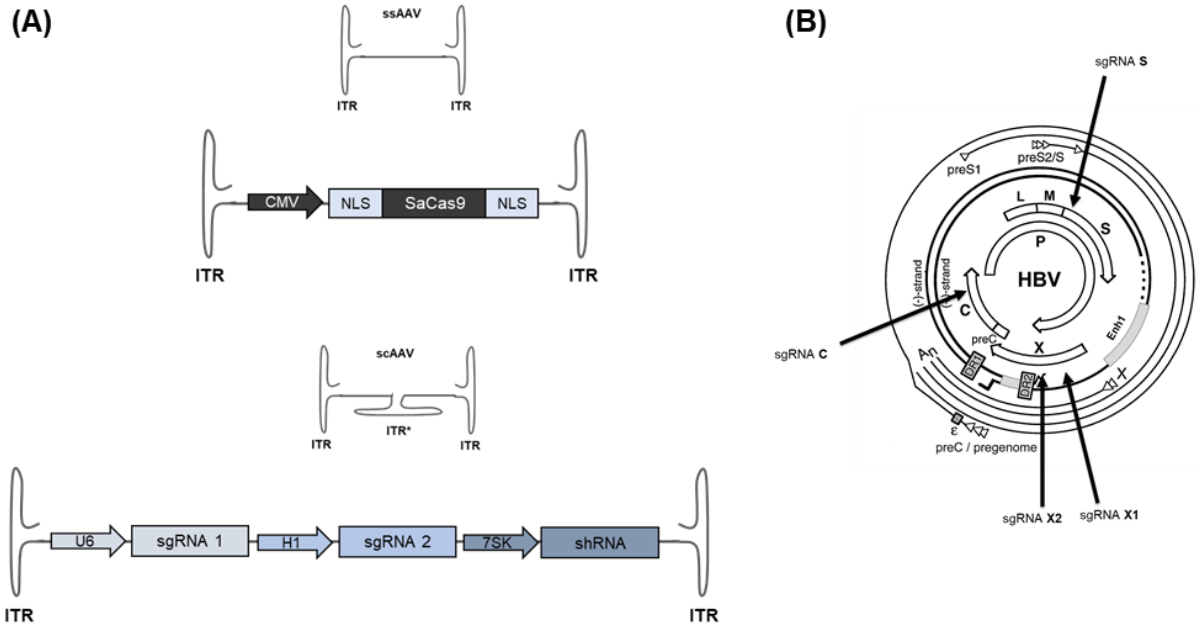

Figure 42: Schematic representation of combinatorial CRISPR/Cas9-RNAi AAV system. (A) ssAAV encoding for SaCas9 under control of CMV promotor (top) and scAAV encoding for sgRNA (anti HBV or control) and shRNA (anti-HBV or control, bottom). (B) CRISPR/Cas9 targeting of different sequences within the HBV genome: sgRNA S (S ORF), sgRNA C (C ORF), sgRNA X1 and sgRNA X2 (X ORF).

To combine both systems we used two separate AAV-based vectors (Fig. 42 A) encoding for Cas9 and a cassette of two sgRNAs and one shRNA to validate our hypothesis. In contrast to our IVT mRNA studies, we used *Staphylococcus aures* (Sa) Cas9 which is smaller than SpCas9 and allows the production of one combinatorial AAV encoding for all elements. For the following experiments we used scAAVs encoding for two sgRNA and one shRNA. In preliminary experiments, we utilized AAV capsid A9.2 which showed very low transduction efficiency *in vitro* (data not shown). Therefore, we tested different capsids identifying LK03 as best candidate for our experiments (data not shown). To evaluate our CRISPR/Cas9 approach we tested different combinations of sgRNAs targeting X (X1 and X2) and C regions of HBV (Fig. 42 B), showing only a low reduction of viral parameters (data not shown). To improve functionality, we exchanged sgRNA targeting C region with a sgRNA against S region which has demonstrated high genome editing efficiency in cell culture (data not shown) and combined it with sgRNA X2.

3.5.2. Efficient reduction of viral parameters using combinatorial AAV system

To analyze functionality of our final constructs, we transduced HepG2.2.15 and infected K7 cells (MOI 500) with MOI 10^5 of AAV-SaCas9 and MOI 10^5 of respective AAV-sgRNA/shRNA. In contrast to our SpCas9 long-term experiments, we performed the experiment for 3 weeks monitoring reduction of viral parameters by HBeAg measurement 2, 6, 10, 16 and 21 d post transduction.

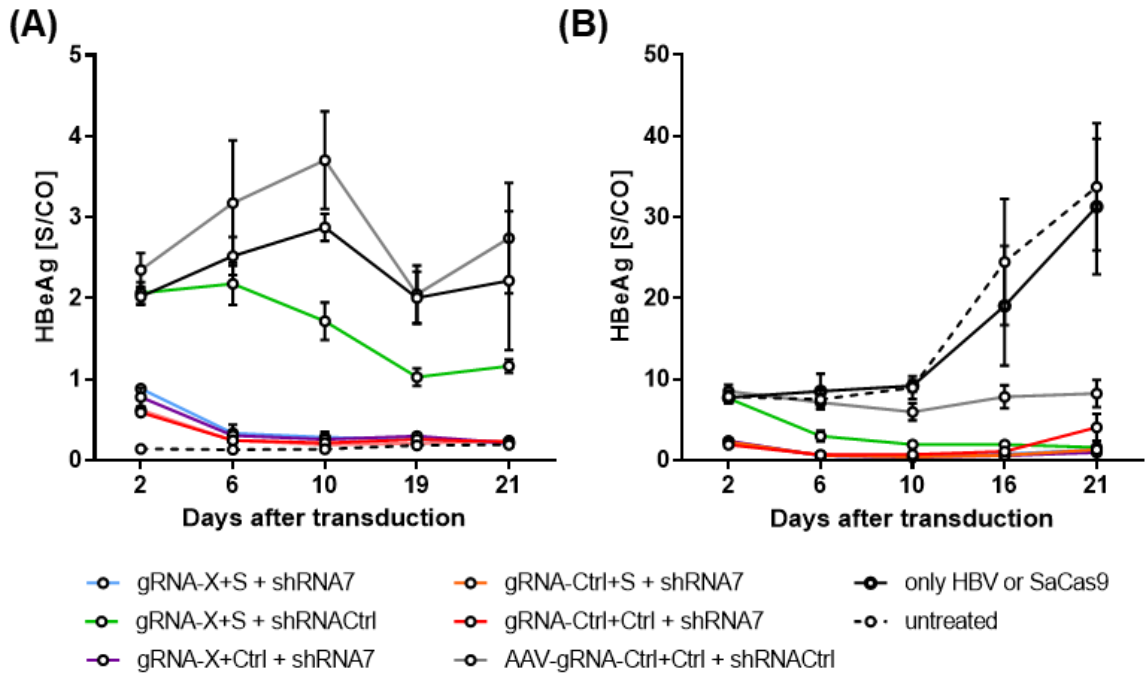

Figure 43: Time dependent antiviral effect using combinatorial system. Infected HepG2-NTCP-K7 (MOI 500 WT HBV, A) and HepG2.2.15 cells (B) were transduced with indicated AAV constructs. Measurement of secreted HBeAg was performed at depicted time points.

Results of HBeAg measurement (Fig. 43) displayed strong reduction with all constructs harboring shHBV7 independent of CRISPR/Cas9 system already 2 days post transduction in infected HepG2-NTCP-K7 (A) and HepG2.2.15 (B). Constructs containing exclusively the CRISPR/Cas9 system and a control shRNA (green line) showed reduction after 10 days in K7 and 6 days in HepG2.2.15 cells post transduction when comparing to control (grey).

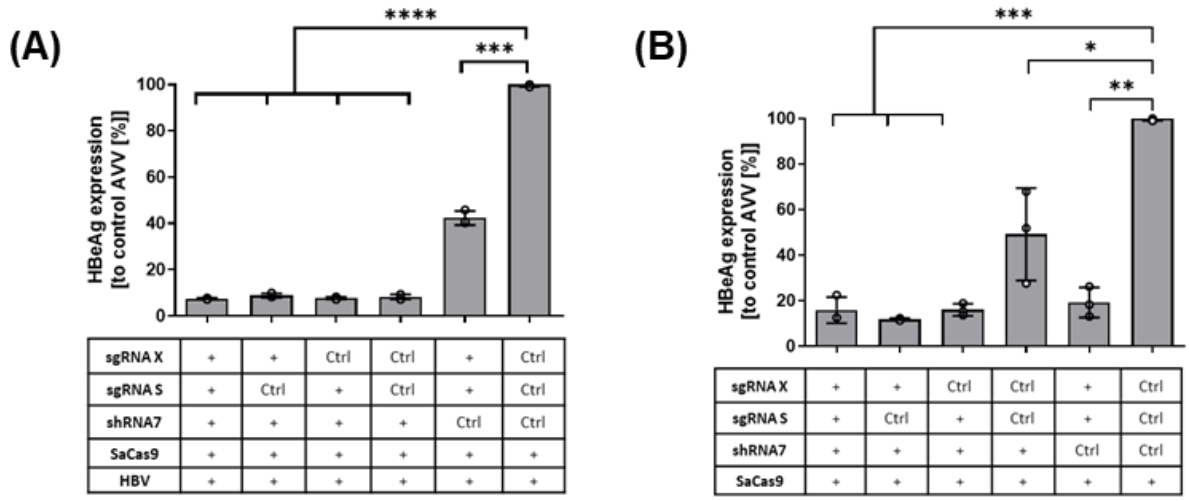

Figure 44: Comparison of anti-HBV effect by combinatorial AAV system (I). Analysis of anti-HBV effects was performed 3 weeks post transduction of indicated AAV constructs. Determination of secreted HBeAg levels in infected HepG2-NTCP-K7 (A) and HepG2.2.15 cells (B) was determined with BEP measurement. Statistical significance was determined using unpaired Students *t*-test with Welsh's correction (*: $p < 0.05$; **: $p < 0.01$; ***: $p < 0.001$; ****: $p < 0.0001$).

Three weeks post transduction, HBeAg measurement (Fig. 44) revealed significant reduction with all constructs in both cell lines compared to control. Interestingly, the structural dependency of this effect was also detectable using AAV-SaCas9 system, showing stronger reduction of HBeAg in HepG2.2.15 (5-fold, B) than K7 (2-fold, A) CRISPR/Cas9 treated cells. To further characterize anti-HBV effects, we performed qPCR analysis for total HBV DNA and total HBV transcripts.

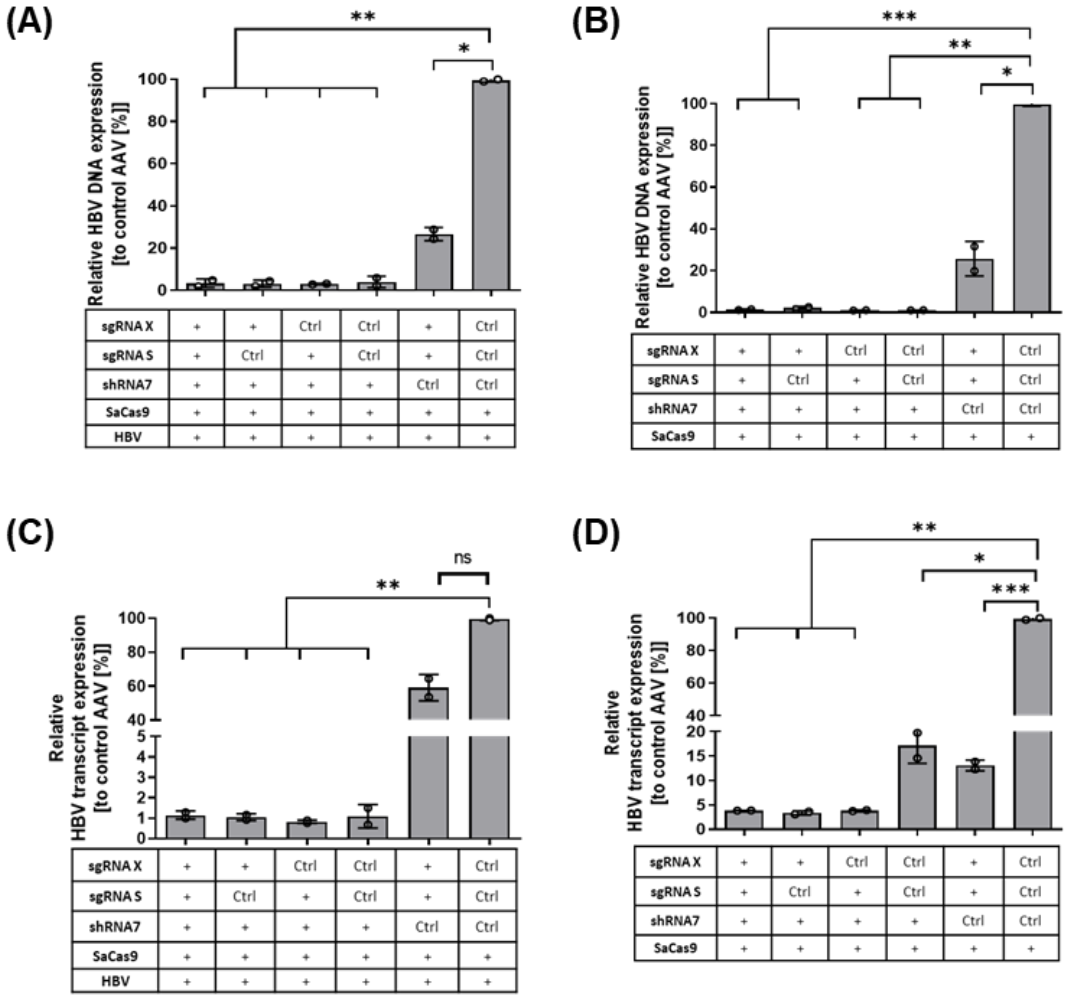

Figure 45: Comparison of anti-HBV effect by combinatorial AAV system (II). Analysis of anti-HBV effects was performed 3 weeks after transduction of indicated AAV constructs. Determination of total HBV DNA and total HBV transcripts in infected HepG2-NTCP-K7 (A, C) and HepG2.2.15. (B, D) was determined with qPCR analysis. Statistical significance was determined using unpaired Students *t*-test with Welsh's correction (*: $p < 0.05$; **: $p < 0.01$; ***: $p < 0.001$; ****: $p < 0.0001$).

Relative quantification of HBV DNA (Fig. 45 A, B) showed significant reduction in both cell lines for all constructs expressing shHBV7 compared to control. For the CRISPR/Cas9 only approach HBV DNA in HepG2.2.15 (B) and in K7 (A) was significantly lower than for control treated cells. Analysis of total HBV transcripts (Fig. 45 C, D) indicated similar significant reduction in both cell lines for all constructs with shHBV7. In contrast, significant reduction in CRISPR/Cas9 only constructs were detectable when targeting HepG2.2.15 (4-fold, D) but not when targeting K7 (2-fold, C) cell line in comparison to control construct.

In summary our results showed a strong reduction of viral parameters using shHBV7 but only a moderate effect when targeting HBV by CRISPR/Cas9. Additionally, no combinatorial effect could be noted due to high efficiency of the RNAi system.

4. Discussion

4.1. Additional optimization steps to further enhance IVT mRNA

During this study we used IVT mRNAs modified with ARCA cap and Ψ-UTP/m^5CTP nucleoside modification. The combination of those modifications has demonstrated best cell viability, transfection efficiency and protein expression in differentiated HepG2 *in vitro* system. This combination was shown to be highly efficient and was already used in previous studies of several groups (Warren et al. 2010, Vaidyanathan et al. 2018). Still, further optimization might be needed to improve this system. We have used ARCA cap which was described to inhibit formation of reversed orientated capped mRNAs compared to standard Cap 0 analog. Thus, transfection efficiency, protein expression and genome editing by CRISPR/Cas9 was more efficient with ARCA capped mRNAs.

Nevertheless, as mentioned before, there are also other eukaryotic Caps (Cap1 and Cap2) available which could be more beneficial. As it was recently described CleanCap (a Cap1 variant) offers higher yields of capped mRNAs compared to the ARCA approach. Cap 2 variants are currently under investigation, probably showing further improved characteristics (Vaidyanathan et al. 2018).

Since we are using HiScribe ARCA kit according to manufacturer's instructions, the ratio of modified to unmodified nucleosides in our produced IVT mRNAs is 50:50. In contrast, other groups reported improved functionality using 100% Ψ-UTP, 25% Ψ-UTP and 25% m^5CTP or 100% Ψ-UTP/ me^1ψ-UTP (Kariko et al. 2012, Levy et al. 2013, Yoshioka et al. 2013, Andries et al. 2015). Therefore, further testing of different modifications and ratios could be important to improve our IVT mRNA system. Besides chemical modifications, optimization of the CDS sequence could be another promising way to enhance functionality. It was shown that uridine depletion of firefly luciferase and SpCas9 IVT mRNA increased protein expression *in vitro* (Vaidyanathan et al. 2018). Further, a study from Kariko *et al.* described higher functionality of unmodified but uridine depleted mRNA *in vivo* when compared to Ψ-UTP variant (Kariko et al. 2012). In a last step, it was demonstrated that a 120 nt poly(A) tail is sufficient to reduce degradation of transfected IVT mRNAs (Holtkamp et al. 2006).

Therefore, introducing 120 nt poly(T) sequences within plasmid or PCR templates could lead to production of identical tailed mRNAs which further enhances downstream applications.

4.2. Transient expression of Cav-1 does not affect HBV uptake

Introduction of Cav-I in HepG2-NTCP-K7 using IVT mRNA led to expression of high amounts of functional protein, which was shown by Western blot analysis and $CTB_{Atto488}$ uptake assay. Interestingly, no effect on HBV entry was detectable, indicating that either Cav-I plays no role in HBV internalization in HepG2-NTCP-K7 cell line or that additional factors of related downstream pathways are not expressed. In contrast to HepaRG cell line, where Cav-I was described as important entry factor, Cav-I protein expression was not detectable in HepG2-NTCP-K7 indicating that other pathways are involved, such as clathrin-mediated endocytosis. This hypothesis is supported by findings in HuS-E/2, an immortalized primary human hepatocyte cell line, in which HBV entry is clathrin-dependent (Macovei et al. 2010, Huang et al. 2012). To analyze if transient expression of Cav-1 affects full cellular functionality and thereby downstream pathways, we generated HepG2-NTCP-K7-Cav-1 cell lines and repeated the experiments. As results indicate, Cav-1 expressing cell lines showed enhanced uptake of HBV in contrast to parental cell lines, indicating that additional factors must be expressed to allow Cav-1 dependent HBV uptake (Chakraborty 2020).

In conclusion, the experiment revealed that transient introduction of Cav-1 by IVT mRNA is not suitable to reconstitute functionality of complete Cav-1 dependent pathway. One way to overcome this problem is either by repeated transfection of IVT mRNA or transfection of multiple IVT mRNAs involved in one pathway. The latter was shown to be suitable for reprogramming of human fibroblasts into induced pluripotent stem cells (iPSCs) (Warren et al. 2010). Additionally, preliminary experiments using IVT mRNAs encoding for EGFP and RFP (data not shown) showed almost 100% of double positive cells. This indicate that efficient introduction of multiple IVT mRNAs in cells encoding for proteins involved in certain pathways might become a promising tool for whole pathway analyzes.

4.3. Advantages of IVT mRNA in contrast to AAV or pDNA vectors

Transfection of IVT mRNA showed high transfection efficiency, low cytotoxicity and high protein expression in our differentiated hepatoma cell lines, as well as in primary cells. In comparison to pDNA, transfection with mRNA led to much higher numbers of transfected cells and increased protein expression. This is due to the large size of complexed pDNA and the need to enter the nucleus to be transcribed whereas IVT mRNA can directly be translated in the cytoplasm (Rettig et al. 2010, Steinle et al. 2017). Thus, pDNA transfection of dividing cells like HEK293 is much higher compared to non-dividing and differentiated cells like HepG2, which nearly stop cell division (de Los Milagros Bassani Molinas et al. 2014, Leonhardt et al. 2014). Another important advantage over pDNA is the fact that no additional elements (like ori, antibiotic selection) are introduced to cell lines which can have adverse effects (e.g. triggering immune responses), as IVT mRNAs exclusively harbor the coding sequence and regulatory elements (Hemmi et al. 2000).

As mentioned already in the introduction, one of the biggest advantages of IVT mRNA over viral vectors is the exclusively transient expression making additional inactivation steps unnecessary. Further, IVT mRNA lack the risk of insertion, and cannot trigger oncogenic mutations which is the main safety concerns against integrating vectors for human therapies (Mallon et al. 2014, Steichen et al. 2014). Therefore, non-integrative vectors like AAV are becoming more important for clinical application. Those vectors face other problems like low transduction efficiency *in vitro* and small packaging space. The transduction efficiency is dependent on the capsid variants, which have to be exchanged for different cell lines (Ellis et al. 2013). In contrast, IVT mRNA can be applied easily to other cell lines showing suitable transfection efficiency and protein expression without complicated adaption. Another promising alternative to the current used vectors and IVT mRNAs could be Sendai viruses (SeV) which are independent of DNA phase and show more efficient reprogramming than IVT mRNA. Additionally, production of SeV is cheaper and already successfully applied in different groups (Hu 2014, Schlaeger et al. 2015).

Still further improvements for this technique are needed, especially concerning *in vivo* applications facing different problems, like immunogenicity, delivery efficiency but also cheaper production (Sahin et al. 2014, Hecker 2016, Slivac et al. 2017). Nevertheless, IVT mRNA is a promising tool for future therapeutic applications to allow safe and efficient treatment of different diseases or chronic viral infections.

4.4. Advantages of NTCP IVT mRNA introduction in contrast to stably expressing NTCP cell lines

Transfection of different amounts of IVT mRNA encoding for NTCP showed increasing expression of protein in transfected cells compared to pDNA or AdV systems which led to dose-dependent effects on bile acid uptake, HBV uptake and infection. The results indicate that our introduced IVT mRNA led to HBV permissivity of otherwise resistant HepG2 cells even when expressing very low levels of NTCP protein. These results demonstrate that HBV needs a certain NTCP threshold on the cellular surface for entry and infection. Our findings are confirmed, when comparing the NTCP expression in other permissive cell lines like HepaRG or primary hepatocytes in which only low endogenous amounts are detectable (Ni et al. 2014). Further, these findings indicate that IVT mRNA transfection is a promising alternative to cell lines since high transfection efficiencies can be achieved. Cell lines which are frequently derived from clones, selected for specific characteristics often show highly different cellular homeostasis compared to the original cell population (Sommeregger et al. 2016). This was shown when performing proteome analysis of differentiated HepG2 and HepG2-NTCP-K7 revealing up–or downregulation of multiple genes (data not shown). Therefore, results and effects obtained from overexpressing cell lines can be artificial and clone specific but do not reflect the natural situation. Instead application of IVT mRNA allows analysis of cellular effects on population level using physiological amounts, leading to more robust and comparable results between cell lines and different research groups. Another important advantage of IVT mRNA is the fast production of different IVT mRNAs using pDNA templates for T7 based synthesis. Further, we showed that production could be accelerated when using PCR based templates harboring a T7 promotor (Stadler et al. 2020). Thus, allowing fast and easy production and subsequent testing of various constructs in different concentrations and combinations within days.

4.5. Unknown missing factors inhibit HBV infection in transfected non-hepatic cells

Transfection of NTCP IVT mRNA into non-hepatic cell lines resulted in high transfection efficiency and protein expression as well as uptake of bile acids. In contrast transfection of NTCP IVT mRNA did not allow uptake or infection with HBV in all tested cell lines. These results are supported by different studies in which cell lines stably expressing NTCP also did not support the full HBV life cycle (Ni et al. 2014, Meredith et al. 2016). Further, these findings indicate that not only cell clones, but also whole populations are not susceptible to HBV infection independent of NTCP expression. To ensure transcriptional activity, we used AdV vectors harboring the HBV sequence. Transduction in non-hepatic cell lines lead to expression of HBeAg indicating that transcription factors specific for HBV sequence are present in nuclei of tested cells. The same results were obtained in human NTCP transgenic mouse models, which do not support infection with viral particles but transcription from AAV-HBV templates. This indicate for missing factors involved in trafficking or repair of rcDNA within the nucleus of infected hepatocytes which can be bypassed using AAV vectors (Yang et al. 2014). In comparison, expression of human NTCP in a mouse hepatocyte cell line AML-12 supported infection with HBV and satellite virus HDV. This result demonstrated that in principle mouse hepatocytes harbor all HBV essential factors but simply lack human NTCP expression (Lempp et al. 2016). In conclusion, the results indicate that additional factors, probably liver specific, are missing or downregulated which are essential for viral life cycle. This is supported by a study of a Chinese group which showed HBV infection of HEK293 cells after introduction of NTCP and three additional factors (Yang et al. 2020).

As mentioned above, IVT mRNA allows transfection of multiple mRNAs with high efficiency and is therefore an interesting tool to introduce not only NTCP, but also additional factors simultaneously into non-hepatic cells to analyze their impact on HBV.

4.6. Improved CRISPR/Cas9 application using modified sgRNAs

Our results indicate that genome editing efficiency is significantly increased when using modified sgRNAs in contrast to IVT sgRNAs. This was already described in a previous study, where the authors compared 2'-O-methyl (M), 2'-O-methyl 3'phosphorothioate (MS) and 2'-O-methyl 3'thioPACE (MSP) modified sgRNAs showing increasing genome editing efficiency (Hendel et al. 2015). Additionally, T7 derived RNAs harbor three 5' phosphate groups which were described to trigger RIG-I immune responses, leading to increased IFNβ levels (Wienert et al. 2018). The activation of RIG-I signalling can be overcome by removing the 5' phosphates using calf-intestinal phosphatase (CIP). Kim *et al.* demonstrated that after CIP treatment, transfection of sgRNA molecules did not trigger RIG-I immune responses (Kim et al. 2018). This indicates that this additional step could improve genome editing efficiency, especially for those CRISPR variants (e.g. SaCas9, Cas12a), where no chemical synthesis or modification are commercially available. Furthermore, we confirmed previous observations that Ψ-UTP/m^5CTP modified mRNA did not trigger RIG-I dependent immune responses, allowing higher protein expression and reduced cytotoxicity in our cell culture models (Kariko et al. 2008, Henning 2019).

4.7. Low levels of Cas9:sgRNA complexes cause reduced targeting efficiency against multiple targets

CRISPR/Cas9 targeting of HBV integrates showed reduced anti-viral effects correlating with increasing copy number of the target (HepG2-H1.3.: 1; HepG2.2.15: 2; HepG2-911: 13-16). This indicates that CRISPR/Cas9 efficiency is dependent on the number of target sequences, losing efficiency if several sequences are located inside one cell. Interestingly, this effect is more pronounced when using IVT mRNA and sgRNA transfection, as compared to Cas9 RNP, long-term or stable expression of CRISPR/Cas9 system. An explanation for Cas9 RNP could be that Cas9 RNP and sgRNAs are complexed before transfection hindering degradation or dilution of sgRNA within the target cells and therefore increases genome editing efficiency (Kim et al. 2014, Ma et al. 2016).

In IVT mRNA applications sgRNAs are transfected separately and due to delayed Cas9 protein expression, efficient formation of Cas9:sgRNA complexes is reduced, leading to dilution or degradation of sgRNAs by intracellular nucleases (Ma et al. 2016). Since it was shown that the introduced modification MS reduces sgRNA degradation, the latter explanation could be excluded (Hendel et al. 2015). In contrast to transient systems, a strong promotor (like CMV or TTR) or stable expression of Cas9 protein and sgRNAs can compensate for intracellular degradation and therefore mimic the target depending effect, as high amounts of both factors are present within the cells (Seeger and Sohn 2014, Kennedy et al. 2015). A last explanation for this effect is based on the probability to introduce multiple InDel mutations that lead to stop codon or frameshift mutations in several target sites simultaneously. In high copy number situation separate frameshift mutations can easily be compensated by the remaining templates, which is not the case in a single copy situation. Therefore, successful targeting of HBV sequence within HepG2-H1.3. (1 copy/cell), in contrast to HepG2-911 (13-16 copies/cell), leads to significantly reduced viral parameter expression (Meyers et al. 2017).

4.8. Accessibility of episomal structures and cellular repair mechanism hinder efficient CRISPR/Cas9 targeting

The results of CRISPR/Cas9 targeting against pEpi-H1.3. episomal HBV DNA showed only slight reductions of viral parameters in contrast to cccDNA. Compared to targeting efficiency against integrated or episomal targets with equal copy numbers, efficiency is highly reduced in the episomal situation, indicating that CRISPR/Cas9 targeting is dependent on targeting localization. These observations are supported by several studies in which CRISPR/Cas9 targeting was aiming against integrated or pDNA-based HBV sequences or cccDNA demonstrating increased efficiency against integrated targets (Kennedy et al. 2015, Ramanan et al. 2015). Furthermore, it was described that targeting of mitochondrial DNA (mtDNA) by endonucleases like CRISPR/Cas shows low efficiency when compared to targeting of genome DNA. This indicates that CRISPR/Cas9 has lower efficiency against smaller and episomal structures in comparison to genome sequences (Jo et al. 2015, Antón et al. 2020). One explanation for this effect could be different binding efficiencies between integrated, linear and episomal, coiled sequences.

Probably, the rigid characteristics of long integrated sequences enables efficient screening for PAM sequences and full binding of sgRNAs whereas dynamic and shorter episomal structures, hinder those steps (Farasat et al. 2016). This would lead to lower genome editing rates within target sequences which would significantly reduce effects on viral parameters. Another explanation could be related to differences concerning repair of DSB introduced in integrated or episomal structures. As HDR is limited to certain cell phases when sister alleles for repair are present within the cells, integrated sequences are mostly repaired by NHEJ. In contrast, HBV infected cells harbor up to 10 copies of cccDNA per cell which can act as template for HDR, leading to correct repair and inhibiting the CRISPR/Cas9 based effects (Ko et al. 2018). This could also be an explanation for increased efficiency of CRISPR/Cas9 in single copy situation, where no repair template is present within the cells.

4.9. Improvements to counteract binding limitations of CRISPR to episomal structures

Transfection of silenced dSpCas9 resulted in significant reduction of HBV DNA in HepG2-H1.3. but no effect was detectable in HepG2-pEpi-H1.3. This result supports the findings obtained from experiments using functional SpCas9, indicating reduced binding to episomal structures by the Cas9:sgRNA complexes. Furthermore, results show that binding of the CRISPR/Cas9 complex it-self reduces transcriptional activity of targeted sequences probably through blocking the binding of transcription factors or even the whole transcriptional machinery (Farasat and Salis 2016). In contrast, functional SpCas9 shows a significantly increased reduction compared to silenced variant indicating that additional introduction of DSB further inhibits transcription from target sequence (Shanbhag et al. 2010, Pankotai et al. 2012). In summary, these findings lead to the conclusion that binding or genome editing characteristics of SpCas9 against episomal structures must be optimized to render CRISPR/Cas9 targeting more effective. One option could be a new variant of SpCas9 which is fused to the N-terminus of human codon-optimized RecA protein. RecA is a bacterial protein involved in single strand DNA (ssDNA) binding and in bacterial homologous recombination. It was described that genome editing efficiency using SpCas9-RecA is significantly increased compared to SpCas9 which is presumably based on enhanced DSB repair using single strand annealing (SSA).

First preliminary experiments using our pDNA based SSA-assay support this hypothesis, showing significantly increased numbers of $EGFP^+$ cells as well as increased MFI values 24 h after treatment with SpCas9-RecA compared to SpCas9 (data not shown). This result indicates that SpCas9-RecA can lead to more efficient and faster editing, reflected by higher protein expression within the first 24 h. Furthermore, this fusion-protein might enhance DSB repair by SSA/MMEJ pathway which could further improve inactivation of HBV sequences (Lin et al. 2017). Another alternative was described by Tsui et al. using a Cas9 variant from *Acidothermus cellulolyticus (*AceCas9) showing enhanced cleavage activity against negative supercoils (plasmid), which could be more suitable for targeting plasmid based or cccDNA molecules (Tsui et al. 2017).

4.10. Reduced numbers of InDel events in episomal target sites

NGS analysis of sgRNA S target site showed highly reduced numbers of genome editing events in HepG2-pEpi-H1.3. in comparison to HepG2-H1.3. This result supports the findings obtained from our dSpCas9 experiment indicating, that binding of SpCas9 to episomal targets is limited which further leads to strong reduction of genome editing. Since we only analyzed genome editing with sgRNA S target site, as it was shown that this region is targeted more efficiently by CRISPR/Cas9 (data not shown), we have to repeat this experiment with our other used sgRNA target sites. Furthermore, PCR for our sequencing templates needs to be further improved, as we utilized primers also recognizing rcDNA molecules. Since our cells produce high amounts of rcDNA which is not targeted by CRISPR/Cas9 the absolute number of genome editing events in our cell lines remain elusive. Therefore, application of nested-PCR for H1.3. template, not amplifying rcDNA sequences, would be beneficial. Nevertheless, the results of our experiments indicate that targeting of episomal structures is limited by binding of SpCas9 protein, leading to reduced genome editing and finally to highly reduced anti-viral effects.

4.11. Compensation of binding limitations by long-term expression

As mentioned above, transient expression of SpCas9 demonstrates significant differences in CRISPR/Cas9 efficiency against different HBV DNA forms. In contrast long-term expression using AAV systems revealed a compensation of the effect in single copy situation, showing comparable reduction of viral parameters when targeting HepG2-H1.3. and HepG2-pEpi-H1.3. The data indicate that one way to overcome the limitation of binding and subsequent reduced genome editing might be achieved through over- and long-term expression of Cas9 and sgRNA. Saturation of the system with functional Cas9:sgRNA complexes could allow repeated targeting of episomal structures, finally leading to binding and genome editing. In the transient situation the targeting frequency is limited and related to half-life of introduced IVT mRNA, lowering the chances to introduce DSB. Another option is based on sgRNA transcription from templates which reside already in the nucleus. Thus, intracellular produced sgRNAs are not diluted or degraded in the cytoplasm as exogenously derived sgRNAs leading to increased Cas9:sgRNA complex formation and enhanced functionality. As mentioned above, this efficient compensation is restricted to single copy situation as our data (Results Chapter 5.) and other studies showed reduced efficiency of CRISPR/Cas9 when targeting high copy templates (like cccDNA) (Kennedy et al. 2015, Seeger and Mason 2015). For future applications, long-term exposure or overexpression CRISPR/Cas9 systems are not desirable, as the risk of off-targeting is a major safety issue (Kleinstiver et al. 2016). Therefore, application of IVT mRNA reduces the risk of off-targeting simply by exclusively transient expression. Since IVT mRNA is degraded by cellular mechanisms no additional inactivation system has to be implemented to ensure controllable expression of CRISPR/Cas9 within target cells (Plews et al. 2010, Warren et al. 2010). Still, further optimizations of IVT mRNA have to be implemented to overcome insufficient effects which are based on transient expression.

4.12. Alternative CRISPR/Cas systems

In the current study we are mainly focusing on IVT mRNA SpCas9 CRISPR/Cas9 system, as it is the best described and most frequently used variant. Since this system shows limited efficiency against episomal structures, comparison of different Cas9 variants with improved features could be an additional step for future research. Until now different optimized SpCas9 versions were described (e.g. eSpCas9(1.1) and SpCas9-HF1) which mainly reduced the risks of off-targeting (Kleinstiver et al. 2016, Slaymaker et al. 2016). Further, protein engineering approaches were aiming to modulate the PI domain, enabling recognition of different PAM sequences to allow broader targeting (Ma et al. 2019). In contrast the optimization of SpCas9, application of other CRISPR systems from different species has become of great interest. One very prominent example is Cas9 from *Staphylococcus aureus* which is 1 kb smaller (3.2 kb) than SpCas9 (4.2 kb) allowing application in viral vectors like AAV having limited packaging space. In contrast to SpCas9, PAM sequence of SaCas9 is more complex limiting targeting capability. Another interesting candidate for targeting DNA is Cas12a form *Lachnospiricae bacterium ND2006*, has the same size like SpCas9 but recognizes a T-rich PAM motif allowing broader application (Swarts and Jinek 2019).

In contrast to SpCas9 and SaCas9, Cas12a can process its own guide RNA, allowing easy and efficient multiplexing. Additionally, studies in patients revealed pre-existing immunity against Sp and SaCas9 as both were derived from pathogenic bacteria (Charlesworth et al. 2019). In contrast, LbCas12a is originated from non-pathogenic bacteria with presumably no pre-existing immunity which would be of great interest for clinical translation. First preliminary studies of IVT mRNAs encoding for SaCas9 and LbCas12a showed protein expression and functionality but have to be further optimized in terms of their guide RNAs to become promising alternatives to target HBV.

4.13. Combinatorial treatment

The results of our combinatorial treatment system for chronic HBV, showed significant reduction of viral parameters when using RNAi containing vectors. Since the shRNA sequence (shHBV7) was already evaluated *in vitro* and *in vivo* our results confirmed its highly efficient anti-viral effect also in a multiplexed system. Targeting by CRISPR/Cas9 also showed significant reduction of viral parameters, independent of the RNAi system, which was increased in HepG2.2.15. Again, those findings support the assumption that targeting of different HBV DNA forms results in varying functionality of CRISPR/Cas9. Unfortunately, since reduction of viral parameters by shHBV7 alone is highly efficient, no additional effect of CRISPR/Cas9 was observable in our settings. To ensure the combinatorial effect for further studies, either the shHBV7 must be replaced by a less potent shRNA or a weaker promotor has to be implemented to reduce expression. Furthermore, the longer PAM sequence of SaCas9 compared to SpCas9 lead to reduced numbers of targeting sites, which limit its applicability. An opportunity to improve this could be to exchange PI domain of SaCas9 to allow targeting of smaller or alternative PAM sequences. This would allow targeting of additional sequences which could improve genome editing efficiency (Ma et al. 2019). Another option to improve the system could be based on a split-SpCas9 system, in which the C- and N-terminal part of SpCas9 protein are expressed from two individual AAVs. After transduction of both AAVs, the full SpCas9 is formed over intein-linkages (Schmelas and Grimm 2018). The advantage of such a system is that expression can be enhanced using scAAV systems leading to higher protein yield within cells and increased genome editing efficiency. Since Split-Cas9 systems are smaller, additional sgRNAs can be inserted into the AAV vectors. To further optimize the system, safety aspects also have to be taken into account. As mentioned above, long-term expression of CRISPR systems can increase the risk of off-target events therefore, different inactivation strategies like SpCas9 inhibitor, self-inactivation systems or coupling of Cas9 to artificial inhibitory domains have to be evaluated (Li et al. 2019, Song et al. 2019, Aschenbrenner et al. 2020). Besides CRISPR, also RNAi long-term expression can lead to undesired off-target effects. Co-delivery of decoys called “TuD” were shown to reduce such effects, through binding of sense strand shRNA sequences reducing off-target gene regulation (Mockenhaupt et al. 2015, Michler et al. 2016).

4.14. Summary and conclusion

In this work we established and optimized our IVT mRNA-based system by implementation of ARCA cap and ψ-UTP/m^5CTP modification. The system supports high transfection efficiency and protein expression without cytotoxicity in different non-dividing and dividing cell lines. Furthermore, we improved an mRNA based CRISPR/Cas9 system showing high genome editing efficiency using modified sgRNAs in our established SSA assay platform. We applied the IVT mRNA technique to analyze Cav-1 dependent effect on HBV uptake in HepG2-NTCP-K7 cell line and NTCP HBV dose-dependent effects in HepG2 cell line. Additionally, we investigated the effect on HBV uptake and infection in IVT mRNA NTCP transfected non-hepatic cell lines. With our optimized CRISPR/Cas9 system we analyzed transient efficiency of SpCas9 targeting different localized HBV DNA forms, leading us to the conclusion that binding is the limiting step reducing CRISPR/Cas9 targeting efficiency against episomal structures. Thus, we showed that long-term expression of CRISPR/Cas9 using AAV-delivery systems could compensate for reduced binding of SpCas9. Finally, we improved our combinatorial RNAi CRISPR/Cas9 system targeting HBV in cooperation with AG Grimm (Schmelas 2020). The established system enables significant reduction of viral parameters after long-term expression. Those results allow us to continue with further experiments in different mouse models, analysing the capability of the system to reconstitute anti-HBV immunity.

In conclusion, the results in this study revealed, that IVT mRNA is a powerful tool for different applications in basic and translational biology. With this technique it is possible to analyze impacts of different proteins *in vitro*, simultaneously and in a time saving manner. Besides the results mentioned in this work we used the established IVT mRNA in different applications (e.g. HBV X, ISG20 and TherVacB) showing promising results. Our results concerning the combinatorial system allows us to continue with this project as well as to analyze optimized versions of the system in different mouse models.

5. Materials and Methods

5.1. Materials

In the following chapters, used materials and applied methods are described. Materials This section gives an overview of the used laboratory materials, machines and software applications.

5.1.1. Cell lines

Table 1: Cell lines

Name	Description
HEK293	Human embryonic kidney cells, transformed with fragments of adenovirus type 5 DNA (Graham et al. 1977)
HepG2.2.15	HBV-producing hepatoblastoma cell line (Sells et al. 1987)
HepG2-H1.3.	Human hepatoma cells replicating HBV from a 1.3-fold genome integrate (Untergasser et al. 2004)
HepG2-NTCP-K7	HepG2 derived clone transduced with lentiviral based expression cassette for NTCP (Ko et al. 2018)
HepG2	Hepatocellular carcinoma cell line (Knowles et al. 1980)
U2OS	Bone osteosarcoma cell line (Ponten et al. 1967)
A549	Lung carcinoma cell line (Giard et al. 1973)
HeLa	Cervix adenocarcinoma cell line (Gey et al. 1952)
HepG2-911	Hepatocellular carcinoma cell line, transfected with piggyBac containing 1.3-fold HBV genome
E. coli TOP10	Chemically competent *E. coli* (Thermo Scientific Scientific Scientifc)
Stellar cells	Chemically competent *E. coli* strain HST08 (Takara)

5.1.2. Cell culture media

Table 2: Cell culture media

	Standard medium	Differentiation medium
Dulbecco's Modified Eagle Medium: Nutrient Mixture F-12 (DMEM/F-12)	500 mL	500 mL
Heat-inactivated fetal calf serum (FCS)	10%	10%
Penicillin/streptomycin	100 U/mL	100 U/mL
DMSO		2.5%

5.1.3. Modified sgRNAs

All 2'O-methyl 3'phosphothiorate (MS) modified sgRNAs were ordered from Merck (Billerica, USA).

Table 3: sgRNA sequences

sgRNA	Sequence	Source
PCSK9	GGTGCTAGCCTTGCGTTCCG	(Oswald 2016)
Nonsense	GGGTCTTCGAGAAGACCT	(Wang et al. 2017)
HBV S ORF	TCCTCTGCCGATCCATACTG	(Ramanan et al. 2015)
HBV C ORF	AGCTTGGAGGCTTGAACAGT	(Wang et al. 2015)
HBV X ORF	AGGAGGCTGTAGGCATAAAT	(Wang et al. 2015)

5.1.4. PCR oligonucleotides

PCR oligonucleotides were purchased from Microsynth AG (Balgach, Switzerland).

Table 4: PCR oligonucleotides

Name	Sequence
cccDNA 2251+	AGCTGAGGCGGTATCTA
cccDNA 92-	GCCTATTGATTGGAAAGTATGT
HBV DNA 1745	GGAGGGATACATAGAGGTTCCTTGA
HBV DNA 1844	GTTGCCCGTTTGTCCTCTAATTC
PRNP fw	TGCTGGGAAGTGCCATGAG
PRNP rev	CGGTGCATGTTTTCACGATAGTA
18S fw	AAACGGCTACCACATCCAAG
18S rev	CCTCCAATGGATCCTCGTTA
IFNß fw	GCCGCATTGACCATCT
IFNß rev	AGTTTCGGAGGTAACCTG
HBV1805fw	TCACCAGCACCATGCAAC
HBV1896rev	AAGCCACCCAAGGCACAG
pEpi-H1.3. fw	GACCACTACCAGCAGAACAC
pEpi-H1.3. rev	GAACTCCAGCAGGACCATG
sgRNA 1 [v1]	TAATACGACTCACTATAGGG

sgRNA 1 [v2]	TAATACGACTCACTATA
sgRNA 2	GTTTTAGAGCTAGAAATAGCAAGTTAAAATAAGGCTAGTCCGTTATCAACTTGAAAAAGTGGCACCGAGTCGGTGCTTTTTT
sgRNA 3	TAATACGACTCACTATAGGG**[X]**GTTTTAGAGCTAGAAAT
sgRNA 4	AAAAAAGCACCGACTCGGTG
SaCas9 sgRNA 2	TAATACGACTCACTATAGGG**[X]**GTTTTAGTACTCTGGAA
SaCas9 sgRNA 3	GTTTTAGTACTCTGGAAACAGAATCTACTAAAACAAGGCAAAATGCCGTGTTTATCTCGTCAACTTGTTGGCGAGATTTTTTT
SaCas9 sgRNA 4	AAAAAAATCTCGCCAACAAGTTG
S ORF fwd	GCAGGCTTTCACTTTCTCG
S ORF rev	AGCCTAGCAGCCATGGA

5.1.5. Kits

Table 5: Kits

Product	Supplier
GeneJET Gel Extraction Kit	Fermentas, St. Leon-Rot, Germany
GeneJET Plasmid Miniprep Kit	Thermo Scientific Scientific Scientific, Schwerte, Germany
Lightcycler 480 SYBR Green I Master mix	Roche, Mannheim, Germany
NucleoSpin RNA isolation Kit	Machery-Nagel, Düren, Germany
NucleoSpin Tissue Kit	Machery-Nagel, Düren, Germany
SuperScript III First-Strand Synthesis SuperMix for qRT-PCR	Invitrogen, Carlsbad, CA, USA
HiScribe T7 ARCA	New England Biolabs, Ipswich, USA
High yield T7	New England Biolabs, Ipswich, USA
InFusion	Takara, Kyoto, Japan
Ambion mMessage mMachine T7 Transcription Kit	Invitrogen, Carlsbad, CA, USA

5.1.6. Antibodies

Table 6: Antibodies

Name	Supplier	Catalogue number	Application (dilution)
NTCP (K9)			WB (1:1000)
FLAG	Abcam	Ab49763	WB (1:1000)
Vinculin	Abcam	Ab129002	WB (1:1000)
ß-Actin	Sigma	AC-15	WB (1:1000)
Caveolin-1	Cell Signaling	D46G3	WB (1:1000)
Gαm	Sigma	A0168	WB (1:10000)
Gαr	Sigma	A5420	WB (1:10000)

5.1.7. Plasmids

Table 7: Plasmids

Name	Encoding features	Number
pDNA-SSA	Single-strand annealing Assay template; RFP; EGFP; SpCas9 target site for PCSK9 sgRNA	905
pDNA-SSA-SaCas9	Single-strand annealing Assay template; RFP; EGFP; SaCas9 target site for PCSK9 sgRNA	n.a.
pDNA-SSA-LbCas12a	Single-strand annealing Assay template; RFP; EGFP; LbCas12a target site for DNMT1 crRNA	n.a.
pDNA-T7-SpCas9	Production template SpCas9	793
pDNA-T7-dSpCas9	Production template dSpCas9	n.a.
pDNA-LbCas12a	Production template LbCas12a	1117
pDNA-T7-Caveolin-1	Production template Cavelion-1	
pDNA-T7-NTCP	Production template NTCP	n.a.
pDNA-T7-NTCP-tdTomato	Production template NTCP-tdTomato	n.a.
pDNA-T7-EGFP	Production template EGFP	335
pDNA-T7-RFP	Production template RFP	786

5.1.8. AAV-constructs

Table 8: AAV-constructs

Construct	Encoding features (Promotor
AAV-SpCas9	SpCas9 (CMV)
AAV-sgRNA X/S	sgRNA X (U6), sgRNA S (7SK)
AAV-sgRNA X/C	sgRNA C (U6), sgRNA X (7SK)
AAV-sgRNA C/S	sgRNA C (U6), sgRNA S (7SK)
AAV-sgRNA nonsense	sgRNA nonsense (U6 & 7SK)
AAV-SaCas9	SaCas9 (CMV)
AAV-151	sgRNA X (U6), sgRNA S (H1), shRNA7 (7SK)
AAV-153	sgRNA X (U6), sgRNA S (H1), shRNA Ctrl (7SK)
AAV-14	sgRNA X (U6), sgRNA Ctrl (H1), shRNA7 (7SK)
AAV-154	sgRNA Ctrl (U6), sgRNA S (H1), shRNA7 (7SK)
AAV-19	sgRNA Ctrl (U6), sgRNA Ctrl (H1), shRNA7 (7SK)
AAV-13	sgRNA Ctrl (U6), sgRNA Ctrl (H1), shRNA Ctrl (7SK)

5.1.9. Chemicals and reagents

Table 9: Chemicals and reagents

Chemical or reagent	Supplier
Agar-agar	Roth, Karlsruhe, Germany
Agarose	Peqlab, Erlangen, Germany
Amersham ECL Prime Western Blotting Detection Reagent	GE Healthcare Life Sciences, Freiburg, Germany
Ampicillin	Roth, Karlsruhe, Germany
APS	Roth, Karlsruhe, Germany
Collagen R	Serva Electrophoresis, Heidelberg, Germany
DMSO	Sigma-Adlrich, Steinheim, Germany
Dulbecco's Modified Eagle's Medium:Nutrient Mixture F12	Gibco/Invitrogen, Carlsbad, USA
Ethanol	Roth, Karlsruhe, Germany
FCS (heat-inactivated)	Gibco/Invitrogen, Carlsbad, USA
Formaldehyde	Roth, Karlsruhe, Germany
Geneticin (G418)	Thermo Scientific Scientific Scientific, Rockford, USA
Isopropanol	Roth, Karlsruhe, Germany
LDS Sample Buffer, Non-Reducing (4X)	Thermo Scientific Scientific Scientific, Rockford, USA
Lipofectamine 2000	Life Technologies, Carlsbad, USA
Lipofectamine MessengerMax	Life Technologies, Carlsbad, USA
Methanol	Roth, Karlsruhe, Germany
Milk powder	Roth, Karlsruhe, Germany
NaCl	Roth, Karlsruhe, Germany
OptiMEM	Gibco/Invitrogen, Carlsbad, USA
Page Ruler Plus Prestained protein ladder	Thermo Scientific Scientific Scientific, Rockford, USA
PBS	Gibco/Invitrogen, Carlsbad, USA
PEG6000	Merck, Hohenbrunn, Germany
Penicillin/streptomycin	Gibco/Invitrogen, Carlsbad, USA
Pierce RIPA buffer	Thermo Scientific Scientific Scientific, Rockford, USA
Polyacrylamide	Roth, Karlsruhe, Germany
Protease Inhibitor (cOmplete)	Roche, Mannheim, Germany
RotiSafe	Roth, Karlsruhe, Germany
SDS	Roth, Karlsruhe, Germany
SmartLadder DNA (10kb)	Eurogentec, Seraing, Belgium
ssRNA Ladder	New England Biolabs, Ipswich, USA
Low Range ssRNA Ladder	New England Biolabs, Ipswich, USA
T5 Exonuclease	New England Biolabs, Ipswich, USA
TEMED	Roth, Karlsruhe, Germany
Tris base	Roth, Karlsruhe, Germany
Tris HCl	Roth, Karlsruhe, Germany
Trypan blue	Gibco/Invitrogen, Carlsbad, USA
Trypsin	Gibco/Invitrogen, Carlsbad, USA

Tween 20	Roth, Karlsruhe, Germany
Yeast extract	Roth, Karlsruhe, Germany
Loading Dye 2x RNA	New England Biolabs, Ipswich, USA
EDTA	Roth, Karlsruhe, Germany
Pseudo-UTP (Ψ-UTP)	Jena Bioscience, Jena, Germany
5-Methoxy-UTP	Jena Bioscience, Jena, Germany
N^1-Methylpseudo-UTP	Jena Bioscience, Jena, Germany
5-Methyl-CTP (m^5CTP)	Jena Bioscience, Jena, Germany

5.1.10. Laboratory equipment and consumables

Table 10: Laboratory equipment and consumables

Product	Supplier
Architect	Abbott Laboratories, Chicago, IL, USA
Amersham Hybond PVDF membrane	GE Healthcare Life Sciences, Freiburg, Germany
BEP (HBeAg measurement)	Siemens Molecular Diagnostics, Marburg, Germany
Cell culture flasks and plates	TPP, Trasadingen, Switzerland
Cell culture incubator HERAcell 150i	Thermo Scientific Scientific Scientific, Rockford, USA
Centricon Plus-70	Merck Millipore, Brillerica, USA
Centrifuge 5417C/5417R	Eppendorf, Hamburg, Germany
Cryo vials	Greiner Bio One, Kremsmünster, Austria
Cytoflex	Beckman Coulter, Brea, CA, USA
Falcon tubes 15 mL, 50 mL	Greiner Bio One, Kremsmünster, Austria
Fuorescence microscope LEICA DM8i	Leica Biosystems, Wetzlar, Germany
Freezing container	Thermo Scientific Scientific Scientific, Rockford, USA
Fusion Fx7 (chemiluminescence detection, UV light system)	Peqlab, Erlangen, Germany
Gel chambers (agarose gel electrophoresis)	Peqlab, Erlangen, Germany
Gel chambers (SDS-PAGE)	Bio-Rad, Hercules, USA
Heating block	Eppendorf, Hamburg, Germany
Hemocytometer	Brand, Wertheim, Germany
Lightcycler 480 II	Roche, Mannheim, Germany
Nanodrop Photometer	Thermo Scientific Scientific Scientific, Rockford, USA
Pipette “Accu-jet pro”	Brand, Wertheim, Germany
Pipette filter tips	Starlab, Ahrensburg, Germany
Pipettes	Eppendorf, Hamburg, Germany
PVDF membrane	Bio-Rad, Hercules, USA
Reaction tubes	Eppendorf, Hamburg, Germany
Sterile filters 0,45 µM	Merck Millipore, Brillerica, USA
Sterile hood	Heraeus, Hanau, Germany
Tecan plate reader infinite F200	Tecan, Männedorf, Switzerland

Western Blotting Chamber (Wet Blot)	Bio-Rad, Hercules, USA
Whatman paper	Bio-Rad, Hercules, USA

5.1.11. Software

Table 11: Sofware

Software name	Supplier
Graph Pad Prism 8.4.1.	Graph Pad, La Jolla, USA
Image J	NIH, Bethesda, USA
LightCycler 480 Software	Roche, Mannheim, Germany
Windows 10	Microsoft, Redmond, USA
Galaxy	Web-based platform (Afgan et al. 2018)
Integrative Genomics Viewer (IGV) 2.8.2.	Broad Institute, Cambridge, USA
FlowJo, LLC	BD, Franklin Lakes, USA

5.2. Methods

In the following chapter the methods used in this study are listed in order of their appearance in the results section.

5.2.1. Cell culture

All used cells were maintained under standard sterile cell culture conditions (37°C, 5% CO_2, 95% humidity) and cells were tested frequently for mycoplasma-contamination. For subculturing, old medium was discarded, cells were washed with 1x PBS and detached with 1x trypsin at 37°C for 10–15 min. Detached cells were resuspended in cell culture medium and splitted in 1:6 or 1:10 dilution dependent on density. HepG2-based cells were cultured on collagen-coated (1:10 diluted collagen in dH_2O for 30 min at 37°C) and HEK293 cell line was cultured on poly-L lysine cell culture vessels (1:20 diluted poly-L lysine in 1x PBS for 30 min at 37°C). For seeding cells were diluted 1:2 with trypan blue and counted using a hemocytometer (calculation: average number of two quadrants multiplied with 10^4 to get number of cells per mL). To freeze cells, cell suspension was centrifuged for 10 min at 300 x g. Cell pellet was resuspended in freezing medium (90% fetal calf serum (FCS) and 10% DMSO) and transferred to cryovials stored at freezing container at –80°C. For thawing, cryovials were heated to 37°C. Thawed cells were resuspended, transferred to 10 mL culture medium and centrifuged for 10 min at 300 x g. Pelleted cells were diluted in culture medium and put into respective cell culture flask.

All cell lines were maintained in standard cultivation medium. HepG2-pEpi-H1.3. cells were generated by transfection of pEpi-H1.3. construct, containing a 1.3-fold overlength HBV and EGFP sequence and subsequent selection with 1:100 geneticin (Piechaczek et al. 1999). All experiments performed with HepG2-based cell lines included a pre-differentiation step of 1-3 days using differentiation medium. All experiments in this study were performed in 24 well plates.

5.2.2. Cloning

IVT mRNA production and single strand annealing (SSA) plasmids were generated with standard and InFusion cloning methods, which are generally described in the following paragraphs.

To produce inserts for cloning procedure appropriate primer pairs were designed using Serial Cloner (standard cloning) or Takara InFusion software (InFusion Cloning). For PCR reaction 1 µL template plasmids containing CDS (stock solution: 100 ng/µL) were mixed with 0.75 µL forward primer (20 µM), 0.75 µL reverse primer, 3 µL DMSO, 19.5 µL H_2O and 25 µL 2x Phusion Mastermix (Invitrogen). Samples were transferred to PCR machine using following program: 94°C 5 min (1 Cycle); 72°C 15 s, 70°C 30 s (40 Cycles); 70°C 5 min (1 Cycle), 4°C (cooling). PCR products and 10 kB DNA ladder were loaded on 1% agarose gels (0.5 g agarose solved in 50 mL 1x TAE buffer with 5 µL RotiSafe) and separated for 45 min at 100 V. To visualize bands, gel was placed on UV-table of Fusion Fx7 machine (Peqlab). PCR products were cleaned-up with PCR Clean-up Kit (Roche) according to manufacturer's instructions and eluted in 13.5 µL elution buffer. For standard cloning PCR products and target plasmid, for InFusion cloning only target plasmid were digested with appropriate restriction enzymes. Therefore, 13.5 µL of PCR products or 13.5 µL of prediluted plasmids (~ 10 µg) were mixed with 1.5 µL of each restriction enzyme, 1.5 µL *DpnI* (for PCR products) or 1.5 µL FastAP (for plasmids), 2 µL of FastDigest Buffer (10x) and incubated 1 h at 37°C. Clean up of PCR products (PCR Clean-up Kit) and plasmids (Gen extraction Kit (Quiagen)) was performed according to the manufacturer's protocols. For ligation step, amounts of inserts and plasmids were calculated using NEB ligation calculator. Reaction using T4 Ligase (Invitrogen) was performed according to manufacture's instruction but with incubation at 16°C overnight. InFusion reaction was performed using InFusion HD Cloning Kit (Takara) according to protocol. Transformation was performed in *E.coli* TOP10 (standard cloning) or *Stellar* cells (InFusion cloning) using heat-shock for 40 s at 42°C, recovery for 1 h at 37°C (after addition of 500 µL SOC medium) and incubation overnight on selective antibiotics containing LB plates. Clones were transferred to 3 mL LB medium containing selective antibiotics and incubated overnight at 37°C. Isolation of plasmids was performed using GeneJet Miniprep Kit (Thermo Scientific) according to manufacturer's instructions. To analysis correct clones, restriction digestion was performed as mentioned above using enzymes cutting within backbone and CDS.

Correct sequence was analyzed using Sanger sequencing (GATC). For IVT production and transfection experiments, correct clones were inoculated in 50 mL LB medium, incubated overnight at 37°C and plasmid isolation was performed using Plasmid Plus Kit (Quiagen) according to manufacturer's instructions. Concentration of isolated plasmids was determined with Nanodrop (Invitrogen).

5.2.3. Production of *in vitro* transcribed (IVT) mRNA

For T7 based *in vitro* transcription pDNA templates containing T7 Promotor and coding sequence were linearized. Therefore, 10 µL of plasmid (concentration: 1 µg/µL) were mixed with 2 µL FastDigest Buffer (10x), 5 µL appropriate restriction enzyme, 3 µL H_2O and incubated for 1 h at 37°C. Linearization was checked on 1% agarose gel as described above. Cleanup of linearized plasmid was performed by mixing digestion reaction with 1:20 v/v 0.5 M EDTA, 1:10 v/v 5M NH_4OH, 2 volumes of 100% ethanol and precipitation overnight at -20°C. DNA was pelleted (15 min at max speed), washed two times with 100% ethanol and resuspended in 25 µL nuclease-free Water. Production of T7 derived IVT mRNA was performed with HiScribe T7 ARCA mRNA Kit (with tailing) (NEB) or Ambion mMessage mMachine T7 Transcription Kit (Invitrogen) according to manufacturer's instructions with 30 min synthesis and 25 min poly(A)-tailing steps. For production of modified mRNAs UTP (Pseudo-UTP (Ψ-UTP), 5-Methoxy-UTP (5moUTP), N^1-Methylpseudo-UTP (me^1Ψ-UTP)) and CTP (5-Methyl-CTP (m^5CTP)) analogous (Jena Bioscience) were added to reaction according to protocol. IVT mRNA was cleaned-up using RNA Clean&Concentrator-25 (Zymo Research) according to manufacturer's instructions. To ensure synthesis and poly(A)-tailing, 0.5 µL of untailed and tailed IVT mRNAs were mixed with 5.5 µL nuclease-free water, RNA loading dye (2x) (NEB) and incubated for 10 min at 65°C. Analysis was performed on 2% agarose gel (45 min at 80 V). IVT mRNA concentration was determined with Nanodrop (Thermo Scientific).

5.2.4. IVT guide production

5.2.4.1. SpCas9 sgRNA

For production of IVT sgRNAs v1 and v2 respective primer sgRNA 1 were used. CRISPR/Cas9 crRNA sequence is implemented in primer sgRNA 3 (indicated by brackets). For template production we mixed 1 µL primer sgRNA 1 (10 µM), 1 µL primer sgRNA 2 (1 µM), 1 µL primer sgRNA 3 (1 µM), 1 µL sgRNA 4 (10 µM), 12.5 µL Phusion 2x MM and 8.5 µL H_2O and performed PCR reaction with following program:

Table 12: Program for T7 IVT sgRNA PCR template

	T [°C]	T [s]	Cycles
Denaturation	94	120	1
Annealing 1	94	20	4
	68	20	
	72	20	
Annealing 2	94	20	4
	62	20	
	72	20	
Elongation	94	20	29
	55	20	
	72	20	
Cooling	4	pause	

PCR templates were purified using PCR Clean-up Kit (Roche) according to manufacturer's instructions. For IVT sgRNA production HiScribe T7 High Yield RNA Synthesis Kit (NEB) were used according to protocol, using 5 µL of PCR template. Clean-up and analysis were performed as mentioned above regarding IVT mRNA.

5.2.4.2. SaCas9 sgRNA and LbCas12a crRNA

SaCas9 sgRNAs were produced according to protocol for SpCas9 variants, but using SaCas9 sgRNA primer 2, 3 and 4 instead of sgRNA primer 2, 3 and 4. Production of LbCas12a crRNA PCR template and crRNA molecules is described in the Master thesis of Christine Henning (Henning 2019).

5.2.5. Transfection

For plasmid transfection Lipofectamine 2000 (Invitrogen) was used according to manufacturer's protocol. IVT mRNA transfection was performed with Lipofectamine Messenger Max (Invitrogen) using 1:3 ratio according to manufacturer's instructions.

5.2.6. Transduction

AdV and AAV viral vectors were transduced according to respective titer into standard cultivation medium. 24 h post transduction, cells were washed several times with PBS to remove remaining viral vectors.

5.2.7. CellTiter Blue

Cell Titer Blue assay (CTB) was performed according to manufacturer's instruction (Promega). Measurement of fluorescent (560(20)Ex/590(10)Em) was performed using M200 infinite plate reader (Tecan).

5.2.8. Protein isolation, sodium dodecyl sulphate-polyacrylamide gel electrophoresis (SDS-PAGE) and Western blot analysis

For protein isolation RIPA buffer (Pierce) containing cOmplete protease inhibitor (1:20) (Roche) was added to cells and incubated for 30 min on ice. Cell debris was pelleted by centrifugation for 15 min at max. speed and lysate was transferred to new 1.5 mL reaction tube. For Western blot analysis protein lysates were further treated depending on target protein. NTCP samples were mixed with loading dye (LDS Sample Buffer, Non-reducing (4x)), 0,1 M DTT (Promega). For deglycosylation PNGaseF treatment was performed according to manufacturer's instructions (NEB). All other protein samples were mixed with loading dye (reducing, 6x), cooked for 5 min at 95°C and centrifuged.

Separation of proteins for Western Blot analysis was performed with SDS-PAGE. Therefore, 12.5% or 7.5% gels were prepared according to following table:

Separation gel	7.5 %	12.5 %
Acrylamide (40 %)	1.5 mL	2.5 mL
Tris (1M, pH 8.8)	3 mL	3 mL
SDS (10 %)	80 µL	80 µL
H_2O	3.4 mL	2 mL
TEMED	7 µL	7 µL
APS (10 %)	40 µL	40 µL
Total volume	8 mL	8 mL

Collection Gel	5 %
Acrylamide (40 %)	0.24 mL
Tris (1M, pH 8.8)	0.5 mL
SDS (10 %)	20 µL
H_2O	1.25 mL
TEMED	2 µL
APS (10 %)	15 µL
Total volume	2 mL

Depending on protein size 7.5% (> 2.5 kB) or 12.5% (< 2.5 kB) gels were used together with 10 µL prestained protein ladder (Page Ruler Plus). Separation was performed in 1x Running Buffer with 15 mA per gel for 1.5 hours.

For all proteins a wet blot procedure was applied using 1x transfer buffer and 0.2 µM PVDF membranes (Bio-Rad). Blotting was performed in Bio-Rad blotting chambers with 200 mA per gel for 2 hours. After protein transfer, membranes were blocked with 5% milk (milk powder solved in 1x TBS-T) for 1 h and incubated with appropriate primary antibody diluted in blocking solution overnight at 4°C.

After incubation, blots were washed three times with 1x TBS-T and incubated with diluted secondary antibody for 2 hours at room temperature. Development of blots was performed after three times washing using Amersham ECL Prime Western Blotting Detection Reagent with Fusion machine (Intas).

5.2.9. Fluorescence microscopy

Fluorescence images were obtained with 10x or 20x objectives in phase contrast, Fluorescein isothiocyanate (FITC; Excitation: 480/40; Emission: 460/50) and Texas Red (TXR; Excitation: 560/40; Emission: 630/75) channels using Leica DMi8 fluorescence microscope. Procession of data was performed with LAS X Expert software (Leica).

5.2.10. Flow cytometry

For flow cytometry analysis cells were washed with 1x PBS, detached with 1x Trypsin for 15 min at 37°C, resuspended in FACS Buffer (1x PBS with 1% FBS and 0,5 mM EDTA) and transferred to 96 U well plates through 0.2 µM cell strainer. Cells were washed twice and were resuspended in FACS Buffer. Flow cytometry analysis was performed with Cytoflex machine using following gating strategy: FSC-A–SSC-A (for cell population), FSC-A : FSC-H (for single cells), SSC-A: FITC-A (for EGFP or $Atto_{488}$) or SSC-A: PE-A (for RFP or tdTomato), respectively. Data processing was performed using FloJow software.

5.2.11. Cholera Toxin $B_{Atto488}$ ($CTB_{Atto488}$) assay

Cav-I dependent uptake assay was performed using 4 µg/mL $CTB_{Atto488}$ per well and added to cells for 1 h at 4°C, followed by 1.5 h incubation at 37°C. Internalized $CTB_{Atto488}$ substrate was measured using flow cytometry analysis.

5.2.12. $Atto_{488}$ labeled Myrcludex B staining

For analysis of NTCP expression, 10 µM Atto488 labeled Myrcludex B ($MyrB_{Atto488}$) were added to culture medium and incubated for 30 min at 37°C. Unbound $MyrB_{Atto488}$ was removed by washing with PBS.

5.2.13. Taurocholate Uptake assay

Analysis of [^{3}H] taurocholate uptake for all cell lines was performed as previously described (Kubitz et al. 2004). Briefly, negative samples were incubated for 15 min at 37 °C with 200 nM MyrB diluted in 250 µL basal medium. Next, Hot Mix stock (1940 µL basal medium, 66 µL 15 mM cold TC (Sigma-Aldrich) and 1 µL hot TC (Hartmann Analytic, Braunschweig, Germany) was diluted 1:10 in basal medium, 25 µL were added to the preincubated samples and incubated for 15 min at 37 °C. After incubation, cells were placed on iced, Hot Mix was removed and cells were washed 3 times with ice-cold PBS. Next, 500 µL lysis buffer (0.05 % SDS, 0.25 mM NaOH) were added and lysed cells were transferred to scintillation vials.

Afterwards, 4 mL scintillation liquid was added, vials were closed and vortexed for 30 s. Measurement of [^{3}H] taurocholate was performed with scintillation analyzer.

5.2.14. HBV uptake and infection assay

HBV uptake was performed as described previously using MOI 200 (Chakraborty 2020). For HBV infection virus was mixed with standard cultivation medium, 4% polyethylengylcol (PEG) solution and 2.5% DMSO, vortexed and added to cells. To block viral entry, Myrcludex B (MyrB), a synthetic N-acylated preS1 lipopeptide, was used, which inhibits viral interaction with NTCP receptor (Gripon et al. 2005, Urban et al. 2014). For treatment 10 µM Myrcludex B was added to infection mixture. One day post infection, cells were washed with 1x PBS and fresh differentiation medium was added.

5.2.15. HBeAg measurement: BEP III and Architect

For qualitative measurement of HBeAg BEP III (Siemens) was used. Sample/Cutoff was determined using internal cutoff value. Measurement of quantitative amounts of HBeAg was performed using Architect machine (Abbott).

5.2.16. DNA isolation

Total, cellular DNA was extracted using Genomic DNA from tissue kit (Machery&Nagel). Briefly, 200 µL T1 buffer, 25 µL Proteinase K and 200 µL B3 buffer were added to each sample and incubated 10 min at 70°C. To adjust DNA binding conditions 210 µL 96–100% ethanol was added, mixed and transferred to Nucleospin column. Columns were centrifuged for 1 min at 11.000x g and placed in new collection tube. To wash silica membrane first washing step was performed with 500 µL BW buffer and second with 600 µL B5. After an additional dry centrifugation step (2 min, 11.000x g), DNA was eluted in 1.5 mL reaction tube with 100 µL BE elution buffer.

5.2.17. DNA T5 digestion

DNA T5 digestion was performed according to protocol (Xia et al. 2017). 8.5 µL DNA is mixed with 1 µL NEBuffer 4 (10x) and 0.5 µL of T5 Exonuclease (10 U) (NEB). Samples are incubated for 30 min at 37°C with subsequent heat inactivation for 5 min at 99°C. Since remaining buffer components can interfere with qPCR reaction, samples are 4-fold diluted with 30 µL ddH_2O.

5.2.18. Isolation of total RNA and cDNA synthesis

RNA purification was performed using RNA isolation kit (Machery&Nagel) according to manufacturer's instruction. Cells were lysed with 350 µL RA1 buffer, transferred to NucleoSpin Filter columns and centrifuged for 1 min at 11.000 x g. To adjust RNA binding conditions, 350 µL 70% ethanol is added to flow-through and mixed by pipetting. Lysates are loaded on NucleoSpin RNA columns and centrifuged for 30 s at 11.000 x g.

To desalt membrane 350 µL MDB buffer is added and columns are again centrifuged for 30 s at 11.000 x g. On column DNA digestion is performed using 10 µL reconstituted rDNAse and 90 µL Reaction Buffer for rDNAse, added to filter membrane and incubated for 15 min at RT. After, removal of DNA contamination three subsequent washing steps were performed using, 200 µL Buffer RAW2 (1st), 600 µL Buffer RA3 (2st) and 250 µL RA3 (3rd) and with in between centrifugation steps for 30 s at 11.000 x g. After an additional dry centrifugation step (2 min, 11.000 x g), RNA is eluted in 60 µL of RNAse-free H_2O and collected in 1.5 mL nuclease-free reaction tubes. For cDNA synthesis Superscript III kit (Invitrogen) was used according to modified manufacturer's instruction using half reaction volume per sample. Briefly, 4 µL isolated RNA, 5 µL 2X RT Reaction mix and 1 µL RT Enzyme Mix was mixed and placed into PCR machine using following program: 10 min at 25°C, 30 min at 50°C and 5 min at 85°C before cooling to 4°C. To degrade RNA template 0.5 µL (2U) *E.coli* RNase H was added and incubated for 20 min at 37°C. Finally, 90 µL of ddH_2O is added and cDNA is stored at -20°C.

5.2.19. Quantification of viral HBV markers using qPCR

Relative amounts of total intracellular HBV DNA (primer: HBV 1745, HBV 1844); cccDNA (primers: cccDNA 92-, cccDNA 2251+), HBV pgRNA (primers: pgRNA fw, pgRNA rev) as well as reference genes PRNP (primers: PRNP fw, PRNP rev) and 18S (primers: 18S fw, 18S rev) were determined by qPCR using LightCycler480 Real-time PCR system (Roche). qPCR data was analyzed with advanced relative quantification using normalization to reference gene. For each reaction, 0,5 µL forward primer (20 µM), 0.5 µL reverse primer (20 µM), 5 µL LightCycler 480 SYBR Green I Master mix (Roche) and 4 µL of DNA or cDNA template were mixed.

Measurement of total intracellular HBV DNA and PRNP was using following qPCR program:

Table 13: qPCR program for HBV DNA and PRNP

	T [°C]	T [s]	Ramp [°C/s]	Acquisition mode	Cycles
Denaturation	95	300	4.4		1
Amplification	95	25	4.4		40
	60	10	2.2		
	72	30	4.4	Single	
Melting	95	1	4.4		1
	65	60	2.2		
	95		0.11	Continuous: 5/°C	
Cooling	40	30	2.2		1

Measurement of cccDNA was using following qPCR program:

Table 14: qPCR program for cccDNA

	T [°C]	T [s]	Ramp [°C/s]	Acquisition mode	Cycles
Denaturation	95	600	4.4		1
Amplification	95	15	4.4		50
	60	5	2.2		
	72	45	4.4		
	88	2	4.4	Single	
Melting	95	1	4.4		1
	65	15	2.2		
	95		0.11	Continuous: 5/°C	
Cooling	40	30	2.2		1

Measurement of total HBV transcripts and 18S was using following qPCR program “GE_C3”:

Table 15: qPCR program („GE_C3”) for total HBV transcripts and 18S

	T [°C]	T [s]	Ramp [°C/s]	Acquisition mode	Cycles
Denaturation	95	300	4.4		1
Amplification	95	15	4.4		45
	60	10	2.2		
	72	25	4.4	Single	
Melting	95	1	4.4		1
	65	60	2.2		
	95		0.11	Continuous: 5/°C	
Cooling	40	30	2.2		1

5.2.20. Next generation sequencing (NGS)

For NGS analysis, ORF S target region of HepG2-H1.3., HepG2-pEpi-H1.3., HepG2.2.15. and infected HepG2-NTCP-K7 were amplified with PCR (primer: S ORF fw, S ORF rev) using PCR program: 94°C 5 min (1 Cycle); 72°C 15 s, 70°C 30 s (40 Cycles); 70°C 5 min (1 Cycle), 4°C (cooling). PCR amplicons were analyzed using microbial amplicon-based metagenomics sequencing on Illumina PE250 machine (Novogene). Subsequent data analysis was performed using free-web based Galaxy software and IGV program (Afgan et al. 2018).

5.2.21. Statistical analysis

Numeric values are presented as means with standard deviation. Calculation of p-values was performed with Student's unpaired two-tailed *t*-test with Welch's correction or one-way *ANOVA* using Prism 8.4.1 software.

6. References

Afgan, E., D. Baker, B. Batut, M. van den Beek, D. Bouvier, M. Cech, J. Chilton, D. Clements, N. Coraor, B. A. Gruning, A. Guerler, J. Hillman-Jackson, S. Hiltemann, V. Jalili, H. Rasche, N. Soranzo, J. Goecks, J. Taylor, A. Nekrutenko and D. Blankenberg (2018). "The Galaxy platform for accessible, reproducible and collaborative biomedical analyses: 2018 update." Nucleic Acids Res **46**(W1): W537-W544.

Ahi, Y. S., D. S. Bangari and S. K. Mittal (2011). "Adenoviral vector immunity: its implications and circumvention strategies." Curr Gene Ther **11**(4): 307-320.

Al Mahtab, M., S. M. F. Akbar, J. C. Aguilar, G. Guillen, E. Penton, A. Tuero, O. Yoshida, Y. Hiasa and M. Onji (2018). "Treatment of chronic hepatitis B naive patients with a therapeutic vaccine containing HBs and HBc antigens (a randomized, open and treatment controlled phase III clinical trial)." PLoS One **13**(8): e0201236.

Allweiss, L., T. Volz, K. Giersch, J. Kah, G. Raffa, J. Petersen, A. W. Lohse, C. Beninati, T. Pollicino, S. Urban, M. Lutgehetmann and M. Dandri (2018). "Proliferation of primary human hepatocytes and prevention of hepatitis B virus reinfection efficiently deplete nuclear cccDNA in vivo." Gut **67**(3): 542-552.

Anderson, B. R., H. Muramatsu, B. K. Jha, R. H. Silverman, D. Weissman and K. Kariko (2011). "Nucleoside modifications in RNA limit activation of 2'-5'-oligoadenylate synthetase and increase resistance to cleavage by RNase L." Nucleic Acids Res **39**(21): 9329-9338.

Anderson, B. R., H. Muramatsu, S. R. Nallagatla, P. C. Bevilacqua, L. H. Sansing, D. Weissman and K. Kariko (2010). "Incorporation of pseudouridine into mRNA enhances translation by diminishing PKR activation." Nucleic Acids Res **38**(17): 5884-5892.

Andries, O., S. Mc Cafferty, S. C. De Smedt, R. Weiss, N. N. Sanders and T. Kitada (2015). "N(1)-methylpseudouridine-incorporated mRNA outperforms pseudouridine-incorporated mRNA by providing enhanced protein expression and reduced immunogenicity in mammalian cell lines and mice." J Control Release **217**: 337-344.

Antón, Z., G. Mullally, H. Ford, M. W. van der Kamp, M. D. Szczelkun and J. D. Lane (2020). "Variability in mitochondrial import, mitochondrial health and mtDNA copy number using Type II and Type V CRISPR effectors." bioRxiv.

Appelman, M. D., A. Chakraborty, U. Protzer, J. A. McKeating and S. F. van de Graaf (2017). "N-Glycosylation of the Na+-Taurocholate Cotransporting Polypeptide (NTCP) Determines Its Trafficking and Stability and Is Required for Hepatitis B Virus Infection." PLoS One **12**(1): e0170419.

Aschenbrenner, S., S. M. Kallenberger, M. D. Hoffmann, A. Huck, R. Eils and D. Niopek (2020). "Coupling Cas9 to artificial inhibitory domains enhances CRISPR-Cas9 target specificity." Sci Adv **6**(6): eaay0187.

Backes, S., C. Jager, C. J. Dembek, A. D. Kosinska, T. Bauer, A. S. Stephan, A. Dislers, G. Mutwiri, D. H. Busch, L. A. Babiuk, G. Gasteiger and U. Protzer (2016). "Protein-prime/modified vaccinia virus Ankara vector-boost vaccination overcomes tolerance in high-antigenemic HBV-transgenic mice." Vaccine **34**(7): 923-932.

Barrangou, R. (2013). "CRISPR-Cas systems and RNA-guided interference." Wiley Interdiscip Rev RNA **4**(3): 267-278.

Barrangou, R. and J. van der Oost (2015). "Bacteriophage exclusion, a new defense system." EMBO J **34**(2): 134-135.

Barrett, L. W., S. Fletcher and S. D. Wilton (2012). "Regulation of eukaryotic gene expression by the untranslated gene regions and other non-coding elements." Cell Mol Life Sci **69**(21): 3613-3634.

Bestor, T. H. (2000). "Gene silencing as a threat to the success of gene therapy." J Clin Invest **105**(4): 409-411.

Bloom, K., A. Ely, C. Mussolino, T. Cathomen and P. Arbuthnot (2013). "Inactivation of hepatitis B virus replication in cultured cells and in vivo with engineered transcription activator-like effector nucleases." Mol Ther **21**(10): 1889-1897.

Bock, C. T., P. Schranz, C. H. Schroder and H. Zentgraf (1994). "Hepatitis B virus genome is organized into nucleosomes in the nucleus of the infected cell." Virus Genes **8**(3): 215-229.

Bock, C. T., S. Schwinn, S. Locarnini, J. Fyfe, M. P. Manns, C. Trautwein and H. Zentgraf (2001). "Structural organization of the hepatitis B virus minichromosome." J Mol Biol **307**(1): 183-196.

Boni, C., V. Barili, G. Acerbi, M. Rossi, A. Vecchi, D. Laccabue, A. Penna, G. Missale, C. Ferrari and P. Fisicaro (2019). "HBV Immune-Therapy: From Molecular Mechanisms to Clinical Applications." Int J Mol Sci **20**(11).

Chakraborty, A. (2020). "Characterization of early events in hepatitis b virus infection." PhD thesis.

Chandrasegaran, S. and D. Carroll (2016). "Origins of Programmable Nucleases for Genome Engineering." J Mol Biol **428**(5 Pt B): 963-989.

Charlesworth, C. T., P. S. Deshpande, D. P. Dever, J. Camarena, V. T. Lemgart, M. K. Cromer, C. A. Vakulskas, M. A. Collingwood, L. Zhang, N. M. Bode, M. A. Behlke, B. Dejene, B. Cieniewicz, R. Romano, B. J. Lesch, N. Gomez-Ospina, S. Mantri, M. Pavel-Dinu, K. I. Weinberg and M. H. Porteus (2019). "Identification of preexisting adaptive immunity to Cas9 proteins in humans." Nat Med **25**(2): 249-254.

Chen, L., K. Shi, Z. Yin and H. Aihara (2013). "Structural asymmetry in the Thermus thermophilus RuvC dimer suggests a basis for sequential strand cleavages during Holliday junction resolution." Nucleic Acids Res **41**(1): 648-656.

Cong, L., F. A. Ran, D. Cox, S. Lin, R. Barretto, N. Habib, P. D. Hsu, X. Wu, W. Jiang, L. A. Marraffini and F. Zhang (2013). "Multiplex genome engineering using CRISPR/Cas systems." Science **339**(6121): 819-823.

Cox, D. B. T., J. S. Gootenberg, O. O. Abudayyeh, B. Franklin, M. J. Kellner, J. Joung and F. Zhang (2017). "RNA editing with CRISPR-Cas13." Science **358**(6366): 1019-1027.

Cradick, T. J., K. Keck, S. Bradshaw, A. C. Jamieson and A. P. McCaffrey (2010). "Zinc-finger nucleases as a novel therapeutic strategy for targeting hepatitis B virus DNAs." Mol Ther **18**(5): 947-954.

Crowther, R. A., N. A. Kiselev, B. Bottcher, J. A. Berriman, G. P. Borisova, V. Ose and P. Pumpens (1994). "Three-dimensional structure of hepatitis B virus core particles determined by electron cryomicroscopy." Cell **77**(6): 943-950.

Dane, D. S., C. H. Cameron and M. Briggs (1970). "Virus-like particles in serum of patients with Australia-antigen-associated hepatitis." Lancet **1**(7649): 695-698.

de Los Milagros Bassani Molinas, M., C. Beer, F. Hesse, M. Wirth and R. Wagner (2014). "Optimizing the transient transfection process of HEK-293 suspension cells for protein production by nucleotide ratio monitoring." Cytotechnology **66**(3): 493-514.

Devarkar, S. C., C. Wang, M. T. Miller, A. Ramanathan, F. Jiang, A. G. Khan, S. S. Patel and J. Marcotrigiano (2016). "Structural basis for m7G recognition and 2'-O-methyl discrimination in capped RNAs by the innate immune receptor RIG-I." Proc Natl Acad Sci U S A **113**(3): 596-601.

Diebold, S. S., T. Kaisho, H. Hemmi, S. Akira and C. Reis e Sousa (2004). "Innate antiviral responses by means of TLR7-mediated recognition of single-stranded RNA." Science **303**(5663): 1529-1531.

DiLillo, D. J., G. S. Tan, P. Palese and J. V. Ravetch (2014). "Broadly neutralizing hemagglutinin stalk-specific antibodies require FcgammaR interactions for protection against influenza virus in vivo." Nat Med **20**(2): 143-151.

Dimitriadis, G. J. (1978). "Translation of rabbit globin mRNA introduced by liposomes into mouse lymphocytes." Nature **274**(5674): 923-924.

Doring, B., T. Lutteke, J. Geyer and E. Petzinger (2012). "The SLC10 carrier family: transport functions and molecular structure." Curr Top Membr **70**: 105-168.

Durbin, A. F., C. Wang, J. Marcotrigiano and L. Gehrke (2016). "RNAs Containing Modified Nucleotides Fail To Trigger RIG-I Conformational Changes for Innate Immune Signaling." mBio **7**(5).

Eckstein, F. (2007). "Phosphorothioation of DNA in bacteria." Nat Chem Biol **3**(11): 689-690.

Eid, A. and M. M. Mahfouz (2016). "Genome editing: the road of CRISPR/Cas9 from bench to clinic." Exp Mol Med **48**(10): e265.

Ellis, B. L., M. L. Hirsch, J. C. Barker, J. P. Connelly, R. J. Steininger, 3rd and M. H. Porteus (2013). "A survey of ex vivo/in vitro transduction efficiency of mammalian primary cells and cell lines with Nine natural adeno-associated virus (AAV1-9) and one engineered adeno-associated virus serotype." Virol J **10**: 74.

Farasat, I. and H. M. Salis (2016). "A Biophysical Model of CRISPR/Cas9 Activity for Rational Design of Genome Editing and Gene Regulation." PLoS Comput Biol **12**(1): e1004724.

Festag, M. M., J. Festag, S. P. Frassle, T. Asen, J. Sacherl, S. Schreiber, M. A. Muck-Hausl, D. H. Busch, K. Wisskirchen and U. Protzer (2019). "Evaluation of a Fully Human, Hepatitis B Virus-Specific Chimeric Antigen Receptor in an Immunocompetent Mouse Model." Mol Ther **27**(5): 947-959.

Fischer, S. E. J. (2015). "RNA Interference and MicroRNA-Mediated Silencing." Curr Protoc Mol Biol **112**: 26 21 21-26 21 25.

Follenzi, A., L. Santambrogio and A. Annoni (2007). "Immune responses to lentiviral vectors." Curr Gene Ther **7**(5): 306-315.

Fu, Y., J. D. Sander, D. Reyon, V. M. Cascio and J. K. Joung (2014). "Improving CRISPR-Cas nuclease specificity using truncated guide RNAs." Nat Biotechnol **32**(3): 279-284.

Furuichi, Y. and A. J. Shatkin (2000). "Viral and cellular mRNA capping: past and prospects." Adv Virus Res **55**: 135-184.

Gasiunas, G., R. Barrangou, P. Horvath and V. Siksnys (2012). "Cas9-crRNA ribonucleoprotein complex mediates specific DNA cleavage for adaptive immunity in bacteria." Proc Natl Acad Sci U S A **109**(39): E2579-2586.

Gerlich, W. H. and W. S. Robinson (1980). "Hepatitis B virus contains protein attached to the 5' terminus of its complete DNA strand." Cell **21**(3): 801-809.

Gey, G. O., W. D. Coffman and M. T. Kubicek (1952). "Tissue culture studies of the proliferative capacity of cervical carcinoma and normal epithelium." Cancer Res **12**: 264-265.

Giard, D. J., S. A. Aaronson, G. J. Todaro, P. Arnstein, J. H. Kersey, H. Dosik and W. P. Parks (1973). "In vitro cultivation of human tumors: establishment of cell lines derived from a series of solid tumors." J Natl Cancer Inst **51**(5): 1417-1423.

Gish, R. G., M. F. Yuen, H. L. Chan, B. D. Given, C. L. Lai, S. A. Locarnini, J. Y. Lau, C. I. Wooddell, T. Schluep and D. L. Lewis (2015). "Synthetic RNAi triggers and their use in chronic hepatitis B therapies with curative intent." Antiviral Res **121**: 97-108.

Graham, F. L., J. Smiley, W. C. Russell and R. Nairn (1977). "Characteristics of a human cell line transformed by DNA from human adenovirus type 5." J Gen Virol **36**(1): 59-74.

Gripon, P., I. Cannie and S. Urban (2005). "Efficient inhibition of hepatitis B virus infection by acylated peptides derived from the large viral surface protein." J Virol **79**(3): 1613-1622.

Grudzien-Nogalska, E., J. Stepinski, J. Jemielity, J. Zuberek, R. Stolarski, R. E. Rhoads and E. Darzynkiewicz (2007). "Synthesis of anti-reverse cap analogs

(ARCAs) and their applications in mRNA translation and stability." Methods Enzymol **431**: 203-227.

Gustafsson, C., S. Govindarajan and J. Minshull (2004). "Codon bias and heterologous protein expression." Trends Biotechnol **22**(7): 346-353.

Hagenbuch, B. and P. J. Meier (1994). "Molecular cloning, chromosomal localization, and functional characterization of a human liver Na+/bile acid cotransporter." J Clin Invest **93**(3): 1326-1331.

Hecker, J. G. (2016). "Non-Viral, Lipid-Mediated DNA and mRNA Gene Therapy of the Central Nervous System (CNS): Chemical-Based Transfection." Methods Mol Biol **1382**: 307-324.

Heckl, D., M. S. Kowalczyk, D. Yudovich, R. Belizaire, R. V. Puram, M. E. McConkey, A. Thielke, J. C. Aster, A. Regev and B. L. Ebert (2014). "Generation of mouse models of myeloid malignancy with combinatorial genetic lesions using CRISPR-Cas9 genome editing." Nat Biotechnol **32**(9): 941-946.

Heil, F., H. Hemmi, H. Hochrein, F. Ampenberger, C. Kirschning, S. Akira, G. Lipford, H. Wagner and S. Bauer (2004). "Species-specific recognition of single-stranded RNA via toll-like receptor 7 and 8." Science **303**(5663): 1526-1529.

Hemmi, H., O. Takeuchi, T. Kawai, T. Kaisho, S. Sato, H. Sanjo, M. Matsumoto, K. Hoshino, H. Wagner, K. Takeda and S. Akira (2000). "A Toll-like receptor recognizes bacterial DNA." Nature **408**(6813): 740-745.

Hendel, A., R. O. Bak, J. T. Clark, A. B. Kennedy, D. E. Ryan, S. Roy, I. Steinfeld, B. D. Lunstad, R. J. Kaiser, A. B. Wilkens, R. Bacchetta, A. Tsalenko, D. Dellinger, L. Bruhn and M. H. Porteus (2015). "Chemically modified guide RNAs enhance CRISPR-Cas genome editing in human primary cells." Nat Biotechnol **33**(9): 985-989.

Henning, C. E. (2019). "Establishment of a functional, mRNA-based CRISPR-Cas12a approach for genome editing." Master's Thesis.

Hirano, H., J. S. Gootenberg, T. Horii, O. O. Abudayyeh, M. Kimura, P. D. Hsu, T. Nakane, R. Ishitani, I. Hatada, F. Zhang, H. Nishimasu and O. Nureki (2016). "Structure and Engineering of Francisella novicida Cas9." Cell **164**(5): 950-961.

Ho, J. K., B. Jeevan-Raj and H. J. Netter (2020). "Hepatitis B Virus (HBV) Subviral Particles as Protective Vaccines and Vaccine Platforms." Viruses **12**(2).

Ho, R. H., B. F. Leake, R. L. Roberts, W. Lee and R. B. Kim (2004). "Ethnicity-dependent polymorphism in Na+-taurocholate cotransporting polypeptide (SLC10A1) reveals a domain critical for bile acid substrate recognition." J Biol Chem **279**(8): 7213-7222.

Hoe, N. P., K. Nakashima, S. Lukomski, D. Grigsby, M. Liu, P. Kordari, S. J. Dou, X. Pan, J. Vuopio-Varkila, S. Salmelinna, A. McGeer, D. E. Low, B. Schwartz, A. Schuchat, S. Naidich, D. De Lorenzo, Y. X. Fu and J. M. Musser (1999). "Rapid selection of complement-inhibiting protein variants in group A Streptococcus epidemic waves." Nat Med **5**(8): 924-929.

Holtkamp, S., S. Kreiter, A. Selmi, P. Simon, M. Koslowski, C. Huber, O. Tureci and U. Sahin (2006). "Modification of antigen-encoding RNA increases stability, translational efficacy, and T-cell stimulatory capacity of dendritic cells." Blood **108**(13): 4009-4017.

Hornung, V., M. Guenthner-Biller, C. Bourquin, A. Ablasser, M. Schlee, S. Uematsu, A. Noronha, M. Manoharan, S. Akira, A. de Fougerolles, S. Endres and G. Hartmann (2005). "Sequence-specific potent induction of IFN-alpha by short interfering RNA in plasmacytoid dendritic cells through TLR7." Nat Med **11**(3): 263-270.

Hu, J. and K. Liu (2017). "Complete and Incomplete Hepatitis B Virus Particles: Formation, Function, and Application." Viruses **9**(3).

Hu, K. (2014). "Vectorology and factor delivery in induced pluripotent stem cell reprogramming." Stem Cells Dev **23**(12): 1301-1315.

Hu, X., J. Jiang, C. Ni, Q. Xu, S. Ye, J. Wu, F. Ge, Y. Han, Y. Mo, D. Huang and L. Yang (2019). "HBV Integration-mediated Cell Apoptosis in HepG2.2.15." J Cancer **10**(17): 4142-4150.

Huang, H. C., C. C. Chen, W. C. Chang, M. H. Tao and C. Huang (2012). "Entry of hepatitis B virus into immortalized human primary hepatocytes by clathrin-dependent endocytosis." J Virol **86**(17): 9443-9453.

Ishino, Y., H. Shinagawa, K. Makino, M. Amemura and A. Nakata (1987). "Nucleotide sequence of the iap gene, responsible for alkaline phosphatase isozyme conversion in Escherichia coli, and identification of the gene product." J Bacteriol **169**(12): 5429-5433.

Jalkanen, A. L., S. J. Coleman and J. Wilusz (2014). "Determinants and implications of mRNA poly(A) tail size--does this protein make my tail look big?" Semin Cell Dev Biol **34**: 24-32.

Jansen, R., J. D. Embden, W. Gaastra and L. M. Schouls (2002). "Identification of genes that are associated with DNA repeats in prokaryotes." Mol Microbiol **43**(6): 1565-1575.

Jemielity, J., T. Fowler, J. Zuberek, J. Stepinski, M. Lewdorowicz, A. Niedzwiecka, R. Stolarski, E. Darzynkiewicz and R. E. Rhoads (2003). "Novel "anti-reverse" cap analogs with superior translational properties." RNA **9**(9): 1108-1122.

Jiang, B., K. Himmelsbach, H. Ren, K. Boller and E. Hildt (2015). "Subviral Hepatitis B Virus Filaments, like Infectious Viral Particles, Are Released via Multivesicular Bodies." J Virol **90**(7): 3330-3341.

Jiang, F., K. Zhou, L. Ma, S. Gressel and J. A. Doudna (2015). "STRUCTURAL BIOLOGY. A Cas9-guide RNA complex preorganized for target DNA recognition." Science **348**(6242): 1477-1481.

Jinek, M., K. Chylinski, I. Fonfara, M. Hauer, J. A. Doudna and E. Charpentier (2012). "A programmable dual-RNA-guided DNA endonuclease in adaptive bacterial immunity." Science **337**(6096): 816-821.

Jinek, M., A. East, A. Cheng, S. Lin, E. Ma and J. Doudna (2013). "RNA-programmed genome editing in human cells." Elife **2**: e00471.

Jo, A., S. Ham, G. H. Lee, Y. I. Lee, S. Kim, Y. S. Lee, J. H. Shin and Y. Lee (2015). "Efficient Mitochondrial Genome Editing by CRISPR/Cas9." Biomed Res Int **2015**: 305716.

Judge, A. D., G. Bola, A. C. Lee and I. MacLachlan (2006). "Design of noninflammatory synthetic siRNA mediating potent gene silencing in vivo." Mol Ther **13**(3): 494-505.

Kabadi, A. M., D. G. Ousterout, I. B. Hilton and C. A. Gersbach (2014). "Multiplex CRISPR/Cas9-based genome engineering from a single lentiviral vector." Nucleic Acids Res **42**(19): e147.

Karayiannis, P. (2017). "Hepatitis B virus: virology, molecular biology, life cycle and intrahepatic spread." Hepatol Int **11**(6): 500-508.

Kariko, K., M. Buckstein, H. Ni and D. Weissman (2005). "Suppression of RNA recognition by Toll-like receptors: the impact of nucleoside modification and the evolutionary origin of RNA." Immunity **23**(2): 165-175.

Kariko, K., H. Muramatsu, J. M. Keller and D. Weissman (2012). "Increased erythropoiesis in mice injected with submicrogram quantities of pseudouridine-containing mRNA encoding erythropoietin." Mol Ther **20**(5): 948-953.

Kariko, K., H. Muramatsu, F. A. Welsh, J. Ludwig, H. Kato, S. Akira and D. Weissman (2008). "Incorporation of pseudouridine into mRNA yields superior nonimmunogenic vector with increased translational capacity and biological stability." Mol Ther **16**(11): 1833-1840.

Kazlauskiene, M., G. Kostiuk, C. Venclovas, G. Tamulaitis and V. Siksnys (2017). "A cyclic oligonucleotide signaling pathway in type III CRISPR-Cas systems." Science **357**(6351): 605-609.

Kennedy, E. M., L. C. Bassit, H. Mueller, A. V. R. Kornepati, H. P. Bogerd, T. Nie, P. Chatterjee, H. Javanbakht, R. F. Schinazi and B. R. Cullen (2015). "Suppression of hepatitis B virus DNA accumulation in chronically infected cells using a bacterial CRISPR/Cas RNA-guided DNA endonuclease." Virology **476**: 196-205.

Kennedy, E. M., A. V. Kornepati, M. Goldstein, H. P. Bogerd, B. C. Poling, A. W. Whisnant, M. B. Kastan and B. R. Cullen (2014). "Inactivation of the human papillomavirus E6 or E7 gene in cervical carcinoma cells by using a bacterial CRISPR/Cas RNA-guided endonuclease." J Virol **88**(20): 11965-11972.

Kettlun, C., D. L. Galvan, A. L. George, Jr., A. Kaja and M. H. Wilson (2011). "Manipulating piggyBac transposon chromosomal integration site selection in human cells." Mol Ther **19**(9): 1636-1644.

Kim, S., D. Kim, S. W. Cho, J. Kim and J. S. Kim (2014). "Highly efficient RNA-guided genome editing in human cells via delivery of purified Cas9 ribonucleoproteins." Genome Res **24**(6): 1012-1019.

Kim, S., T. Koo, H. G. Jee, H. Y. Cho, G. Lee, D. G. Lim, H. S. Shin and J. S. Kim (2018). "CRISPR RNAs trigger innate immune responses in human cells." Genome Res.

Kleinstiver, B. P., V. Pattanayak, M. S. Prew, S. Q. Tsai, N. T. Nguyen, Z. Zheng and J. K. Joung (2016). "High-fidelity CRISPR-Cas9 nucleases with no detectable genome-wide off-target effects." Nature **529**(7587): 490-495.

Knowles, B. B., C. C. Howe and D. P. Aden (1980). "Human hepatocellular carcinoma cell lines secrete the major plasma proteins and hepatitis B surface antigen." Science **209**(4455): 497-499.

Ko, C., R. Bester, X. Zhou, Z. Xu, C. Blossey, J. Sacherl, F. W. R. Vondran, L. Gao and U. Protzer (2019). "A New Role for Capsid Assembly Modulators To Target Mature Hepatitis B Virus Capsids and Prevent Virus Infection." Antimicrob Agents Chemother **64**(1).

Ko, C., A. Chakraborty, W. M. Chou, J. Hasreiter, J. M. Wettengel, D. Stadler, R. Bester, T. Asen, K. Zhang, K. Wisskirchen, J. A. McKeating, W. S. Ryu and U. Protzer (2018). "Hepatitis B virus genome recycling and de novo secondary infection events maintain stable cccDNA levels." J Hepatol **69**(6): 1231-1241.

Ko, C., T. Michler and U. Protzer (2017). "Novel viral and host targets to cure hepatitis B." Curr Opin Virol **24**: 38-45.

Koch, G. (1973). "Interaction of poliovirus-specific RNAs with HeLa cells and E. coli." Curr Top Microbiol Immunol **62**: 89-138.

Koniger, C., I. Wingert, M. Marsmann, C. Rosler, J. Beck and M. Nassal (2014). "Involvement of the host DNA-repair enzyme TDP2 in formation of the covalently closed circular DNA persistence reservoir of hepatitis B viruses." Proc Natl Acad Sci U S A **111**(40): E4244-4253.

Koonin, E. V., K. S. Makarova and Y. I. Wolf (2017). "Evolutionary Genomics of Defense Systems in Archaea and Bacteria." Annu Rev Microbiol **71**: 233-261.

Kosinska, A. D., A. Moeed, N. Kallin, J. Festag, J. Su, K. Steiger, M. L. Michel, U. Protzer and P. A. Knolle (2019). "Synergy of therapeutic heterologous prime-boost hepatitis B vaccination with CpG-application to improve immune control of persistent HBV infection." Sci Rep **9**(1): 10808.

Kovall, R. A. and B. W. Matthews (1999). "Type II restriction endonucleases: structural, functional and evolutionary relationships." Curr Opin Chem Biol **3**(5): 578-583.

Kozak, M. (1987). "An analysis of 5'-noncoding sequences from 699 vertebrate messenger RNAs." Nucleic Acids Res **15**(20): 8125-8148.

Kramvis, A. (2014). "Genotypes and genetic variability of hepatitis B virus." Intervirology **57**(3-4): 141-150.

Kruse, R. L., T. Shum, H. Tashiro, M. Barzi, Z. Yi, C. Whitten-Bauer, X. Legras, B. Bissig-Choisat, U. Garaigorta, S. Gottschalk and K. D. Bissig (2018). "HBsAg-redirected T cells exhibit antiviral activity in HBV-infected human liver chimeric mice." Cytotherapy **20**(5): 697-705.

Kubitz, R., G. Sutfels, T. Kuhlkamp, R. Kolling and D. Haussinger (2004). "Trafficking of the bile salt export pump from the Golgi to the canalicular membrane is regulated by the p38 MAP kinase." Gastroenterology **126**(2): 541-553.

Labrie, S. J., J. E. Samson and S. Moineau (2010). "Bacteriophage resistance mechanisms." Nat Rev Microbiol **8**(5): 317-327.

Lempp, F. A., P. Mutz, C. Lipps, D. Wirth, R. Bartenschlager and S. Urban (2016). "Evidence that hepatitis B virus replication in mouse cells is limited by the lack of a host cell dependency factor." J Hepatol **64**(3): 556-564.

Leonhardt, C., G. Schwake, T. R. Stogbauer, S. Rappl, J. T. Kuhr, T. S. Ligon and J. O. Radler (2014). "Single-cell mRNA transfection studies: delivery, kinetics and statistics by numbers." Nanomedicine **10**(4): 679-688.

Levy, O., W. Zhao, L. J. Mortensen, S. Leblanc, K. Tsang, M. Fu, J. A. Phillips, V. Sagar, P. Anandakumaran, J. Ngai, C. H. Cui, P. Eimon, M. Angel, C. P. Lin, M. F. Yanik and J. M. Karp (2013). "mRNA-engineered mesenchymal stem cells for targeted delivery of interleukin-10 to sites of inflammation." Blood **122**(14): e23-32.

Li, A., C. M. Lee, A. E. Hurley, K. E. Jarrett, M. De Giorgi, W. Lu, K. S. Balderrama, A. M. Doerfler, H. Deshmukh, A. Ray, G. Bao and W. R. Lagor (2019). "A Self-Deleting AAV-CRISPR System for In Vivo Genome Editing." Mol Ther Methods Clin Dev **12**: 111-122.

Li, D., W. He, X. Liu, S. Zheng, Y. Qi, H. Li, F. Mao, J. Liu, Y. Sun, L. Pan, K. Du, K. Ye, W. Li and J. Sui (2017). "A potent human neutralizing antibody Fc-dependently reduces established HBV infections." Elife **6**.

Li, H., C. Sheng, H. Liu, S. Wang, J. Zhao, L. Yang, L. Jia, P. Li, L. Wang, J. Xie, D. Xu, Y. Sun, S. Qiu and H. Song (2018). "Inhibition of HBV Expression in HBV Transgenic Mice Using AAV-Delivered CRISPR-SaCas9." Front Immunol **9**: 2080.

Li, K., G. Wang, T. Andersen, P. Zhou and W. T. Pu (2014). "Optimization of genome engineering approaches with the CRISPR/Cas9 system." PLoS One **9**(8): e105779.

Liang, X., J. Potter, S. Kumar, Y. Zou, R. Quintanilla, M. Sridharan, J. Carte, W. Chen, N. Roark, S. Ranganathan, N. Ravinder and J. D. Chesnut (2015). "Rapid and highly efficient mammalian cell engineering via Cas9 protein transfection." J Biotechnol **208**: 44-53.

Lin, L., T. S. Petersen, K. T. Jensen, L. Bolund, R. Kuhn and Y. Luo (2017). "Fusion of SpCas9 to E. coli Rec A protein enhances CRISPR-Cas9 mediated gene knockout in mammalian cells." J Biotechnol **247**: 42-49.

Lino, C. A., J. C. Harper, J. P. Carney and J. A. Timlin (2018). "Delivering CRISPR: a review of the challenges and approaches." Drug Deliv **25**(1): 1234-1257.

Liu, M., S. Rehman, X. Tang, K. Gu, Q. Fan, D. Chen and W. Ma (2018). "Methodologies for Improving HDR Efficiency." Front Genet **9**: 691.

Liu, Y., M. Zhao, M. Gong, Y. Xu, C. Xie, H. Deng, X. Li, H. Wu and Z. Wang (2018). "Inhibition of hepatitis B virus replication via HBV DNA cleavage by Cas9 from Staphylococcus aureus." Antiviral Res **152**: 58-67.

Lok, A. S., F. Zoulim, G. Dusheiko and M. G. Ghany (2017). "Hepatitis B cure: From discovery to regulatory approval." J Hepatol **67**(4): 847-861.

Loo, Y. M. and M. Gale, Jr. (2011). "Immune signaling by RIG-I-like receptors." Immunity **34**(5): 680-692.

Lucifora, J., S. Arzberger, D. Durantel, L. Belloni, M. Strubin, M. Levrero, F. Zoulim, O. Hantz and U. Protzer (2011). "Hepatitis B virus X protein is essential to initiate and maintain virus replication after infection." J Hepatol **55**(5): 996-1003.

Ma, D., Z. Xu, Z. Zhang, X. Chen, X. Zeng, Y. Zhang, T. Deng, M. Ren, Z. Sun, R. Jiang and Z. Xie (2019). "Engineer chimeric Cas9 to expand PAM recognition based on evolutionary information." Nat Commun **10**(1): 560.

Ma, H., L. C. Tu, A. Naseri, M. Huisman, S. Zhang, D. Grunwald and T. Pederson (2016). "CRISPR-Cas9 nuclear dynamics and target recognition in living cells." J Cell Biol **214**(5): 529-537.

Macovei, A., C. Radulescu, C. Lazar, S. Petrescu, D. Durantel, R. A. Dwek, N. Zitzmann and N. B. Nichita (2010). "Hepatitis B virus requires intact caveolin-1 function for productive infection in HepaRG cells." J Virol **84**(1): 243-253.

Maddalo, D., E. Manchado, C. P. Concepcion, C. Bonetti, J. A. Vidigal, Y. C. Han, P. Ogrodowski, A. Crippa, N. Rekhtman, E. de Stanchina, S. W. Lowe and A. Ventura (2014). "In vivo engineering of oncogenic chromosomal rearrangements with the CRISPR/Cas9 system." Nature **516**(7531): 423-427.

Makarova, K. S., V. Anantharaman, L. Aravind and E. V. Koonin (2012). "Live virus-free or die: coupling of antivirus immunity and programmed suicide or dormancy in prokaryotes." Biol Direct **7**: 40.

Makarova, K. S., D. H. Haft, R. Barrangou, S. J. Brouns, E. Charpentier, P. Horvath, S. Moineau, F. J. Mojica, Y. I. Wolf, A. F. Yakunin, J. van der Oost and E. V. Koonin (2011). "Evolution and classification of the CRISPR-Cas systems." Nat Rev Microbiol **9**(6): 467-477.

Makarova, K. S., Y. I. Wolf, O. S. Alkhnbashi, F. Costa, S. A. Shah, S. J. Saunders, R. Barrangou, S. J. Brouns, E. Charpentier, D. H. Haft, P. Horvath, S. Moineau, F. J. Mojica, R. M. Terns, M. P. Terns, M. F. White, A. F. Yakunin, R. A. Garrett, J. van der Oost, R. Backofen and E. V. Koonin (2015). "An updated evolutionary classification of CRISPR-Cas systems." Nat Rev Microbiol **13**(11): 722-736.

Makarova, K. S., Y. I. Wolf, J. Iranzo, S. A. Shmakov, O. S. Alkhnbashi, S. J. J. Brouns, E. Charpentier, D. Cheng, D. H. Haft, P. Horvath, S. Moineau, F. J. M. Mojica, D. Scott, S. A. Shah, V. Siksnys, M. P. Terns, C. Venclovas, M. F. White, A. F. Yakunin, W. Yan, F. Zhang, R. A. Garrett, R. Backofen, J. van der Oost, R. Barrangou and E. V. Koonin (2020). "Evolutionary classification of CRISPR-Cas systems: a burst of class 2 and derived variants." Nat Rev Microbiol **18**(2): 67-83.

Makarova, K. S., Y. I. Wolf and E. V. Koonin (2013). "The basic building blocks and evolution of CRISPR-CAS systems." Biochem Soc Trans **41**(6): 1392-1400.

Mallon, B. S., R. S. Hamilton, O. A. Kozhich, K. R. Johnson, Y. C. Fann, M. S. Rao and P. G. Robey (2014). "Comparison of the molecular profiles of human embryonic and induced pluripotent stem cells of isogenic origin." Stem Cell Res **12**(2): 376-386.

Mason, W. S., G. Seal and J. Summers (1980). "Virus of Pekin ducks with structural and biological relatedness to human hepatitis B virus." J Virol **36**(3): 829-836.

McCarty, D. M. (2008). "Self-complementary AAV vectors; advances and applications." Mol Ther **16**(10): 1648-1656.

Mekler, V., L. Minakhin, E. Semenova, K. Kuznedelov and K. Severinov (2016). "Kinetics of the CRISPR-Cas9 effector complex assembly and the role of 3'-terminal segment of guide RNA." Nucleic Acids Res **44**(6): 2837-2845.

Meredith, L. W., K. Hu, X. Cheng, C. R. Howard, T. F. Baumert, P. Balfe, K. F. van de Graaf, U. Protzer and J. A. McKeating (2016). "Lentiviral hepatitis B pseudotype entry requires sodium taurocholate co-transporting polypeptide and additional hepatocyte-specific factors." J Gen Virol **97**(1): 121-127.

Meyers, R. M., J. G. Bryan, J. M. McFarland, B. A. Weir, A. E. Sizemore, H. Xu, N. V. Dharia, P. G. Montgomery, G. S. Cowley, S. Pantel, A. Goodale, Y. Lee, L. D. Ali, G. Jiang, R. Lubonja, W. F. Harrington, M. Strickland, T. Wu, D. C. Hawes, V. A. Zhivich, M. R. Wyatt, Z. Kalani, J. J. Chang, M. Okamoto, K. Stegmaier, T. R. Golub, J. S. Boehm, F. Vazquez, D. E. Root, W. C. Hahn and A. Tsherniak (2017). "Computational correction of copy number effect improves specificity of CRISPR-Cas9 essentiality screens in cancer cells." Nat Genet **49**(12): 1779-1784.

Michler, T., S. Grosse, S. Mockenhaupt, N. Roder, F. Stuckler, B. Knapp, C. Ko, M. Heikenwalder, U. Protzer and D. Grimm (2016). "Blocking sense-strand activity improves potency, safety and specificity of anti-hepatitis B virus short hairpin RNA." EMBO Mol Med **8**(9): 1082-1098.

Michler, T., A. D. Kosinska, J. Festag, T. Bunse, J. Su, M. Ringelhan, H. Imhof, D. Grimm, K. Steiger, C. Mogler, M. Heikenwalder, M. L. Michel, C. A. Guzman, S. Milstein, L. Sepp-Lorenzino, P. Knolle and U. Protzer (2020). "Knockdown of Virus Antigen Expression Increases Therapeutic Vaccine Efficacy in High-Titer Hepatitis B Virus Carrier Mice." Gastroenterology.

Michler, T., A. D. Kosinska, J. Festag, T. Bunse, J. Su, M. Ringelhan, H. Imhof, D. Grimm, K. Steiger, C. Mogler, M. Heikenwalder, M. L. Michel, C. A. Guzman, S. Milstein, L. Sepp-Lorenzino, P. Knolle and U. Protzer (2020). "Knockdown of Virus Antigen Expression Increases Therapeutic Vaccine Efficacy in High-Titer Hepatitis B Virus Carrier Mice." Gastroenterology **158**(6): 1762-1775 e1769.

Mockenhaupt, S., S. Grosse, D. Rupp, R. Bartenschlager and D. Grimm (2015). "Alleviation of off-target effects from vector-encoded shRNAs via codelivered RNA decoys." Proc Natl Acad Sci U S A **112**(30): E4007-4016.

Moore, J. K. and J. E. Haber (1996). "Cell cycle and genetic requirements of two pathways of nonhomologous end-joining repair of double-strand breaks in Saccharomyces cerevisiae." Mol Cell Biol **16**(5): 2164-2173.

Nassal, M. (2015). "HBV cccDNA: viral persistence reservoir and key obstacle for a cure of chronic hepatitis B." Gut **64**(12): 1972-1984.

Neumann, A. U., S. Phillips, I. Levine, S. Ijaz, H. Dahari, R. Eren, S. Dagan and N. V. Naoumov (2010). "Novel mechanism of antibodies to hepatitis B virus in blocking viral particle release from cells." Hepatology **52**(3): 875-885.

Ni, Y., F. A. Lempp, S. Mehrle, S. Nkongolo, C. Kaufman, M. Falth, J. Stindt, C. Koniger, M. Nassal, R. Kubitz, H. Sultmann and S. Urban (2014). "Hepatitis B and D viruses exploit sodium taurocholate co-transporting polypeptide for species-specific entry into hepatocytes." Gastroenterology **146**(4): 1070-1083.

Nishimasu, H., L. Cong, W. X. Yan, F. A. Ran, B. Zetsche, Y. Li, A. Kurabayashi, R. Ishitani, F. Zhang and O. Nureki (2015). "Crystal Structure of Staphylococcus aureus Cas9." Cell **162**(5): 1113-1126.

Nishimasu, H., F. A. Ran, P. D. Hsu, S. Konermann, S. I. Shehata, N. Dohmae, R. Ishitani, F. Zhang and O. Nureki (2014). "Crystal structure of Cas9 in complex with guide RNA and target DNA." Cell **156**(5): 935-949.

Oswald, A. (2016). "Establishment of a mRNA based CRISPR/Cas9 system for genom editing." Master's Thesis.

Pankotai, T., C. Bonhomme, D. Chen and E. Soutoglou (2012). "DNAPKcs-dependent arrest of RNA polymerase II transcription in the presence of DNA breaks." Nat Struct Mol Biol **19**(3): 276-282.

Paquet, D., D. Kwart, A. Chen, A. Sproul, S. Jacob, S. Teo, K. M. Olsen, A. Gregg, S. Noggle and M. Tessier-Lavigne (2016). "Efficient introduction of specific homozygous and heterozygous mutations using CRISPR/Cas9." Nature **533**(7601): 125-129.

Pardi, N., S. Tuyishime, H. Muramatsu, K. Kariko, B. L. Mui, Y. K. Tam, T. D. Madden, M. J. Hope and D. Weissman (2015). "Expression kinetics of nucleoside-modified mRNA delivered in lipid nanoparticles to mice by various routes." J Control Release **217**: 345-351.

Pasquinelli, A. E., J. E. Dahlberg and E. Lund (1995). "Reverse 5' caps in RNAs made in vitro by phage RNA polymerases." RNA **1**(9): 957-967.

Patel, S., A. Athirasala, P. P. Menezes, N. Ashwanikumar, T. Zou, G. Sahay and L. E. Bertassoni (2019). "Messenger RNA Delivery for Tissue Engineering and Regenerative Medicine Applications." Tissue Eng Part A **25**(1-2): 91-112.

Patient, R., C. Hourioux, P. Y. Sizaret, S. Trassard, C. Sureau and P. Roingeard (2007). "Hepatitis B virus subviral envelope particle morphogenesis and intracellular trafficking." J Virol **81**(8): 3842-3851.

Pelegrin, M., M. Naranjo-Gomez and M. Piechaczyk (2015). "Antiviral Monoclonal Antibodies: Can They Be More Than Simple Neutralizing Agents?" Trends Microbiol **23**(10): 653-665.

Pichlmair, A., O. Schulz, C. P. Tan, T. I. Naslund, P. Liljestrom, F. Weber and C. Reis e Sousa (2006). "RIG-I-mediated antiviral responses to single-stranded RNA bearing 5'-phosphates." Science **314**(5801): 997-1001.

Piechaczek, C., C. Fetzer, A. Baiker, J. Bode and H. J. Lipps (1999). "A vector based on the SV40 origin of replication and chromosomal S/MARs replicates episomally in CHO cells." Nucleic Acids Res **27**(2): 426-428.

Plews, J. R., J. Li, M. Jones, H. D. Moore, C. Mason, P. W. Andrews and J. Na (2010). "Activation of pluripotency genes in human fibroblast cells by a novel mRNA based approach." PLoS One **5**(12): e14397.

Pollicino, T., L. Belloni, G. Raffa, N. Pediconi, G. Squadrito, G. Raimondo and M. Levrero (2006). "Hepatitis B virus replication is regulated by the acetylation status of hepatitis B virus cccDNA-bound H3 and H4 histones." Gastroenterology **130**(3): 823-837.

Ponten, J. and E. Saksela (1967). "Two established in vitro cell lines from human mesenchymal tumours." Int J Cancer **2**(5): 434-447.

Pourkarim, M. R., S. Amini-Bavil-Olyaee, F. Kurbanov, M. Van Ranst and F. Tacke (2014). "Molecular identification of hepatitis B virus genotypes/subgenotypes: revised classification hurdles and updated resolutions." World J Gastroenterol **20**(23): 7152-7168.

Protzer, U. and H. Schaller (2000). "Immune escape by hepatitis B viruses." Virus Genes **21**(1-2): 27-37.

Qasim, W., M. Brunetto, A. J. Gehring, S. A. Xue, A. Schurich, A. Khakpoor, H. Zhan, P. Ciccorossi, K. Gilmour, D. Cavallone, F. Moriconi, F. Farzhenah, A. Mazzoni, L. Chan, E. Morris, A. Thrasher, M. K. Maini, F. Bonino, H. Stauss and A. Bertoletti (2015). "Immunotherapy of HCC metastases with autologous T cell receptor redirected T cells, targeting HBsAg in a liver transplant patient." J Hepatol **62**(2): 486-491.

Rajbhandari, R. and R. T. Chung (2016). "Treatment of Hepatitis B: A Concise Review." Clin Transl Gastroenterol **7**(9): e190.

Ramanan, V., A. Shlomai, D. B. Cox, R. E. Schwartz, E. Michailidis, A. Bhatta, D. A. Scott, F. Zhang, C. M. Rice and S. N. Bhatia (2015). "CRISPR/Cas9 cleavage of viral DNA efficiently suppresses hepatitis B virus." Sci Rep **5**: 10833.

Ramanathan, A., G. B. Robb and S. H. Chan (2016). "mRNA capping: biological functions and applications." Nucleic Acids Res **44**(16): 7511-7526.

Ran, F. A., L. Cong, W. X. Yan, D. A. Scott, J. S. Gootenberg, A. J. Kriz, B. Zetsche, O. Shalem, X. Wu, K. S. Makarova, E. V. Koonin, P. A. Sharp and F. Zhang (2015). "In vivo genome editing using Staphylococcus aureus Cas9." Nature **520**(7546): 186-191.

Ran, F. A., P. D. Hsu, J. Wright, V. Agarwala, D. A. Scott and F. Zhang (2013). "Genome engineering using the CRISPR-Cas9 system." Nat Protoc **8**(11): 2281-2308.

Ranganathan, R. and M. C. Foster (2016). "The Limitations and Promise of Immunotherapy With Chimeric Antigen-Modified T Cells." Oncology (Williston Park) **30**(10): 889-890.

Rehermann, B. and M. Nascimbeni (2005). "Immunology of hepatitis B virus and hepatitis C virus infection." Nat Rev Immunol **5**(3): 215-229.

Rettig, L., S. P. Haen, A. G. Bittermann, L. von Boehmer, A. Curioni, S. D. Kramer, A. Knuth and S. Pascolo (2010). "Particle size and activation threshold: a new dimension of danger signaling." Blood **115**(22): 4533-4541.

Riviere, L., L. Gerossier, A. Ducroux, S. Dion, Q. Deng, M. L. Michel, M. A. Buendia, O. Hantz and C. Neuveut (2015). "HBx relieves chromatin-mediated transcriptional repression of hepatitis B viral cccDNA involving SETDB1 histone methyltransferase." J Hepatol **63**(5): 1093-1102.

RKI (2018). "Virushepatitis B und D im Jahr 2018." Epidemiologisches Bulletin - Aktuelle Daten und Informationen zu Infektionskrankheiten und public health.

Roehm, P. C., M. Shekarabi, H. S. Wollebo, A. Bellizzi, L. He, J. Salkind and K. Khalili (2016). "Inhibition of HSV-1 Replication by Gene Editing Strategy." Sci Rep **6**: 23146.

Sahin, U., K. Kariko and O. Tureci (2014). "mRNA-based therapeutics--developing a new class of drugs." Nat Rev Drug Discov **13**(10): 759-780.

Schaefer, S. (2007). "Hepatitis B virus taxonomy and hepatitis B virus genotypes." World J Gastroenterol **13**(1): 14-21.

Scheid, J. F., J. A. Horwitz, Y. Bar-On, E. F. Kreider, C. L. Lu, J. C. Lorenzi, A. Feldmann, M. Braunschweig, L. Nogueira, T. Oliveira, I. Shimeliovich, R. Patel, L. Burke, Y. Z. Cohen, S. Hadrigan, A. Settler, M. Witmer-Pack, A. P. West, Jr., B. Juelg, T. Keler, T. Hawthorne, B. Zingman, R. M. Gulick, N. Pfeifer, G. H. Learn, M. S. Seaman, P. J. Bjorkman, F. Klein, S. J. Schlesinger, B. D. Walker, B. H. Hahn, M. C. Nussenzweig and M. Caskey (2016). "HIV-1 antibody 3BNC117 suppresses viral rebound in humans during treatment interruption." Nature **535**(7613): 556-560.

Schiwon, M., E. Ehrke-Schulz, A. Oswald, T. Bergmann, T. Michler, U. Protzer and A. Ehrhardt (2018). "One-Vector System for Multiplexed CRISPR/Cas9 against Hepatitis B Virus cccDNA Utilizing High-Capacity Adenoviral Vectors." Mol Ther Nucleic Acids **12**: 242-253.

Schlaeger, T. M., L. Daheron, T. R. Brickler, S. Entwisle, K. Chan, A. Cianci, A. DeVine, A. Ettenger, K. Fitzgerald, M. Godfrey, D. Gupta, J. McPherson, P. Malwadkar, M. Gupta, B. Bell, A. Doi, N. Jung, X. Li, M. S. Lynes, E. Brookes, A. B. Cherry, D. Demirbas, A. M. Tsankov, L. I. Zon, L. L. Rubin, A. P. Feinberg, A. Meissner, C. A. Cowan and G. Q. Daley (2015). "A comparison of non-integrating reprogramming methods." Nat Biotechnol **33**(1): 58-63.

Schmelas, C. (2020). "One for all, all for one: Combining and improving AAV, RNAi and CRISPR technologies to combat HBV infection and HBV/HDV co-infections." PhD thesis.

Schmelas, C. and D. Grimm (2018). "Split Cas9, Not Hairs - Advancing the Therapeutic Index of CRISPR Technology." Biotechnol J **13**(9): e1700432.

Schmitz, A., A. Schwarz, M. Foss, L. Zhou, B. Rabe, J. Hoellenriegel, M. Stoeber, N. Pante and M. Kann (2010). "Nucleoporin 153 arrests the nuclear import of hepatitis B virus capsids in the nuclear basket." PLoS Pathog **6**(1): e1000741.

Schoofs, T., F. Klein, M. Braunschweig, E. F. Kreider, A. Feldmann, L. Nogueira, T. Oliveira, J. C. Lorenzi, E. H. Parrish, G. H. Learn, A. P. West, Jr., P. J. Bjorkman, S. J. Schlesinger, M. S. Seaman, J. Czartoski, M. J. McElrath, N. Pfeifer, B. H. Hahn, M. Caskey and M. C. Nussenzweig (2016). "HIV-1 therapy with monoclonal antibody 3BNC117 elicits host immune responses against HIV-1." Science **352**(6288): 997-1001.

Schreiner, S. and M. Nassal (2017). "A Role for the Host DNA Damage Response in Hepatitis B Virus cccDNA Formation-and Beyond?" Viruses **9**(5).

Schulze, A., P. Gripon and S. Urban (2007). "Hepatitis B virus infection initiates with a large surface protein-dependent binding to heparan sulfate proteoglycans." Hepatology **46**(6): 1759-1768.

Schwank, G., B. K. Koo, V. Sasselli, J. F. Dekkers, I. Heo, T. Demircan, N. Sasaki, S. Boymans, E. Cuppen, C. K. van der Ent, E. E. Nieuwenhuis, J. M. Beekman and H. Clevers (2013). "Functional repair of CFTR by CRISPR/Cas9 in intestinal stem cell organoids of cystic fibrosis patients." Cell Stem Cell **13**(6): 653-658.

Schweitzer, A., J. Horn, R. T. Mikolajczyk, G. Krause and J. J. Ott (2015). "Estimations of worldwide prevalence of chronic hepatitis B virus infection: a systematic review of data published between 1965 and 2013." Lancet **386**(10003): 1546-1555.

Seeger, C. and W. S. Mason (2015). "Molecular biology of hepatitis B virus infection." Virology **479-480**: 672-686.

Seeger, C. and J. A. Sohn (2014). "Targeting Hepatitis B Virus With CRISPR/Cas9." Mol Ther Nucleic Acids **3**: e216.

Seeger, C., F. Zoulim and W. S. Mason (2007). "Hepadnaviruses." In: Knipe DM, Howley PM, editors. Fields Virology.: 2977-3029.

Sells, M. A., M. L. Chen and G. Acs (1987). "Production of hepatitis B virus particles in Hep G2 cells transfected with cloned hepatitis B virus DNA." Proc Natl Acad Sci U S A **84**(4): 1005-1009.

Semenova, E., M. M. Jore, K. A. Datsenko, A. Semenova, E. R. Westra, B. Wanner, J. van der Oost, S. J. Brouns and K. Severinov (2011). "Interference by clustered regularly interspaced short palindromic repeat (CRISPR) RNA is governed by a seed sequence." Proc Natl Acad Sci U S A **108**(25): 10098-10103.

Shanbhag, N. M., I. U. Rafalska-Metcalf, C. Balane-Bolivar, S. M. Janicki and R. A. Greenberg (2010). "ATM-dependent chromatin changes silence transcription in cis to DNA double-strand breaks." Cell **141**(6): 970-981.

Slaymaker, I. M., L. Gao, B. Zetsche, D. A. Scott, W. X. Yan and F. Zhang (2016). "Rationally engineered Cas9 nucleases with improved specificity." Science **351**(6268): 84-88.

Slivac, I., D. Guay, M. Mangion, J. Champeil and B. Gaillet (2017). "Non-viral nucleic acid delivery methods." Expert Opin Biol Ther **17**(1): 105-118.

Sommeregger, W., P. Mayrhofer, W. Steinfellner, D. Reinhart, M. Henry, M. Clynes, P. Meleady and R. Kunert (2016). "Proteomic differences in recombinant CHO cells producing two similar antibody fragments." Biotechnol Bioeng **113**(9): 1902-1912.

Song, G., F. Zhang, X. Zhang, X. Gao, X. Zhu, D. Fan and Y. Tian (2019). "AcrIIA5 Inhibits a Broad Range of Cas9 Orthologs by Preventing DNA Target Cleavage." Cell Rep **29**(9): 2579-2589 e2574.

Spellman, M. and J. T. Martin (2011). "TREATMENT OF CHRONIC HEPATITIS B INFECTION WITH DV-601, A THERAPEUTIC VACCINE." J Hepatol **54**: S302.

Stadler, D., M. Kächele, J. Hess, A. N. Jones, C. Urban, S. Schneider, Y. Xia, A. Oswald, F. Nebioglu, R. Bester, F. Lasitschka, M. Ringelhan, C. Ko, W. M. Chou, M. van der Klundert, J. M. Wettengel, P. Schirmacher, M. Heikenwalder, S. Schreiner, A. Pichlmair, R. Bartenschlager, M. Sattler, K. Unger and U. Protzer (2020). "Interferon-induced degradation of the hepatitis B virus persistence form, cccDNA depends on ISG20." EMBO Rep - currently in revision.

Stavrou, E. F., V. M. Lazaris, A. Giannakopoulos, E. Papapetrou, A. Spyridonidis, N. C. Zoumbos, A. Gkountis and A. Athanassiadou (2017). "The beta-globin Replicator greatly enhances the potential of S/MAR based episomal vectors for gene transfer into human haematopoietic progenitor cells." Sci Rep **7**: 40673.

Steichen, C., E. Luce, J. Maluenda, L. Tosca, I. Moreno-Gimeno, C. Desterke, N. Dianat, S. Goulinet-Mainot, S. Awan-Toor, D. Burks, J. Marie, A. Weber, G. Tachdjian, J. Melki and A. Dubart-Kupperschmitt (2014). "Messenger RNA- versus retrovirus-based induced pluripotent stem cell reprogramming strategies: analysis of genomic integrity." Stem Cells Transl Med **3**(6): 686-691.

Steinle, H., A. Behring, C. Schlensak, H. P. Wendel and M. Avci-Adali (2017). "Concise Review: Application of In Vitro Transcribed Messenger RNA for Cellular Engineering and Reprogramming: Progress and Challenges." Stem Cells **35**(1): 68-79.

Stevens, C. E., P. Toy, S. Kamili, P. E. Taylor, M. J. Tong, G. L. Xia and G. N. Vyas (2017). "Eradicating hepatitis B virus: The critical role of preventing perinatal transmission." Biologicals **50**: 3-19.

Stray, S. J. and A. Zlotnick (2006). "BAY 41-4109 has multiple effects on Hepatitis B virus capsid assembly." J Mol Recognit **19**(6): 542-548.

Strecker, J., S. Jones, B. Koopal, J. Schmid-Burgk, B. Zetsche, L. Gao, K. S. Makarova, E. V. Koonin and F. Zhang (2019). "Engineering of CRISPR-Cas12b for human genome editing." Nat Commun **10**(1): 212.

Summers, J., J. M. Smolec and R. Snyder (1978). "A virus similar to human hepatitis B virus associated with hepatitis and hepatoma in woodchucks." Proc Natl Acad Sci U S A **75**(9): 4533-4537.

Swarts, D. C. and M. Jinek (2019). "Mechanistic Insights into the cis- and trans-Acting DNase Activities of Cas12a." Mol Cell **73**(3): 589-600 e584.

Swarts, D. C., K. Makarova, Y. Wang, K. Nakanishi, R. F. Ketting, E. V. Koonin, D. J. Patel and J. van der Oost (2014). "The evolutionary journey of Argonaute proteins." Nat Struct Mol Biol **21**(9): 743-753.

Tatematsu, K., Y. Tanaka, F. Kurbanov, F. Sugauchi, S. Mano, T. Maeshiro, T. Nakayoshi, M. Wakuta, Y. Miyakawa and M. Mizokami (2009). "A genetic variant of hepatitis B virus divergent from known human and ape genotypes isolated from a Japanese patient and provisionally assigned to new genotype J." J Virol **83**(20): 10538-10547.

Thimme, R., S. Wieland, C. Steiger, J. Ghrayeb, K. A. Reimann, R. H. Purcell and F. V. Chisari (2003). "CD8(+) T cells mediate viral clearance and disease pathogenesis during acute hepatitis B virus infection." J Virol **77**(1): 68-76.

Trepo, C., H. L. Chan and A. Lok (2014). "Hepatitis B virus infection." Lancet **384**(9959): 2053-2063.

Tropberger, P., A. Mercier, M. Robinson, W. Zhong, D. E. Ganem and M. Holdorf (2015). "Mapping of histone modifications in episomal HBV cccDNA uncovers an unusual chromatin organization amenable to epigenetic manipulation." Proc Natl Acad Sci U S A **112**(42): E5715-5724.

Tsui, T. K. M., T. H. Hand, E. C. Duboy and H. Li (2017). "The Impact of DNA Topology and Guide Length on Target Selection by a Cytosine-Specific Cas9." ACS Synth Biol **6**(6): 1103-1113.

Untergasser, A. and U. Protzer (2004). "Hepatitis B virus-based vectors allow the elimination of viral gene expression and the insertion of foreign promoters." Hum Gene Ther **15**(2): 203-210.

Urban, S., R. Bartenschlager, R. Kubitz and F. Zoulim (2014). "Strategies to inhibit entry of HBV and HDV into hepatocytes." Gastroenterology **147**(1): 48-64.

Vaidyanathan, S., K. T. Azizian, A. Haque, J. M. Henderson, A. Hendel, S. Shore, J. S. Antony, R. I. Hogrefe, M. S. D. Kormann, M. H. Porteus and A. P. McCaffrey (2018). "Uridine Depletion and Chemical Modification Increase Cas9 mRNA Activity and Reduce Immunogenicity without HPLC Purification." Mol Ther Nucleic Acids **12**: 530-542.

van Belkum, A., S. Scherer, L. van Alphen and H. Verbrugh (1998). "Short-sequence DNA repeats in prokaryotic genomes." Microbiol Mol Biol Rev **62**(2): 275-293.

Velkov, S., J. J. Ott, U. Protzer and T. Michler (2018). "The Global Hepatitis B Virus Genotype Distribution Approximated from Available Genotyping Data." Genes (Basel) **9**(10).

Voets, O., F. Tielen, E. Elstak, J. Benschop, M. Grimbergen, J. Stallen, R. Janssen, A. van Marle and C. Essrich (2017). "Highly efficient gene inactivation by adenoviral CRISPR/Cas9 in human primary cells." PLoS One **12**(8): e0182974.

Wang, J., R. Chen, R. Zhang, S. Ding, T. Zhang, Q. Yuan, G. Guan, X. Chen, T. Zhang, H. Zhuang, F. Nunes, T. Block, S. Liu, Z. Duan, N. Xia, Z. Xu and F. Lu (2017). "The gRNA-miRNA-gRNA Ternary Cassette Combining CRISPR/Cas9 with RNAi Approach Strongly Inhibits Hepatitis B Virus Replication." Theranostics **7**(12): 3090-3105.

Wang, J., Z. W. Xu, S. Liu, R. Y. Zhang, S. L. Ding, X. M. Xie, L. Long, X. M. Chen, H. Zhuang and F. M. Lu (2015). "Dual gRNAs guided CRISPR/Cas9 system inhibits hepatitis B virus replication." World J Gastroenterol **21**(32): 9554-9565.

Wang, M., J. A. Zuris, F. Meng, H. Rees, S. Sun, P. Deng, Y. Han, X. Gao, D. Pouli, Q. Wu, I. Georgakoudi, D. R. Liu and Q. Xu (2016). "Efficient delivery of genome-editing proteins using bioreducible lipid nanoparticles." Proc Natl Acad Sci U S A **113**(11): 2868-2873.

Warren, L., P. D. Manos, T. Ahfeldt, Y. H. Loh, H. Li, F. Lau, W. Ebina, P. K. Mandal, Z. D. Smith, A. Meissner, G. Q. Daley, A. S. Brack, J. J. Collins, C. Cowan, T.

M. Schlaeger and D. J. Rossi (2010). "Highly efficient reprogramming to pluripotency and directed differentiation of human cells with synthetic modified mRNA." Cell Stem Cell **7**(5): 618-630.

Waters, C. A., N. T. Strande, J. M. Pryor, C. N. Strom, P. Mieczkowski, M. D. Burkhalter, S. Oh, B. F. Qaqish, D. T. Moore, E. A. Hendrickson and D. A. Ramsden (2014). "The fidelity of the ligation step determines how ends are resolved during nonhomologous end joining." Nat Commun **5**: 4286.

WHO (2017). "World Health Organization - Global hepatitis report, 2017." Global HIV, Hepatitis and Sexually Transmitted Infections Programmes: 83.

Wiedenheft, B., E. van Duijn, J. B. Bultema, S. P. Waghmare, K. Zhou, A. Barendregt, W. Westphal, A. J. Heck, E. J. Boekema, M. J. Dickman and J. A. Doudna (2011). "RNA-guided complex from a bacterial immune system enhances target recognition through seed sequence interactions." Proc Natl Acad Sci U S A **108**(25): 10092-10097.

Wienert, B., J. Shin, E. Zelin, K. Pestal and J. E. Corn (2018). "In vitro-transcribed guide RNAs trigger an innate immune response via the RIG-I pathway." PLoS Biol **16**(7): e2005840.

Wisskirchen, K., J. Kah, A. Malo, T. Asen, T. Volz, L. Allweiss, J. M. Wettengel, M. Lutgehetmann, S. Urban, T. Bauer, M. Dandri and U. Protzer (2019). "T cell receptor grafting allows virological control of Hepatitis B virus infection." J Clin Invest **129**(7): 2932-2945.

Xia, Y., D. Stadler, C. Ko and U. Protzer (2017). "Analyses of HBV cccDNA Quantification and Modification." Methods Mol Biol **1540**: 59-72.

Yamano, T., H. Nishimasu, B. Zetsche, H. Hirano, I. M. Slaymaker, Y. Li, I. Fedorova, T. Nakane, K. S. Makarova, E. V. Koonin, R. Ishitani, F. Zhang and O. Nureki (2016). "Crystal Structure of Cpf1 in Complex with Guide RNA and Target DNA." Cell **165**(4): 949-962.

Yan, H., G. Zhong, G. Xu, W. He, Z. Jing, Z. Gao, Y. Huang, Y. Qi, B. Peng, H. Wang, L. Fu, M. Song, P. Chen, W. Gao, B. Ren, Y. Sun, T. Cai, X. Feng, J. Sui and W. Li (2012). "Sodium taurocholate cotransporting polypeptide is a functional receptor for human hepatitis B and D virus." Elife **3**.

Yang, D., L. Liu, D. Zhu, H. Peng, L. Su, Y. X. Fu and L. Zhang (2014). "A mouse model for HBV immunotolerance and immunotherapy." Cell Mol Immunol **11**(1): 71-78.

Yang, H., H. Wang, C. S. Shivalila, A. W. Cheng, L. Shi and R. Jaenisch (2013). "One-step generation of mice carrying reporter and conditional alleles by CRISPR/Cas-mediated genome engineering." Cell **154**(6): 1370-1379.

Yang, X., W. Cai, X. Sun, Y. Bi, C. Zeng, X. Zhao, Q. Zhou, T. Xu, Q. Xie, P. Sun and X. Zhou (2020). "Defined host factors support HBV infection in non-hepatic 293T cells." J Cell Mol Med **24**(4): 2507-2518.

Yao, R., D. Liu, X. Jia, Y. Zheng, W. Liu and Y. Xiao (2018). "CRISPR-Cas9/Cas12a biotechnology and application in bacteria." Synth Syst Biotechnol **3**(3): 135-149.

Yin, H., W. Xue, S. Chen, R. L. Bogorad, E. Benedetti, M. Grompe, V. Koteliansky, P. A. Sharp, T. Jacks and D. G. Anderson (2014). "Genome editing with Cas9 in adult mice corrects a disease mutation and phenotype." Nat Biotechnol **32**(6): 551-553.

Yoshioka, N., E. Gros, H. R. Li, S. Kumar, D. C. Deacon, C. Maron, A. R. Muotri, N. C. Chi, X. D. Fu, B. D. Yu and S. F. Dowdy (2013). "Efficient generation of human iPSCs by a synthetic self-replicative RNA." Cell Stem Cell **13**(2): 246-254.

Zangi, L., K. O. Lui, A. von Gise, Q. Ma, W. Ebina, L. M. Ptaszek, D. Spater, H. Xu, M. Tabebordbar, R. Gorbatov, B. Sena, M. Nahrendorf, D. M. Briscoe, R. A. Li, A. J. Wagers, D. J. Rossi, W. T. Pu and K. R. Chien (2013). "Modified mRNA directs the fate of heart progenitor cells and induces vascular regeneration after myocardial infarction." Nat Biotechnol **31**(10): 898-907.

Zetsche, B., J. S. Gootenberg, O. O. Abudayyeh, I. M. Slaymaker, K. S. Makarova, P. Essletzbichler, S. E. Volz, J. Joung, J. van der Oost, A. Regev, E. V. Koonin and F. Zhang (2015). "Cpf1 is a single RNA-guided endonuclease of a class 2 CRISPR-Cas system." Cell **163**(3): 759-771.

Zhang, T. Y., Q. Yuan, J. H. Zhao, Y. L. Zhang, L. Z. Yuan, Y. Lan, Y. C. Lo, C. P. Sun, C. R. Wu, J. F. Zhang, Y. Zhang, J. L. Cao, X. R. Guo, X. Liu, X. B. Mo, W. X. Luo, T. Cheng, Y. X. Chen, M. H. Tao, J. W. Shih, Q. J. Zhao, J. Zhang, P. J. Chen, Y. A. Yuan and N. S. Xia (2016). "Prolonged suppression of HBV in mice by a novel antibody that targets a unique epitope on hepatitis B surface antigen." Gut **65**(4): 658-671.

Zhu, W., R. Lei, Y. Le Duff, J. Li, F. Guo, M. A. Wainberg and C. Liang (2015). "The CRISPR/Cas9 system inactivates latent HIV-1 proviral DNA." Retrovirology **12**: 22.

Zoulim, F., F. Lebosse and M. Levrero (2016). "Current treatments for chronic hepatitis B virus infections." Curr Opin Virol **18**: 109-116.

Zuris, J. A., D. B. Thompson, Y. Shu, J. P. Guilinger, J. L. Bessen, J. H. Hu, M. L. Maeder, J. K. Joung, Z. Y. Chen and D. R. Liu (2015). "Cationic lipid-mediated delivery of proteins enables efficient protein-based genome editing in vitro and in vivo." Nat Biotechnol **33**(1): 73-80.

Zust, R., L. Cervantes-Barragan, M. Habjan, R. Maier, B. W. Neuman, J. Ziebuhr, K. J. Szretter, S. C. Baker, W. Barchet, M. S. Diamond, S. G. Siddell, B. Ludewig and V. Thiel (2011). "Ribose 2'-O-methylation provides a molecular signature for the distinction of self and non-self mRNA dependent on the RNA sensor Mda5." Nat Immunol **12**(2): 137-143.

Acknowledgements

First, I want to thank Dr. Prof. Ulrike Protzer for giving me the chance to work on interesting, different and challenging topics in her laboratory. Additionally, I want to thank her for all the help and support during my PhD thesis, great discussions and especially her support during the finalization of my thesis and the NTCP-paper!

Next, I want to thank Prof. Dr. Michael Pfaffl as my second advisor in the committee meeting, who gave me the chance to present my data at the GQE 2019. Also, I want to thank him for all the feedback he gave me during my committee meeting and the annual seminars.

I'd like to thank our cooperation partner from the university Heidelberg, Prof. Dr. Grimm and Carolin Schmelas, who were involved in the generation of our combinatorial AAV system. I want to thank Prof. Dr. Grimm for his discussion at my TAC meeting and for his support during my lab rotation. Especially, I want to thank Carolin Schmelas, who spent a lot of work for our shared project but also for the CRISPR/Cas9 topic. Additionally, I want to thank her also for the great discussions we had about both topics and the help and supervision during my stay at Heidelberg.

Since lab work can be really frustrating and stressfull, you need to have good colleagues. So, I want to thank Anindita Chakraborty, Stoyan Velkov, Till Bunse, Samuel Jeske, Martin Kächele, Julia Sacherl, Fuwang Chen, Jochen M. Wettengel, Daniela Stadler, Thomas Michler, Lisa Wolff and Chunkyu Ko. Some of you also have become good friends, who made and make the daily work much more enjoyable!

The next big thanks goes to those who helps us with the daily lab routine, office stuff and remind us to also do our general duties. I'd like to thank Theresa Asen, Romina Beister, Philipp Hagen and Daniela Rizzi. Without you, I guess most of us would be really lost and I guess the lab wouldn't run as smoothly as it does (most of the times).

Of course, I want to thank my parents for their constant support during my studies and my PhD thesis. You know that you helped me a lot, without asking and without doubts about what I'm doing. That is and was always very important for me and I'm glad to have such wonderful and fantastic parents as you are!

Last but not least, I'd like to thank someone very special who has become a major part of my life. Verena, you helped me a lot during the last months not only concerning work but mainly concerning my well-being. Especially, during the lockdown, but also before, you supported and loved me tremendously. I'm so happy to have you in my life!!

Publications and meetings

Publications:

Schiwon, M., E. Ehrke-Schulz, **A. Oswald**, T. Bergmann, T. Michler, U. Protzer and A. Ehrhardt (2018). *"One-Vector System for Multiplexed CRISPR/Cas9 against Hepatitis B Virus cccDNA Utilizing High-Capacity Adenoviral Vectors."* Mol Ther Nucleic Acids **12**: 242-253

Stadler, D., Kächele, M., Hess, J., Jones, A.N., Urban, C., Schneider, S., Xia, Y., **Oswald, A.**, Nebioglu, F., Bester, R., Lasitschka, F., Ringelhan, M., Ko, C., Chou, W.-M., van der Klundert, M., Wettengel, J. M., Schirmacher, P., Heikenwälder, M., Schreiner, S., Pichlmair, A., Bartenschlager, R., Sattler, M., Unger, K., Protzer, U. *"Interferon-induced degradation of the hepatitis B virus persistence form, cccDNA, depends on ISG20."* Resubmitted after revision

Oswald, A., Chakraborty, A., Ni, Y., Wettengel, M. J. Urban, S., Protzer, U. *"Concentration of the Na^+-taurocholin cotransporting polypeptide expressed after transfection of in vitro transcribed mRNA determines susceptibility of hepatoma cells for hepatitis B virus"* Manuscript submitted

Oswald, A., Schmelas, C., Jones, J., Moeini, H., Sattler, M., Grimm, D., Protzer, U. *"Reduced targeting characteristics of SpCas9 to episomal DNA limits efficiency against HBV cccDNA."* Manuscript in preparation

Meetings:

Oswald, A., "*Using in vitro transcribed mRNA for gene therapy of chronic hepatitis B infection.*" – Poster presentation, International HBV meeting 2018, Taormina

Oswald, A., Protzer, U. "*Using in vitro transcribed mRNA for gene therapy of chronic hepatitis B infection.*" – Poster presentation, Gene Quantification Event (GQE) 2019, Freising

Oswald, A., Schmelas, C., Grimm, D., Protzer, U. "*Comparing CRISPR/Cas9 effects against differently localized structures of the HBV genome using an mRNA-based system*"